ASSESSING DIFFERENT COAL COMBUSTION RESIDUE BACKFILL SCENARIOS IN OPENCAST COAL MINES, MPUMALANGA, SOUTH AFRICA

UNIVERSITY *of the*
WESTERN CAPE

A dissertation submitted to the University of the Western Cape in the fulfilment of the degree of Magister Scientiae (MSc)

by

ANNALISA SARGA VICENTE

Department of Earth Sciences
Faculty of Natural Sciences University of the Western Cape

Supervisor:
Dr. Jacobus NEL

Co-supervisor:
Dr. Thokozani KANYERERE

26 March2020
Bellville, South Africa

DECLARATION

I declare that 'Assessing different coal combustion residue (CCR) backfill scenarios in opencast coal mines, Mpumalanga, South Africa' is my own work, that is has not been submitted for any degree or examination in any other university, and that all the sources I have used or quoted have been indicated and acknowledged by complete references.

Full Name: Annalisa Sarga Vicente

_____.

Date: 26 March2020

ABSTRACT

ASSESSING DIFFERENT COAL COMBUSTION RESIDUE BACKFILL SCENARIOS IN OPENCAST COAL MINES, MPUMALANGA, SOUTH AFRICA

Abstract:

Coal-fired power stations produce large volumes of coal combustion residues (CCRs), which are disposed of in hold ponds or landfill sites. These ash storage facilities are limited in space and are approaching the end of their capacities, thus additional land is required for extensions. If new land is not sourced, power plants will be forced to cease operations, resulting in increased expenditure costs and environmental liability. A proposed disposal solution is to backfill opencast coal mines with CCR monoliths. However, there is limited knowledge on the hydraulic behaviour of CCRs in an opencast coal mine environment. This leads to an inability to assess this applications feasibility and determine whether this activity will have a positive, negligible or negative effect on groundwater quality. This study aims to address this gap in knowledge by assessing the flow and transport properties of CCRs under numerous theoretical backfilling conditions.

In order to fulfil the aim of this study, the first objective was to conceptualise theoretical backfilling scenarios. These scenarios/conceptual models were constructed using the hydraulic properties of CCRs, mine spoils and geological formations of the Witbank Coal Fields of the Mpumalanga Province, South Africa. The second objective was to simulate the changes in the hydrogeological flow regime, such as the hydraulic head and flow direction, using numerical groundwater flow models. The third objective was to identify changes in contaminant concentrations and plume migrations, using numerical solute transport models. The final objective was to contextualise the risks associated with each theoretical backfill scenario by using a risk assessment approach.

Based on the aforementioned objectives, a total of six theoretical backfilling scenarios were conceptualized, namely: (1) No CCRs/mine spoils only (current practice and Base Case), (2) CCRs backfilled below the water table, (3) CCRs backfilled above the water table, (4) CCRs backfilled from the middle of the mine pit to the surface topography, (5) CCRs backfilled down-gradient of the pit up to surface topography, and (6) CCRs backfilled in the middle of the pit up to the weathered zone.. In order to assess the feasibility of this activity, all CCR backfilling scenarios were compared against backfilling without CCRs/mine spoils only (Scenario 1/ Base Case Scenario).

Comparisons of the hydrogeological flow regimes indicated that Scenarios 2 and 3 obtained similar water levels to the Base Case scenario, whereas Scenarios 4, 5 and 6 raised static water levels by 11 - 12%. Scenario 5 achieved the greatest pit water level rise (12%) over the largest area, keeping a larger volume of mine spoils saturated. This is deemed as a favourable outcome, as mine spoil saturation is likely to reduce oxygen ingress, potentially limiting the formation of acid mine drainage (AMD). The observed water level trend is that placing coal ash above or below the water table had a negligible effect on water levels, whereas coal ash placed in a position which intercepted the water table, inhibited the flow of water and raised the water table. Salt load comparisons indicated that all CCR backfill scenarios reduced salt load concentrations leaving the pit. The highest salt load was observed in Scenario 1. Scenario 2 displayed similar salt loads, offering a minor 4% reduction. Scenarios 3, 4 and 6 offer a significant improvement to groundwater quality by reducing salt loads by 31 - 50%, whereas Scenario 5 exhibited the greatest improvement to groundwater quality, reducing salt loads by 79%.

Contaminant plumes extended 150 – 200 m down-gradient under all scenarios, with the exception of Scenario 5 which displayed a 100 m lateral contaminant plume. Scenarios 1 and 2 produce the greatest contaminant plume, whereas Scenarios 3, 4 and 6 offered a 13 - 22% improvement in down-gradient groundwater quality. Scenario 5 was the only scenario to successfully retain the majority of the plume within the mine pit, offering an 84% improvement to down-gradient water quality.

The changes in water levels, salt loads and contaminant plumes were integrated into a long-term comparative risk assessment. In ranking the risks associated with these factors, it was apparent that the Base Case Scenario (Scenario 1) produced the greatest negative environmental impact, whereas backfilling with CCRs (under any scenario) provided an environmental improvement. Scenarios 2 and 3 were ranked as ‘High’ negative risk scenarios. Scenarios 6 and 4 were both classified as ‘Medium’ risk scenarios and Scenario 5 was the only ‘Low’ negative risk scenario.

It is thus concluded that all CCR backfilling scenarios provide an environmental improvement to groundwater quality. The beneficial extent is dependent on the placement/design of the CCR monolith in relation to site specific receptors (humans, vegetation, rivers etc.). For example, if the receptors are located down gradient, Scenario 5 would be the most favourable scenario. This is because it retains the contaminant plume within the pit, reducing down-gradient salt loads and plume migrations. However, should receptors be positioned adjacent to the pit

(perpendicular to the groundwater flow direction), Scenarios 4 and 6 would be the most favourable because they limit the lateral plume migration. Therefore, it is concluded that each scenario has the potential to provide an improvement (relative to the Base case) and can be beneficially applied under different site conditions.

It is recommended that a field-based pilot study and site-specific flow model, with the intent of giving an accurate depiction of groundwater level changes, be implemented. Understanding the potential benefits in a site-specific context may assist ESKOM in reducing their on-site ash disposal volumes, whilst providing environmental benefits with CCR monolith backfilling into opencast coal mines.

ACKNOWLEDGEMENTS

I would like to express my sincere gratitude towards every family member, friend and colleague who has been involved in my life during these past two years. You have contributed a great deal towards my-wellbeing; being it mentally, physically or emotionally.

I would like to acknowledge my heartfelt thanks to the following individuals and organisations:

- My grandmother, Gloria Street, for being my rock. You have always given me the best you possibly could and for that, I will be eternally grateful for your love and support.
- My mother, Aileen Vicente, for silently being proud. Your indirect affection and guidance have compelled me towards being the best version of myself.
- My supervisor, Dr Jaco Nel, for being the definition of 'greatness'. Whether it be a braai, a field trip or a modelling project. You always strive to be the best; this example is admirable, and your guidance is greatly appreciated.
- My departmental mother, Marlese Nel, for being an intelligent and friendly person. You have always been such an ease to confide in, whether it be for work or play.
- My co-supervisor, Dr Thokozani Kanyerere, for always having faith in me and filling me with passion throughout the years.
- My project partner, Angelo Johnson, for being as genuine as they come. Thank you for picking my brain and making every field trip a good memory.
- The Eskom 'Boss', Kelley Reynolds-Clausen, for your knowledge, support, humour and funding.
- The postgraduate students: Errol Malijani, Nomanesi Makhonco, Raven Pietersen, Malikah Van Der Schyff, Vincent Banda, Phumlani Mqondeki, Retang Mokau, you are thanked for your friendship and assistance.
- A good friend, Josh Silent, for unfailingly being able to guide me by being a good voice of reason. Your effortless support has kept me grounded and happy.
- Eskom for providing me with an interesting project and financial support.
- The National Research Foundation for providing me with financial support.

TABLE OF CONTENTS

LIST OF FIGURES

LIST OF TABLES

LIST OF ACRONYMS

a	annum
AMD	Acid Mine Drainage
c.	circa (approximately)
CCR	Coal Combustion Residue
g/m^3	grams per cubic metre
K	Hydraulic conductivity
m	metres
m/d	metres per day
mamsl	metres above mean sea level
mbgl	metres below ground level
mm	millimetres
mm/a	millimetres per annum
Mt	Million tons
S	Storativity
T	Transmissivity

GLOSSARY

Acid mine drainage	Also known as acid rock drainage, is acidic water from the mine when sulphide-bearing minerals, often in the form of pyrite (iron-sulphide or FeS^2), are exposed to oxygen and water.
Ash monolith	A large single upright block of ash.
Aquifer	A formation, group of formations, or part of a formation that contains sufficient saturated permeable material to store and transmit water; and to yield economical quantities of water to boreholes or springs. An aquifer is the storage medium from which groundwater is abstracted
Coal ash	Also known as coal combustion residues, is the byproduct of coa combustion, which includes fly ash, bottom ash and slag.
Coal combustion residue	Also known as CCR's, is a collective term referring to the residues produced during the combustion of coal, which includes. fly ash, bottom ash, boiler slag and fluidised bed combustion ash and other solid fine particles.
Contaminant plume	An area of degraded water in a stream or aquifer resulting from migration of a contaminant.
Flow regime	The range of magnitude, duration, timing and frequency the groundwater flows.
Formation	A body of rock identified by lithic characteristics and stratigraphic position. Different formations have different hydrogeological properties.
Groundwater	Water found in the subsurface in the saturated zone below the water table. Groundwater is a source of water and is an integral part of the hydrological system.
Hydraulic conductivity	Measure of the ease with which water will pass through the earth's material; defined as the rate of flow through a cross-section of one square metre under a unit hydraulic gradient at right angles to the direction of flow (m/d).
Hydrogeology	In South Africa the term geohydrology and hydrogeology are used interchangeably. In theory hydrogeology is the study of geology from the perspective of its role and influence in

	hydrology, while geohydrology is the study of hydrology from the perspective of the influence on geology
Mine backfilling	This is described as soil, overburden or mine tailings used to replace excavated zones created by mining operations. It is used as a means to aid the stabilization of mining-related voids and the disposing of mining wastes.
Mine overburden	Refers to all earth and other natural materials which are removed from the mine to gain access to the desired minerals in the process of surface mining.
Mine spoils	Earth and rock excavated from a mine.
Opencast coal mine	Also known as open-pit or open-cut mining, is a surface mining technique of extracting rock or minerals from the earth by their removal from an open pit or borrow.
Porosity	The ratio of the volume of void spaces in a rock or sediment to the total volume of the rock or sediment
Recharge	The addition of water to the saturated zone, either by the downward percolation of precipitation or surface water and/or the lateral migration of groundwater from adjacent aquifers. Recharge is crucial for the ongoing replenishment of aquifers.
Remediate	To restore something to its original state
Saturated	The capacity to hold as much water or moisture as can be absorbed thoroughly soaked
Solute	A liquid, solid or gas which is dissolved to make a solution
Specific yield	The ratio of the volume of water a rock or soil will yield by gravity drainage to the volume of the rock or soil
Storativity	The volume of water released from storage per unit of aquifer storage area per unit change in head.
Transient (time)	A system is said to be transient when a process variable or variables have been changed and the system has not yet reached a steady state
Transmissivity	The rate at which water of a prevailing density and viscosity is transmitted through a unit width of an aquifer or confining bed under a unit hydraulic gradient

Water table	The upper surface of the saturated zone of an unconfined aquifer at which pore pressure is equal to that of the atmosphere. It marks the top of the groundwater body.

1 INTRODUCTION

1.1 Research background

South Africa relies heavily on coal to generate low-cost electricity and meet the countries energy demands. Coal is abundant and affordable making it a very popular energy source (Ratshomo and Nembahe, 2013), supplying more than 90% of the country's electricity (National Electricity Regulator 2004). In 2016, approximately 109 million tons of coal were consumed (Eskom, 2016), placing South Africa as the seventh largest coal producing country globally (Hans-Wilhelm, 2016; British Petroleum, 2017).

The burning of coal for power generation produces large quantities of coal by-products such as fly ash, bottom ash and gasification ash (Murarka, 2016). Collectively, these three by-products are termed coal combustion residues (CCRs) or coal ash (Indiana Department of Environmental Management, 2017). In 2016, Eskom (South Africa's energy producer), produced 25 million tonnes (Mt) of coal ash, of which only 7% was utilised (Eskom, 2016).

This low reuse percentage is attributed to CCRs previously being classified as a 'hazardous waste' under the Waste Act 59 of 2008 (Department of Environmental Affairs). However, in 2017, the national government excluded 'ash from combustion plants' from the definitions of 'waste'. Therefore, the new classification of CCRs has prompted its use in specific deregulated applications without a Waste Management License.

Eskom has embarked on a process to enhance the utilisation of ash, with the aim of increasing revenue whilst avoiding the cost of ash disposal. Multiple power stations are running out of storage space on their ash handling facilities and are required to source additional land for extensions. This would increase operational and expenditure costs which could be avoided if ash is utilised in various applications.

In order to reduce the disposal of ash, Eskom is currently undergoing research assessing the feasibility of various coal ash applications, namely: cement and brick production, treatment of acid mine drainage (AMD), soil fertilization, polymerisation, heavy metal extraction and mine void backfilling. This project focuses on CCR mine void backfilling in opencast coal mines, as there is a limited amount of knowledge to assess its feasibility in South Africa.

The feasibility of CCR backfilling in opencast coal mines is dependent on the hydraulic and transport properties which occur within the coal ash, mine spoils and geology (Ward et al., 2009). Comparatively assessing the changes to the hydrogeological flow regimes and contaminant concentrations from various CCR backfilling scenarios will provide insight as to

whether this application will have a positive, negligible or negative impact on groundwater resources.

1.2 Research problem

Ash storage facilities are nearing the end of their capacities, thus additional land is required for extensions. If new land is not sourced, power plants will be forced to cease their operations. This would be a costly operation which would increase expenditure costs and environmental liability.

The utilisation of large quantities of CCRs may resolve or postpone these problems. A proposed disposal solution is to backfill opencast mines with CCRs, however, there is a limited understanding of the groundwater flow and solute transport processes which occur within this application. This gap in knowledge leads to an inability to predict the changes in flow and transport processes under different CCR backfilling scenarios as well as whether CCR backfilling has a positive, negligible or negative impact on groundwater resources.

1.3 Research questions

Would the changes in flow and transport processes under numerous CCR backfilling scenarios have a positive, negligible or negative impact on groundwater?

1.4 Aim and objectives

The aim of this study is to assess the groundwater flow and transport processes of different CCR monolith backfilling scenarios into opencast mines. Understanding the flow and transport processes will provide insight to the changes in hydrogeological flow regimes, contaminant concentrations and plume migrations. This will help deduce whether the application of CCR backfilling under numerous scenarios will have a positive, negligible or negative impact on groundwater resources.

The objectives of this study are as follows:

1. To develop practical CCR monolith backfilling scenarios:
   Constructing conceptual models of practical CCR backfilling scenarios will serve as the basis to assess flow and transport properties;
2. To determine the influence of CCR monolith placement on the hydrogeological flow regime:

Simulating the hydraulic head, rate and direction of groundwater movement through the subsurface will help establish the changes to in-pit groundwater levels;

3. To identify the influence of CCR monolith placement on salt loads and contaminant plume migrations:

   Simulating contaminant solute transport will aid in predicting the contaminant concentrations and plume migrations per scenario; and

4. To evaluate the relative risks associated with various backfilling scenarios:

Contextualising the relative risks associated with flow regimes, salt loads and plume migrations per scenario using a risk assessment, will aid in assessing whether CCR backfilling will have a positive, negligible or negative impact on groundwater quality.

1.5 Thesis outline

Chapter 1 provides a brief introduction to the research background of coal combustion residues (CCRs). Further discussing the research problem, aims and objectives, thesis outline and research framework.

Chapter 2 outlines literature associated with CCRs, mine spoils, geology and their combined interaction. In addition, this chapter documents the current state of knowledge and highlights substantive findings, which were applied in the assessment of different backfilling scenarios. The end of this section describes the process undertaken when selecting the appropriate groundwater model.

Chapter 3 describes the various components and theoretical knowledge which contributed towards developing the conceptual models for various scenarios.

Chapter 4 describes the construction and input variables used to create numerous flow and transport models. These numerical models were used to simulate future responses to the hydrogeological system under various backfilling conditions.

Chapter 5 describes the results obtained from the constructed flow and transport models. The results include information on flow regimes, contaminant concentrations, salt loads and plume migrations. These results are holistically accounted for in the impact assessment at the end of this chapter.

Chapter 6 summarises the most important findings of the study and what the findings imply to the application of CCR backfilling. Furthermore, providing recommendations for further research within this topic.

1.6 Research approach:

This study followed the methodological research approach presented in Figure 1 below. The approach was initiated by identifying the research problem, reviewing the topic in literature and identifying the gaps in knowledge. The research questions, aims and objectives were formulated from this information. A quantitative research design was used to collect and analyse data using numerical groundwater models. The simulated results were then analysed and evaluated to assess whether CCR backfilling under numerous scenarios would have a positive, negligible or negative impact on groundwater resources.

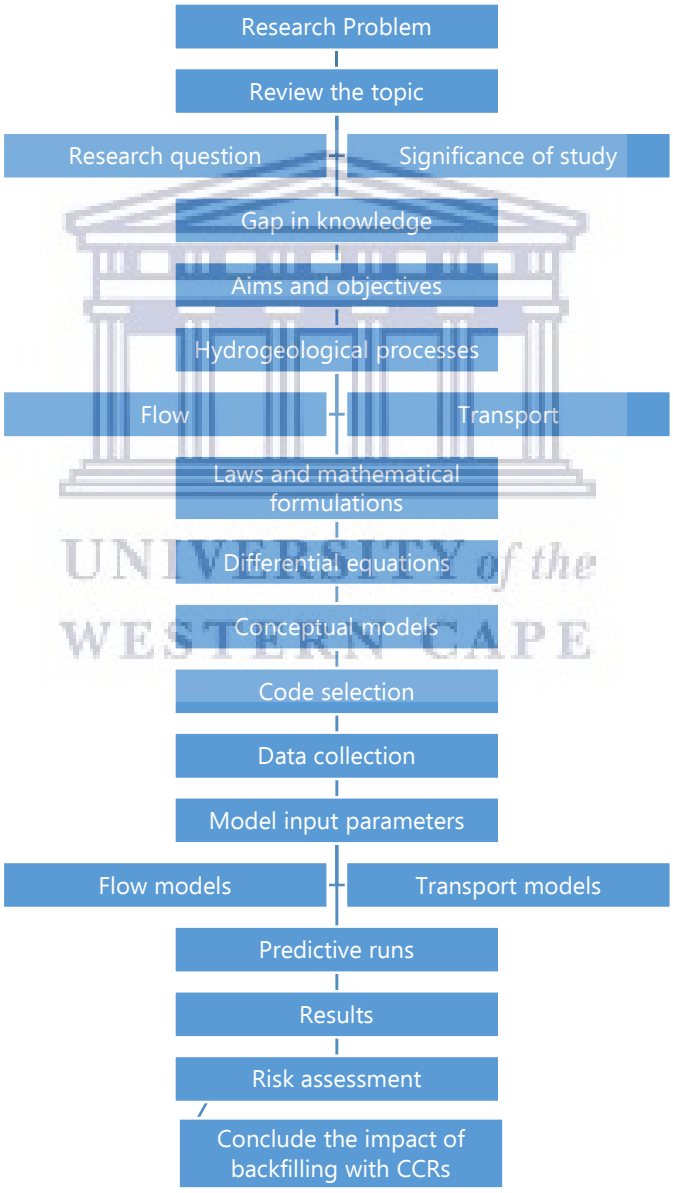

Figure 1: Methodological Framework

2 LITERATURE REVIEW

This chapter evaluates relevant information published regarding CCRs, mine spoils and their combined co-disposal interactions. Documented scholarly articles within these topics give an indication of the current state of knowledge and highlight the substantive findings, which are applied to assess different scenarios. This chapter concludes with the approach undertaken in selecting a suitable groundwater model to achieve the objectives of this study.

2.1 Global and local context of Coal Combustion Residues (CCRs)

The world consumes approximately 7 700 million tonnes (Mt) of coal per annum, used by a variety of sectors such as power generation, liquid fuel, iron and steel production (Hans-Wilhelm, 2016). Globally, coal is the leading source of electricity production as well as the second largest energy source worldwide (Hans-Wilhelm, 2016). The dominance of coal in the global electricity arena is due to its abundance, affordability and widespread distribution (Hans-Wilhelm 2016). The top three coal-consuming countries; namely: China, the United States and India, account for approximately 70% of the world's coal use (Energy international Administration, 2018).

South Africa is ranked as the seventh largest coal producing country (Figure 2), with the tenth largest international coal reserve (Hans-Wilhelm 2016; BP 2017). South Africa relies heavily on coal to generate low-cost electricity and meet the countries growing energy demands (Ratshomo and Nembahe 2013). This is evident as coal supplies approximately 94% of the nation's electricity (National Electricity Regulator, 2004; Eskom, 2009; World Energy Outlook, 2011) . The electricity sector accounts for more than half of the coal consumed in South Africa, followed by Sasol's petrochemical industries, metallurgical industries etc. (BP, 2017).

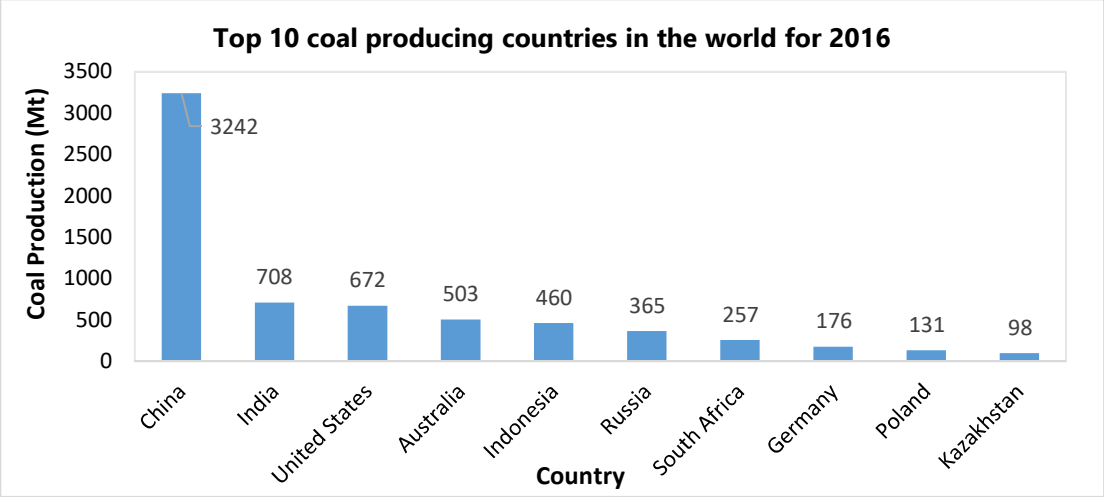

Figure 2: Top 10 coal producing countries in the world for 2016 (Derived from the Agency for Natural Resources and Energy, 2017)

The utilisation of coal for power generation produces large quantities of CCRs (interchangeably referred to as 'coal ash'). It has been estimated that 780 Mt of CCR's are produced worldwide annually, of which only 53.5% is utilised (in applications such as the production of: cement, concrete, structural fill, roadway, pavement materials etc.). The remaining is disposed/stored in ash handling facilities (Zhang, 2014). A country's CCR re-use potential is attributed to its legislation, classifying CCRs as either a 'solid' or 'hazardous' waste. The majority of countries classify CCRs as a solid waste, which encourages its re-use.

In South Africa, CCRs were previously classified as a 'hazardous waste' under the Waste Act 59 of 2008, however in 2017, the national government excluded 'ash from combustion plants' from the definitions of 'waste'. This new classification of CCRs has prompted its use in specific deregulated applications without a Waste Management Licence. South Africa produces approximately 25 Mt of coal ash per annum, of which only 7% was utilised (Reynolds-Clausen and Singh, 2016; Eskom, 2016). These large volumes of underutilised coal ash presented a need to implement innovative utilisation applications. This need is acknowledged by South Africa's energy producer – Eskom, which is currently assessing the feasibility of various coal ash applications, such as cement and brick production, treatment of acid mine drainage, soil fertilization, polymerisation, heavy metal extraction and mine void backfilling.

2.2 Characteristics of Coal Combustion Residue's

This subchapter will provide a holistic review on the physical, hydraulic and chemical properties of coal ash. Further elaborating on the way in which coal ash is disposed of and the environmental impacts associated with its disposal.

2.2.1 Physical properties

Coal ash from coal-fired power stations is comprised of fly ash and bottom ash. 'Fly ash' refers to the lightweight particles that travel with the flue gas whilst it exits the furnace. Fly ash is collected by electrostatic precipitators (Electric Power Research Institute, 2013), whereas 'bottom ash' refers to the heavier particles that fall to the bottom of the furnace (Kikuchi, 2006). Coal ash predominantly comprises fly ash, which accounts for approximately 80 – 90% of its mass weight, whereas bottom ash only accounts for 10 – 20% of its total weight (Yeheyis et al., 2009; Akinyemi, 2011). As fly ash occupies the bulk weight of coal ash, it has a tendency towards obtaining fly ash characteristics, hence 'fly ash' is often referred to as coal ash' throughout this study.

The physical properties of coal ash have been extensively investigated using the scanning electron microscope (SEM). SEM analyses indicate that coal ash particles are typically spherical in shape, being either solid or with vesicles (Figure 3) (Electric Power Research Institute, 2013). The typical solid spherical morphology of coal ash is displayed in 'a' of Figure 3 and the etched or hollow morphologies are displayed in 'b-e' of Figure 3. Coal ash is predominantly comprises non-crystalline alumina-silicate glasses, with smaller amounts of unburnt coal particles and crystalline minerals (Zhang, 2014). The glassy and spherical occurrence of fine ash indicates melting of silicate minerals under high temperatures during the combustion process (Mahlaba et al., 2011).

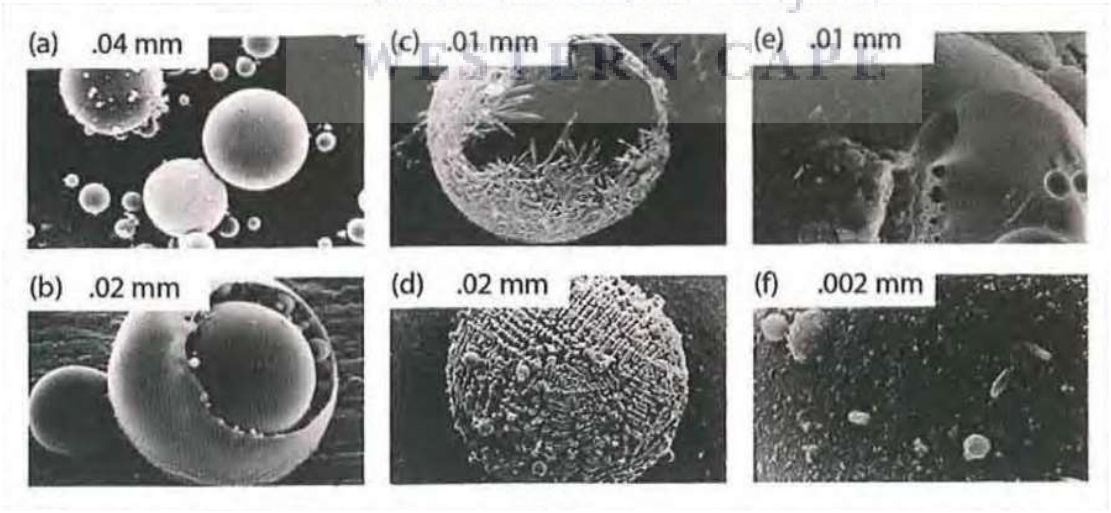

Figure 3: Scanning electron micrographs of coal ash (image sourced from EPRI, 2013): (a) spherical morphology, (b) large hollow sphere (c) etched particle, (d) magnetic spinel, (e) fractured particle, (f) accumulation of ash granules on the surface of a larger particle

Fly ash is generally grey in colour and may vary from light tan to black (Figure 4). The colour of the ash is dependent on the amount of unburnt carbon present and the combustion technology applied (Jayaranjan et al., 2014). The lighter the colour, the lower the carbon content is and vice versa. Bituminous fly ash displays light to dark grey variations (Akinyemi et al., 2011), whereas, lignite and sub-bituminous fly ash is generally tan in colour, indicating a low carbon content as well as the presence of lime or calcium (Akinyemi et al. 2011)

Figure 4: Picture of coal ash

Fly ash is predominantly comprised of silt, clay and sand-sized particles. The particle size distribution of most bituminous fly ash is similar to silt, accounting for 60 – 95% of its composition (Akinyemi, 2011). Although sub-bituminous coal ash is generally silt-sized, it displays coarse properties which may fall into clay and sand-sized ranges. The particle size of fly ash ranges from 0.5 µm to 100 µm with a median particle diameter of 20 – 25 µm (Electric Power Research Institute, 2013). The majority (> 60%) of the particle diameters are less than 50 µm (Swaine, 1995; Kim, 2003; Ahmaruzzaman, 2010).

The specific gravity of fly ash ranges between 2.1 to 3.0 (Akinyemi, 2011; Jayaranjan et al., 2014; Murarka, 2016), whilst it's bulk density ranges from 1 to 1.8 $g \cdot cm^{-3}$ (Campbell et al., 2005; Kim and Prezzi, 2008). The permeability of fly ash typically ranges from 10^{-6} to 10^{-4} cm/s, which is similar to that of silty-clay (Eletric Power Research Institute, 2013). The fine particle size of fly ash allows for a moisture content between 6.1 - 13.4%, with a high water holding capacity of 49 - 66% per weight basis (Campbell et al., 2005). The specific area of fly ash ranges between 0.17 – 1.0 m^2g^{-1} (Theis and Gardner, 1990; Ahmaruzzaman, 2010).

The aforementioned physical properties of coal ash were generalised (Table 1), thus may material vary according to its combustion temperatures, the grade of coal, mineral composition of coal, combustion conditions, the efficiency of particle removal and pollution control

equipment (Kim, 2003; Gitari et al., 2009; Mahlaba et al., 2011). Site-specific factors also play an important role in physical variation, which includes climate/meteorological conditions, the disposal fill design, vegetation, hydrogeological conditions and the extent of weathering (Van der Sloot et al., 1997; Gitari, et al., 2009).

Table 1: Summary of the physical properties of fly ash (Data derived from Campbell et al., 2005; EPRI, 2013; Jayaranjan et al., 2014)

Physical Property	Fly ash
Colour	grey - black
Shape	mainly spherical
Specific gravity (g cm^{-3})	2.1 - 2.9
Bulk density (g cm^{-3})	1 - 1.8
Particle size distribution (mm)	0.001 - 0.075
Specific surface area (m^2 g^{-1})	1 - 9.44
The angle of internal friction (degrees)	25 - 40
Clay (%)	1 - 10
Silt (%)	8 - 85
Sand (%)	7 - 90
Gravel (%)	1 - 10

2.2.2 Hydraulic properties

A vast amount of research has been conducted on the physical and chemical properties of coal ash; however, limited knowledge exists regarding its hydraulic properties. According to Fetter (1994), the main hydraulic property of general concern is 'hydraulic conductivity', which can be defined as the rate at which a material can transmit a liquid under a unit gradient. In an opencast backfill scenario, the hydraulic conductivity is important in understanding the flow of water and air ingress entering the ash (Hodgson and Krantz, 1998).

The hydraulic properties of fly ash vary depending on factors such as its texture, grain size, porosity, saturation, degree of compaction and aggregation (Menghistu, 2010; Jayaranjan et al., 2014). Apart from its initial state, the hydraulic properties of coal ash continue to change over time as it undergoes geochemical weathering and incurs pozzolanic action (Nhan et al., 1996; Kostas et al., 2000). The geochemical processes are initiated by the presence of calcium ions which form gypsum as well as the saturation of coal ash. The gypsum formed accumulates in the void spaces, consequently lowering its hydraulic conductivity (Kostas et al., 2000; Johnson, 2018). This process is known as secondary mineralisation and is responsible for the changes in hydraulic conductivity (Figure 5)(Yeheyis et al., 2009). Although the hydraulic conductivities of coal ash vary, it is generally known to decrease with time (Table 3), until a

proposed steady-state equilibrium is reached (October et al. 2009). The reduction in hydraulic conductivities differ between laboratory and field observations. Field observations display a slow reduction in hydraulic conductivity over time (**Table 2**), whereas laboratory observations display a rapid decrease in hydraulic conductivity (few orders of magnitude) in a relatively short period (Table 3). These differences are attributed to saturation/volumetric water inflow rates as well as the moisture available for curing (Mudd, 2002; October, 2009; Munchingami, 2013; Johnson, 2018). A high moisture content with a longer curing time is known to decrease hydraulic conductivity values by several orders of magnitude (Table 3). This decrease in hydraulic conductivity is attributed to the pozzolanic processes which had taken place due to the calcium oxide and carbon dioxide ingress present (Nhan et al., 1996; Van den Berg et al., 2001; Liu et al., 2009, Akinyemi et al., 2013; Munchingami, 2013). Although hydraulic conductivity values (field vs. laboratory) may differ, a reasonable assumption is that the average hydraulic conductivity of coal ash is within the order of 10^{-1} to 10^{-2} m/d (Hodgson and Krantz, 1998; October, 2011; Johnson, 2018)

Figure 5: A scanning electron micrograph (10µm) of coal ash before and after secondary mineralisation (image sourced from Johnson, 2018).

Table 2: Field hydraulic conductivity values of coal ash over time with a 10 – 15% moisture content (data sourced from Johnson, 2018)

Time (years)	Hydraulic conductivity (meters/day)
1	0.82
5	0.46
10	0.39
20	0.22

Table 3: Laboratory hydraulic conductivity versus moisture content of coal ash (Data sourced from Johnson, 2018)

	Hydraulic Conductivity (meters/day)				
Moisture content (%)	**Week 1 -2**	**Week 3 -4**	**Month 2**	**Month 3**	**Month 4**
40	10^{-1}	10^{-1} - 10^{-2}	10^{-2}	10^{-3}	10^{-3}
50	10^{-1}	10^{-2}	10^{-2}	10^{-2} - 10^{-3}	10^{-3}
60	10^{-1} - 10^{-2}	10^{-2}	10^{-2}	10^{-2} - 10^{-3}	10^{-3}

Coal ash is classified into two classes: Class C and Class F according to the American Society for Testing and Materials (ASTM C618, 2019). These two classes are based on their chemical composition which classes ash into a high-lime and low-lime content. Class F ash is pozzolanic in nature and contains more than 70 wt% SiO_2 + Al_2O_3 + Fe_2O_3 and low lime. This fly ash is produced from the combustion of harder, older anthracite and bituminous coal and is representative of South African coal ash. Class C ash from burning younger lignite or subbituminous coal, in addition to having pozzolanic properties, also has some self-cementing properties (Zhang, 2014). A summary of the different hydraulic conductivities of coal ash according to its source and class are presented in Table 4 below.

Table 4: Literature-based hydraulic conductivities of coal ash

Type of coal ash	Source	Method	Initial hydraulic conductivity (m/d)	Steady-state hydraulic conductivity (m/d)	Author
Class F	Mpumalanga	Field	1.089 – 0.22		Johnson, 2018
Class F	Mpumalanga	Field	0.4	0.12	October, 2011
Class F	Mpumalanga	Lab		0.92	October, 2011
Class F	Mpumalanga	Lab	0.44		Johnson, 2018
Class C	India, Bengal	Lab		0.074	Sivapullaiah, 2004
Class F	Canada	Lab	0.000085	0.0085	Nhan et al., 1996
				0.302 (saturated); 0.167 - 0.886 (unsaturated)	Mudd, 2002
				0.02 -0.1	Van den Berg et al., 2001

The hydraulic conductivity is directly proportional to the porosity of coal ash, which surmises that a lower effective porosity induces a lower hydraulic conductivity. This is a directly proportional relationship, because the hydraulic conductivity is an indication of a liquids ability to flow through coal ash which depends on the void volumes present (porosity). Coal ash has a high total porosity ranging between 42 – 60% (Van den Berg et al., 2001), however not all the porosity is available for flow as part will be occupied by static fluids from surface tension, thus porosity available for fluid flow is termed as effective porosity. Porosity values of Mpumalanga coal ash were examined using laboratory and field tracer tests, resulting in an effective porosity of 13% and 15% respectively (October et al., 2009). This value is a function of the size of the molecules that are being transported to the relative size of the passageways that connect the pores (OhioEPA, 2007). The storativity of coal ash is also an important hydraulic parameter as it indicates the volume of liquid released per volume of ash as a result of a change in head. Due to limited research into the exact storativity value of coal ash, most practical cases infer that specific yield (Sy) values are approximately the same as effective porosity (Bear, 1979; Kasenow, 2001). Coal ash is physically comparable to silt (Mahlaba et al., 2011), thus specific yield can be inferred from Johnson's (1976) soil classifications as 0.08. Furthermore, there is limited knowledge on the recharge value of coal ash, hence it is assumed to be approximately four times greater than natural recharge rate of the geological landscape (Geo Pollution Technologies, 2004).

A summary of the physical properties of coal ash are presented in Table 5 below:

Table 5 The physical properties of coal ash

Parameter	Value (%)	Author
Specific yield	8	Johnson, 1967
Effective Porosity	13	October, 2011
Recharge (m/day)	5 - 10	Geo Pollution Technologies, 2004

2.2.3 Chemical properties

The chemical composition of coal ash consists of a wide range of elements that may influence the environmental impacts that arise from its disposal. Studies show that approximately, 90 - 99% of coal ash is comprised of major ions, namely: Aluminium (Al), Silica (Si), Calcium(Ca), Iron (Fe), Magnesium (Mg), Iron (Fe), Phosphorus, (P), Potassium (K), Sodium (Na), Manganese (Mn) and Sulphur (S) (Campbell et al., 2005; Ahmaruzzaman, 2010 ; Akinyemi, 2011; Kolbe et al., 2011). The remaining chemical composition of coal ash consists

of an average of 26 trace elements, namely: As, B, Ba, Be, Cd, Ce, Co, Cu, Cr, F, Hg, Mn, Mo, Ni, Pb, Rb, Sb, Se, Sn, Ti, Th, U, V, W and Zn (Izquierdo & Querol 2012).

The chemical composition of fly ash varies depending on its particle size, shape, surface area, permeability, heterogeneity, temperature and saturation (van der Sloot et al., 1997). In addition, site-specific conditions play a role as it determines the rate and response of processes such as advection, dispersion, diffusion, sorption and degradation (van der Sloot et al., 1993; Akinyemi, 2011; Eze et al., 2013).

2.2.4 Ash disposal systems

The disposal of coal ash is becoming an increasing economic and environmental liability. The South African power utility company, Eskom, produces approximately 25 Mt of fly ash annually, of which only 7% is reused and the rest is disposed of using wet or dry ash disposal methods (Reynolds-Clausen and Singh 2016; Eskom, 2016).

Wet ash disposal systems involve the mixing of fly ash with water at ratios of 1:10 and 1:5 by volume at the power station (Figure 6) (Hodgson and Krantz, 1998). This type of disposal is a simple operation, which has minimal effects on air quality, however, uses large quantities of water, requires large areas of land and is relatively costly. These factors raise environmental concerns regarding potential groundwater contamination of heavy metal leachate from ash ponds (Sing and Kolay, 2002).

Dry ash disposal systems involve partially wetting coal ash to a 10 – 15% moisture content at the power station (Haynes, 2009) and have less of an environmental impact, as a few studies have concluded that it is unlikely to produce leachate for many years (Simsiman, 1987; Menghistu, 2010).

Figure 6: A dry ash disposal site in Mpumalanga

2.2.5 Environmental impacts of coal ash disposal

Various environmental risks are associated with coal ash disposal, these include air pollution, loss of arable land as well as surface or groundwater contamination due to the leaching of heavy or trace elements from an ash dump (Carlson and Adriano, 1993).

When ash surfaces are exposed to wind, it has the ability to become airborne, thus contributing to dust pollution. Coal ash is composed primarily of an alumina-silicate matrix which is less than 50 μm in size (Liblik and Pensa, 2003; Zhang, 2014), thus it may be inhaled and ingested causing respiratory problems, cardiovascular damage and skin cancer (Pilate and Adams, 1985; Borm, 1997; Kockwood and Evans, 2012). The contribution of coal ash towards dust pollution may be kept at a minimum when the top surface of coal ash is rehabilitated. This will limit surface exposure, lowering the contribution to airborne coal ash. Additionally, ash dust pollution may be limited if further wetting takes place during its dry disposal on the landfill site (Valencic, 2013).

Coal ash disposal may pose a threat to the environment if significant concentrations (that exceed acceptable water quality standards of undesirable elements) leach from the ash towards groundwater and surface water systems (Yuan, et al., 2009). Therefore, it is a growing environmental concern to dispose of fly ash in a sound manner to prevent health issues and heavy metal contamination.

2.3 Characteristics of mine spoils

This subchapter will provide a holistic review on the physical, hydraulic and chemical properties of coal mine spoils. Furthermore, elaborating on its disposal in conjunction with the mining process and the environmental impacts which may occur.

2.3.1 Physical properties

Coal mine spoils are the by-products of coal mining, which refers to the mixture of the coal seam, parent rock and subsoil (Jha and Singh, 1991). Understanding mine spoil hydrology is important for predicting the production of AMD as well as planning for mine reclamation and rehabilitation.

Coal mine spoils are highly heterogeneous and anisotropic (Hodgson and Krantz, 1998), making the general classification of them difficult. They vary in shape and are commonly identified as being irregularly shaped and commonly angular. Due to their heterogeneity, they obtain an extremely poor sorting of sandstone, clays, silt, shale and coal remnants (Jones and

Anderson, 1994). Particle sizes of mine spoils are broad, ranging from clay (< 0.002 mm) to very large boulder (> 2048 mm) sized particles (Rehm et al., 1980; Hawkins, 1998) (Figure 7). The bulk density of mine spoils range from 1.27 to 1.75 g/cm^3 (Maharana and Patel, 2013).

Figure 7: Photograph of the heterogeneity of mine spoils

2.3.2 Hydraulic properties

The structure of mine spoils depend on numerous factors, which include the origin of overburden lithology, methods to strip overburden material, timing and method of recontouring the spoils (Rehm et al., 1980). As mine spoils tend towards being extremely heterogeneous, its hydraulic conductivities span over seven orders of magnitude (Rehm et al., 1980; Hawkins, 1998), ranging from 0.00038 to 654.9 m/d (Hawkins, 1998). These ranges create a large assortment; thus, a better representation is the mean/average hydraulic conductivities. Tabulated mean hydraulic conductivity values are seen in Table 6 below.

Table 6: Hydraulic conductivity values for mine spoils from various locations and authors

Hydraulic Conductivity (m/d)	Location	Author
1.49	Pennsylvania	Hawkins, 1998
1.14	Germany	Buczko et al., 2001
1.46	Appalachian Plateau	Hawkins, 2004
0.07	Dakota, America	Rehm et al., 1980

An acceptable approximation of typical mine spoils hydraulic conductivity is 1 m/d (Hodgson and Krantz, 1998). However, it is important to note that the hydraulic properties of mine spoils evolve with age (Rehm et al., 1980). As the mine spoils age, levelled mine spoils become less permeable due to the decomposition of material, compaction and silting up of channels (Rehm

et al., 1980). The changes in hydraulic conductivity are attributed towards the process of settling, subsidence, compaction and piping within the backfill (Shangoni Aquiscience 2013). Additionally, the recovery of water levels induced vertical and horizontal groundwater movement which catalyses the piping and settling of fine-grained mine spoils causing compaction over time (Hawkins 1998). In contrast to the natural processes, the way in which mine spoils are remediated also play a role in changing the hydraulic conductivity. Rehm (1980) found that spoils which were disaggregated or well compacted during reclamation obtained hydraulic conductivities which were similar to that of undisturbed fine-grained overburden. Besides the alteration of hydraulic conductivities due to spoil reclamation, recharge rates experience the same mechanism. It is noted that remediation conditions and age of spoils determine the amount of recharge mine spoils received. Hodgson and Krantz (1998) conducted a study within the Witbank Coalfields, Mpumalanga, which estimated recharge rates for opencast coal mines under various water contributing conditions. The recharge rates are dependent on the type of rainfall events that occur. Rainfall events that are less than 10 mm have an average recharge of 5.5% and rainfall events over 10 mm have an average recharge of 10%.

The specific yield of mine spoils indicates the volume of water released from storage per unit decline in the water table (Heath, 1983), as this value is uncommon in literature, it is obtained by physically comparing mine spoils to silt (Mahlaba et al., 2011) which is acquired from Johnson's (1976) soil classifications as 0.08. In addition, the void space of unconsolidated material (porosity) influences how groundwater flows. Hodgson and Krantz (1998) equated the effective porosity of mine spoils as 5 – 10% of the total volume.

2.3.3 Chemical properties

Mine spoils and waste rock dumps are regarded as a major source of acid mine drainage (AMD) (Monterroso and Acías, 1998; Fourie, 2007). This is because mine spoils contain an abundant amount of pyrite minerals which get exposed to oxygen and water, consequently forming sulphuric compounds (USEPA, 1994; Brick, 1998; Simate and Ndlovu, 2014). The sulphuric compounds acidify the water forming AMD (Figure 8). AMD has the potential to contaminate

water resources, however the chemical composition of mine spoils, is not a focus of this study, but rather the mine spoils ability to generate AMD.

Figure 8: Photo of acid mine drainage in an opencast coal mine in Mpumalanga

Acid mine drainage prediction tests are used to assess the long-term potential to generate AMD. Mine spoils have a highly variable mineral composition and size, that differ from site to site, the ability to accurately predict the acid potential becomes quite difficult (Brodie et al., 1994). Ferguson and Erickson (1998) have identified primary, secondary and tertiary factors which control the generation of AMD. Primary factors of acid generation include the presence of sulphide minerals, water, oxygen, ferric ions, bacteria and heat. Secondary factors act to either neutralize the acid produced from oxidation reactions or alter effluent characteristics with the addition of heavy metal ions mobilised by residual acid. Tertiary factors affecting AMD production include; the physical characteristics of mine spoils, the placement of acid generating and acid neutralising materials, as well as the hydrologic flow regime in the vicinity.

Although the ability to accurately predict AMD generation needs to be analysed on a site-specific basis, the following oxidation-reduction reactions generally occur when pyritic minerals come into contact with water and oxygen:

1) In this step, S_2^{-2} is oxidised to form hydrogen ions and sulphate, which are the dissociation products of sulphuric acid in solution. The soluble Fe^{+2} ions are free to partake in further oxidation reactions, slowly changing from ferrous ions to ferric ions under low pH values.

$$FeS_{2(s)} + 3.5\ O_2 + H_2O \rightarrow Fe^{+2} + 2\ SO_4^{-2} + 2H^+$$

2) The highly soluble Fe^{2+} species oxidise to relatively insoluble ferric iron (Fe^{3+}) in the presence of oxygen. The reaction is slow but is increased by microbial activity at an optimal pH level between 3.5 – 4.5.

$$Fe^{+2} + 0.25\ O_2 + H^+ \rightarrow Fe^{+3} + 0.5\ H_2O$$

3) This reaction further generates more acid, via the dissolution of pyrite by ferric ion (Fe^{+3}) in conjunction with the oxidation of the ferrous ion. This constitutes the dissolution cycle of pyrite. Furthermore, the ferric ion precipitates as hydrated iron oxides which are presented in the following reaction:

$$FeS_{2(s)} + 14\ Fe^{+3} \rightarrow 15\ Fe^{+2} + 2\ SO_4^{-2} + 16\ H^+$$

4) Fe^{+3} is then hydrolysed by water (at pH > 3) to form the insoluble precipitate ferrihydrite Fe $(OH)_{3(s)}$, which is identifiable as the deposit of amorphous, yellow, orange or red deposits on stream bottom (known as yellow-boy).

$$Fe^{+3} + 3H_2O \rightarrow FeOH_{3(s)} + 3H^+$$

To gain a more site-specific perspective of localised mine spoil AMD, reference is made to Hodgson and Krantz's (1998) study on the impacts of groundwater quality from coal mining activities in the Witbank Coalfields. Their study indicates that the sulphate concentrations remain relatively high in spoil water, especially in stagnated areas in the pit ranging from 2000 to 3000 mg/l, however, sulphate levels are lower in waters that receive the constant recharge. The maximum threshold of sulphate present depends on the concentrations of neutralising calcium ions (lower calcium level produces higher sulphate concentrations and vice versa). Understanding the amount of sulphate present gives an indication of the pH values which are generally below a pH of 2.3. The physicochemical compositions of AMD generated within a Witbank mine in Mpumalanga are illustrated in Table 7 below.

Table 7: The physicochemical composition of AMD from a Witbank mine in Mpumalanga (Reynolds and Petrik, 2001)

Chemical element	Concentration (mg/l)
Sulphate	3654
Aluminium	33.5
Boron	0.06
Barium	0.01
Beryllium	<0.005

Cadmium	0.04
Cobalt	0.54
Chromium	<0.005
Copper	0.05
Iron	122
Manganese	43
Nickel	0.68
Lead	0.03
Strontium	0.71
Zinc	2.8
Parameter	**Value**
pH	2.88
Conductivity (mS/cm)	4.7

2.3.4 Opencast mining process

Opencast coal mining (Figure 9) is the most economical mining method, provided that the targeted coal seams lay at depths that are relatively near to the surface (less than 70 m) (Ratshomo and Nembahe, 2013). This method has the potential to recover over 90% of in-situ coal and is lower in labour costs as it makes use of large scale mining equipment (World Energy Outlook 2011). Approximately half of the coal produced from Mpumalanga is extracted through this method (World Energy Outlook, 2011; Ratshomo and Nembahe, 2013), proving it to be a successful and commonly used technique.

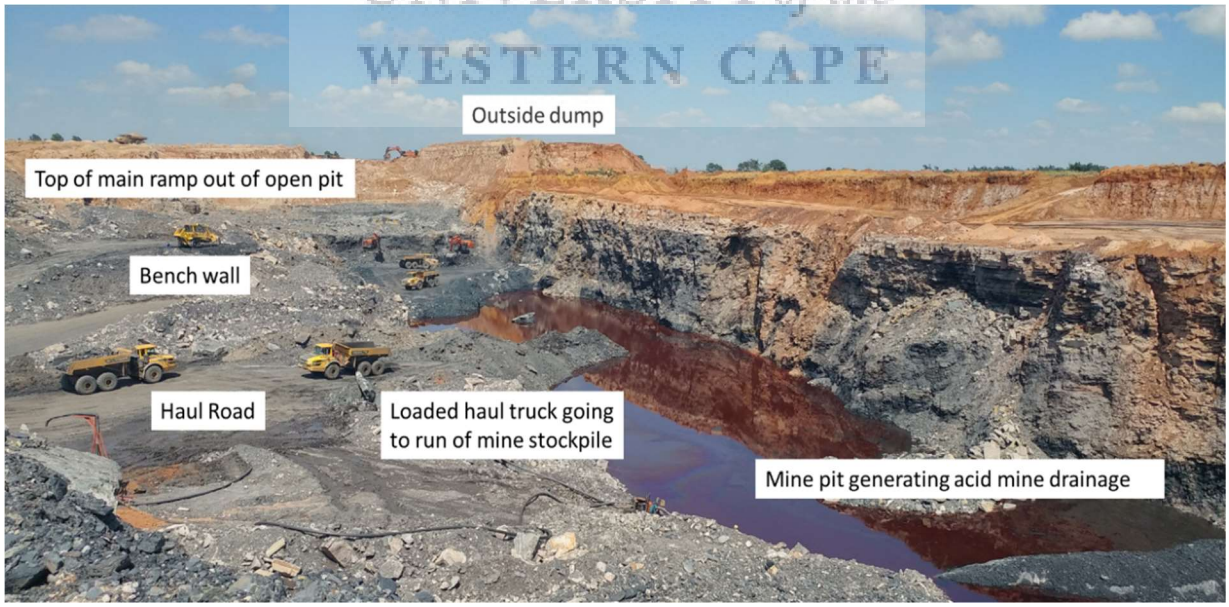

Figure 9: Opencast coal mine in Mpumalanga

The procedure in which opencast mining follows is presented in four distinct mining stages, namely: pre-mining, operational, decommissioning and closure as well as post – closure. These stages are illustrated and denoted from Figures 10 to 12 as follows:

1. Pre-mining stage:

   This stage serves as a baseline, which refers to the condition existing before mining commences against which subsequent changes can be referenced (Figure 10). It is a common occurrence that opencast mines in Mpumalanga are re-mined over the years due to technological advances in coal extraction making it a profitable activity. Therefore, abandoned opencast coal mines may serve as a baseline condition before re-mining begins.

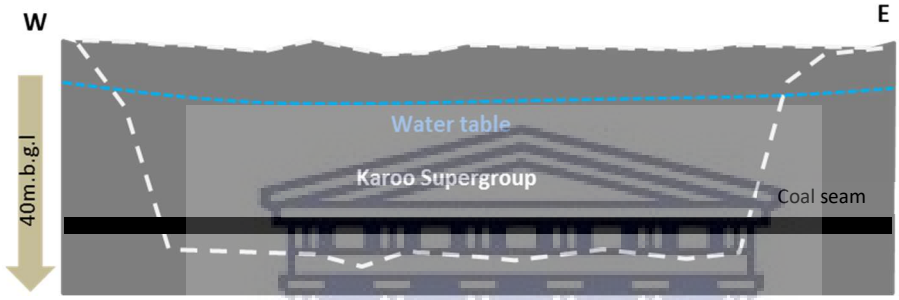

Figure 10: Pre-mining conditions

2. Operational stage:

   This stage involves actively mining out the land (Figure 11). Initially, the mining area is pre-stripped and levelled. Holes are drilled at suitable locations to place and ignite explosives. The explosives break up the rock, exposing a suitable mining workface. The blasting consequently occurs in an orderly fashion, rearranging the mine into stepped benched walls and berms (Figure 11) (Shangoni Aquiscience, 2013). The walls of the pit are dug at lower angles than 90º to avert the risk of rock falls, whilst the berms allow vehicles to manoeuvre around the open pit. The blasted overburden material is then removed and set aside. The targeted coal seam is then removed and transported for use, whereas the piled-up overburden material is backfilled into former voids as successive mining continues.

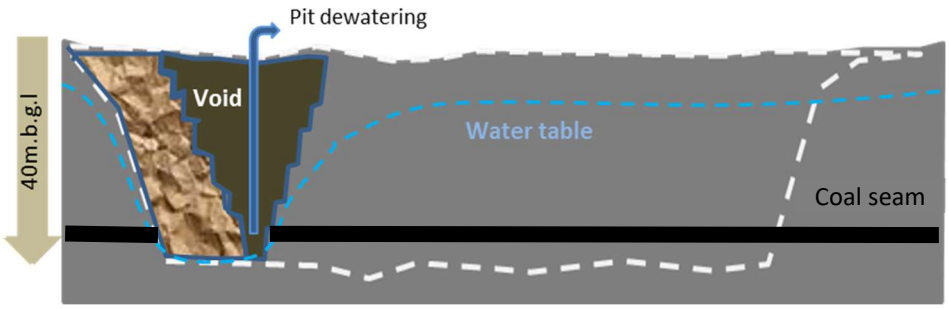

Figure 11: Operational mining stage

3. Decommissioning and closure:

   This stage consists of the closure and decommissioning of the mine (Figure 12), which involves the remediation and reclamation of the site to return the land and watercourses to an acceptable standard. In the process of mining and extracting the coal, a void space often remains in the pit. This void space needs to be filled to ensure that the landform is stable, and that the hydrogeological regime is returned to normal. This process is known as mine remediation, which is typically achieved by removing hazardous materials, reshaping the land, restoring the topsoil, constructing proper drainage control, controlling fugitive dust dispersion and replanting native vegetation (Grobbelaar et al., 2004).

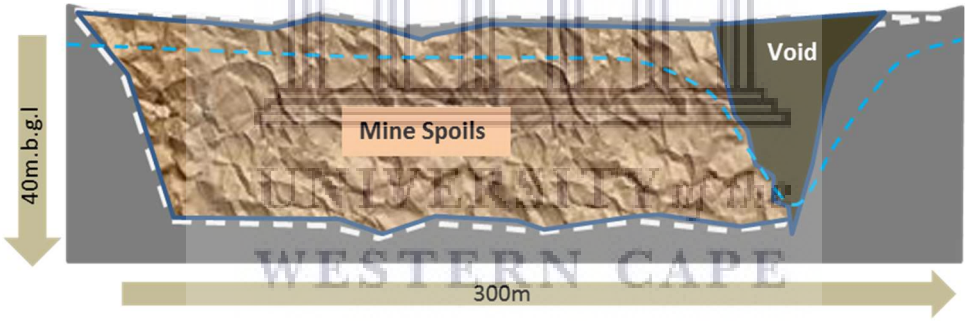

Figure 12: Mine decommissioning and closure stage

4. Post-closure stage:

   This stage involves setting up monitoring programmes which assess the effectiveness of the reclamations and identify any further actions that need implementation. In addition, mines require maintenance after closure to ensure the ongoing treatments of mine discharge water, maintenance of tailings structures and upkeep of vegetation.

2.3.5 Environmental Impacts of mine spoil backfilling

Acid mine drainage has been considered one of the main pollutants from mining activities (Metesh et al., 1998). AMD generation occurs naturally, however mining activities accelerate this by exposing a large amount of rock to weathering in an extremely short geological period (McCarthy, 2011). The pyrite minerals found in mine spoils are exposed to atmospheric

conditions, which cause for oxidation-reduction reactions to occur (refer to section 2.3.3), consequently generating acid mine drainage (Figure 13)(Brick, 1998; Simate and Ndlovu, 2014). The formation of AMD and contaminants associated with it (such as sulphur), are labelled as the largest environmental problem within the mining industry as it has the potential to adversely impact groundwater and surface water quality due to its low pH, high acidity and elevated concentrations of sulphate and metals (Lapakko, 1993; Ferguson and Erickson, 1988; Kuyucak, 2012). Oftentimes, AMD is not evident in groundwater during the operational phase of a mine, because water tables are kept artificially low due to pumping and mine dewatering. However, once the mine is closed and the pumps are turned off, the water table rebound naturally that causes for the migration of AMD, which may continue for many years after the mine is closed (Johnson and Hallberg, 2005).

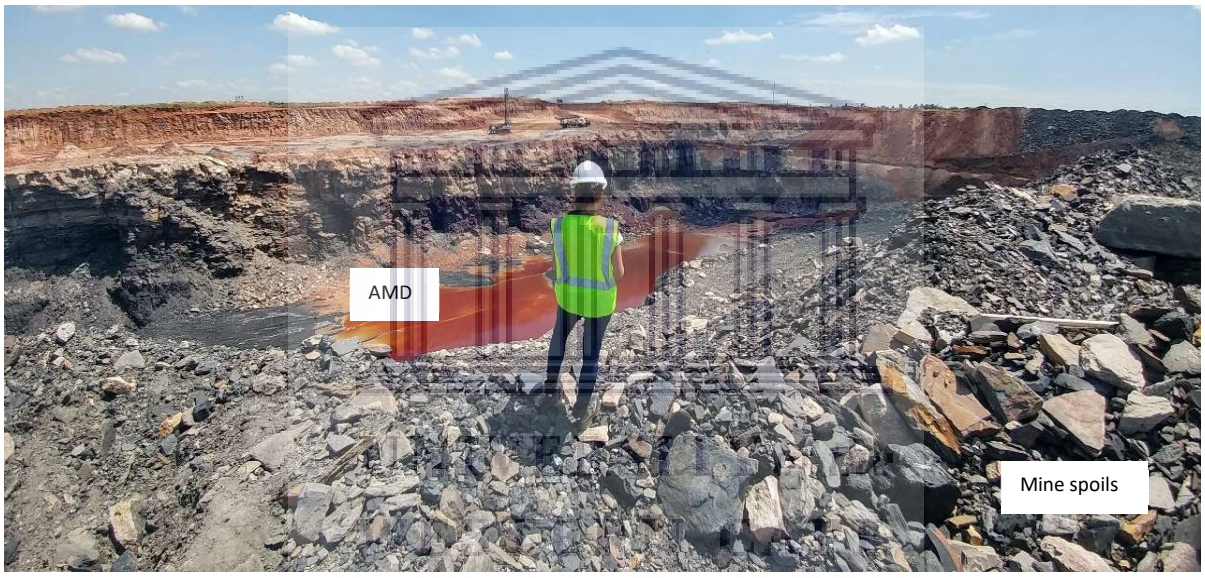

Figure 13: Opencast coal mine with AMD and mine spoils

AMD is highly acidic and saline, which enhances the metal solubility within mine spoils (Zelenková et al., 2009). This results in negative impacts such as the acidification and salinization of aquifers and streams (Zelenková et al., 2009). In other words, the general effect is to render water contaminated to varying degrees depending on local conditions (McCarthy, 2011). Localised conditions, such as the type of water in which the spoils are exposed to may determine the chemical composition of leachate release. AMD may be neutralised by suspensions and reactions with alkaline sediments and various chemical and biological reactions (McCarthy, 2011). In contrast, site-specific geology may catalyse the leaching of heavy and trace metals, particularly feldspars and clay minerals from mine spoils (Zelenkova et al., 2009). Certain constituents such as sulphate, have relatively high solubility's that remain

in the water (McCarthy, 2011), leading to elevated sulphur and salinity concentrations, which will continue to persist until mine spoils are fully oxidised (McCarthy, 2011).

2.4 Treatment of acid mine drainage with coal ash

Acid mine drainage (AMD) and coal ash are both by-products of the increasing demand for power. The mining of coal produces AMD while the burning of coal from thermal power generation produces coal ash. Although these two by-products may cause negative environmental implications, numerous studies show that the combination of them may reduce their negative effect on the natural environment.

Backfilling opencast coal mines with coal ash is the most viable environmental approach as it maximises the utilization of disposed ash (Roy et al. 2017), saving land requirements for ash dumping as well as providing the benefit of reclaiming abandoned coal mines (Roy et al., 2017). Coal ash may serve as a substitute material for sand in backfilling mine voids based on its physical and chemical properties (Siddique 2010).

Physically, coal ash generally obtains a low permeability, which provides structural support and determines the rate at which water will flow within a backfilled mine (Siddique, 2010). In the aims of obtaining low hydraulic conductivities of coal ash, studies have sought out to determine appropriate volumes of coal ash and mine spoils. According to Xenidis et al., (2002), adding ash additives between 10 – 63% to mine spoils, lowers the hydraulic conductivity of the sample by 3 - 500 times, with the optimum reduction in hydraulic conductivity being sought from a 20 – 30% coal ash addition. Concluding that the greater the percentage of coal ash added, the lower the hydraulic conductivity will be. This reduction in hydraulic conductivity is expected to continue as it undergoes geochemical processes and incurs pozzolanic action (Nhan et al., 1996; Kostas et al., 2000), until a presumable steady-state equilibrium is reached (October 2011). This decrease in hydraulic conductivity provides the benefit of reducing the amount of air ingress that enters the ash and the mine pit at large (Hodgson and Krantz, 1998). Besides the permeability of coal ash, it is physically deemed as suitable backfill material based on its content, shear strength, compressibility, moisture content and potential for swell characteristics (Wolfe et al., 2001; Hardin and Daniels, 2011).

Chemically, coal ash is known to be alkaline in nature, which may be used as a reactive barrier, allowing for mine water to pass through it, either neutralising or adsorbing the contaminants in the water (Benner et al., 1997; Metesh et al., 1998). Backfilling with coal ash can be beneficially employed to counter-act the acid generating potential of the mine wastes. Over the

past two decades, numerous studies have focussed on the neutralisation potential of AMD with coal ash. Outcomes indicate that AMD and CCRs, neutralize each other from an initial pH ranging between 2 - 4 to a pH equal or greater than 7 (Xenidis et al., 2002; Gitari et al., 2005; Vadapalli et al., 2007; Prasad and Mondal, 2008; Ram and Masto, 2010; Yang et al., 2011; Alexopoulos et al., 2013; Qureshi et al., 2016). This neutralisation process occurs in two distinct stages; the first stage obtains a rapid increase in pH over a short period of time, whereas the second stage obtains a steady prolonged increase in pH (Petrik et al., 2003; Gitari et al., 2008). The initial rapid increase in pH is attributed to the free calcium oxide (CaO) and magnesium oxide (MgO) within CCRs (Nhan et al. 1996). The second steady increase in pH is attributed to secondary mineralization when AMD and CCRs are in contact, enhancing the formation of gypsum, ettringite, calcite and alumina-silicate minerals (Gitari et al., 2005; Yeheyis et al., 2009).

The main mechanisms which control this neutralisation process, are adsorption, precipitation and co-precipitation (Vadapalli et al. 2007). Furthermore, it has been proven that both types of fly ash, namely calcareous (high CaO content) and siliceous fly ash (High Si content), are effective at absorbing heavy metals from AMD (Qureshi et al. 2016; Alexopoulos et al. 2013). However, the calcareous fly ash achieves neutralisation within a shorter period (Alexopoulos et al. 2013). As different types of coal ash are proven to neutralise AMD, several studies have sought to determine what the effective and optimal CCR: AMD (solid: liquid) ratio is. Observations conclude that any CCR: AMD ratio which is lower than 1: 10 does not have any considerable effect on the pH, whereas ratios greater or equal to 1: 3.5 significantly increases pH, enhancing AMD neutralisation (Petrik et al. 2003). Implying that increasing the amounts of CCRs added to AMD, increases the pH (Yang et al. 2011; Petrik et al. 2003). Optimal heavy metal attenuation occurs at a pH ≥ 10 (Petrik et al., 2003). Based on this literature, it is evident that the physical and chemical properties of coal ash provide numerous backfilling benefits, which include: providing structural support, hydraulic control, adsorption and neutralisation.

Once AMD is produced, it is difficult to control the rate of production and migration into the environment (Kuyucak 2012). Therefore, it is favourable to rather proactively prevent AMD generation. Methods to prevent AMD formation are often targeted at eliminating one of the following variables: water, oxygen, bacteria or sulphides (Brick, 1998). Although it is possible to remove bacteria, it is often a short-lived solution, because bacteria are extremely resilient and will rapidly return (Brick, 1998). In addition to that, limiting bacterial growth is a costly process, thus control and preventative measures are often aimed at reducing the flux of air or

water through sulphide bearing materials (Johnson and Hallberg, 2005; Kuyucak, 2012; Aubertin et al., 2016). Numerous AMD preventative methods exist, which include: water migration, exclusion of oxygen, pH control, sulphide removal and isolation (Kuyucak 2012). Of these methods, the most efficient and practical technique is to use a water retention layer that always maintains a high degree of saturation (Aubertin et al., 2002). This technique efficiently limits oxygen influx caused by advection and diffusion (Aubertin et al., 2002).

A water retention layer may be achieved by using covers (dry or wet), that play a role in isolating or encapsulating sulphide bearing mine spoils, which could limit the access of either oxygen, water or both (Kuyucak, 2012). Dry covers primarily exclude oxygen, which effectively prevents sulphide oxidation. The effectiveness of a dry 'soil' cover is dependent on attaining low hydraulic conductivities and high moisture layer/s (Campbell and Price, 1993; MEND, 1994). Although dry covers are a successful preventative technique, the placement of water (wet) covers is more favourable due to its enhanced ability to prevent the oxidation of wastes (Kuyucak, 2012). This is due to the fact that oxygen has a low solubility and diffusion rate through water, which equates to approximately four orders of magnitude less solubility than air (Kuyucak, 2012). Consequently, reducing the oxidation of mine spoils creating an effective long-term AMD control method.

The same concepts, which limit oxygen ingress, may be applied using the technique of water flooding. This technique involves placing reactive mine spoils underwater to prevent oxidation, which may be achieved by submerging mine spoils (Ouangrawa et al., 2010). A useful construction procedure is to use an elevated water table to prevent mine spoils oxidation. This consists of raising the phreatic surface to a depth less than the height of the saturated capillary fringe in mine spoils, i.e. hydraulic head < air entry value (Aubertin et al., 1999; Ouangrawa et al., 2010). Various studies have proven this technique successful as it greatly reduces sulphide oxidation, infiltration, dissolved oxygen and acid concentrations (Ziemkiewicz and Skousen, 1996; Li et al., 1997; Johnson and Hallberg, 2005; Ouangrawa et al., 2010).

Water table elevation can be achieved by modifying the water balance on site by either increasing the water retention of mine spoils or decreasing lateral flow (Ouangrawa et al., 2010). Its construction comes in various forms, which include: the backfilling of mine pits and allowing the pits to flood naturally and the placement of mine spoils in man-made impoundments or in flooded pits (Donald et al., 1997). A practical impoundment option is to increase the water table of disposed reactive wastes in opencast mining pits (Ouangrawa et al., 2010). Opencast mining pits are recognised as well-accepted depositional environments, as

they are geotechnically and geochemically stable (Donald et al., 1997). Moreover, it is an aesthetic focal point for rehabilitation plans, potentially providing habitats for plants and biota (Donald et al., 1997).

Flooded in-pit mine disposal facilities are based on the concepts of being a ‘porous envelope’, ‘hydraulic cage’ or ‘pervious surround’, designed to limit regional groundwater contamination (Donald et al., 1997). Effective groundwater protection is only achieved if appropriate construction is employed. Factors to consider for in-pit disposal are: the depth to water table, volumetric water content, water pressures, geochemical analysis of the overburden, site hydrology after mining, method of overburden placement, acid-base accounting, diversion flows away from mine spoils (Meek, 1996; Aubertin et al., 1999; Aubertin et al., 2002; Kuyucak, 2012; Aubertin, 2013; Aubertin et al., 2016). This approach has been reported to significantly improve water quality whilst creating a good pH buffer (Donald et al., 1997).

2.5 Groundwater Model Selection

A model is described as 'a simplified representation of a complex system' or 'an approximation of a field situation' (Anderson and Woessner, 1992). A groundwater model provides a quantitative framework for synthesising field information and for conceptualizing hydrogeological processes. The selection of a model should be chosen according to its objective, applicability to the conceptual model and availability of input data (OhioEPA, 2007). Kresic (2007) identified three general purposes of groundwater models, which are to:

- *Predict or forecast*: In this purpose, the expected or artificial changes to the system (aquifer) are studied from a proposed action. This is the most common type of modelling effort, which predicts consequences.
- *Describe* the system: This purpose involves the analysis of various assumptions about the nature and dynamics of the systems. Descriptive models help to gain insight into the controlling parameters in a site-specific setting to better understand the system dynamics.
- Generate a *hypothetical system:* This purpose is to study the fundamental principles of groundwater flow. This is helpful in forming regional regulatory guidelines, as this type of model can be used as a screening tool to identify regions suited for a proposed activity (Anderson and Woessner, 2002).

The reviewed literature highlights the gap in knowledge in understanding the flow and transport processes of coal ash backfilling. Constructing a theoretical model is deemed suitable to address these gaps as it is used as a tool to forecast relative flow and transport behaviour in the system. Theoretical models are developed to a hypothetical system; therefore, no field data is required for calibration.

The applicability of constructing generic flow and transport models is based on selecting a suitable groundwater model. Thus, the rest of this chapter describes the different types of numerical models which exist, narrowing it down to the type of model which was chosen in this study. The methodology followed in making this selection is presented in a hierarchy decision tree below (Figure 14). This hierarchy decision tree was specifically constructed for this study, to provide clarity on the methodology undertaken as well as displaying the following descriptive subchapters that follow.

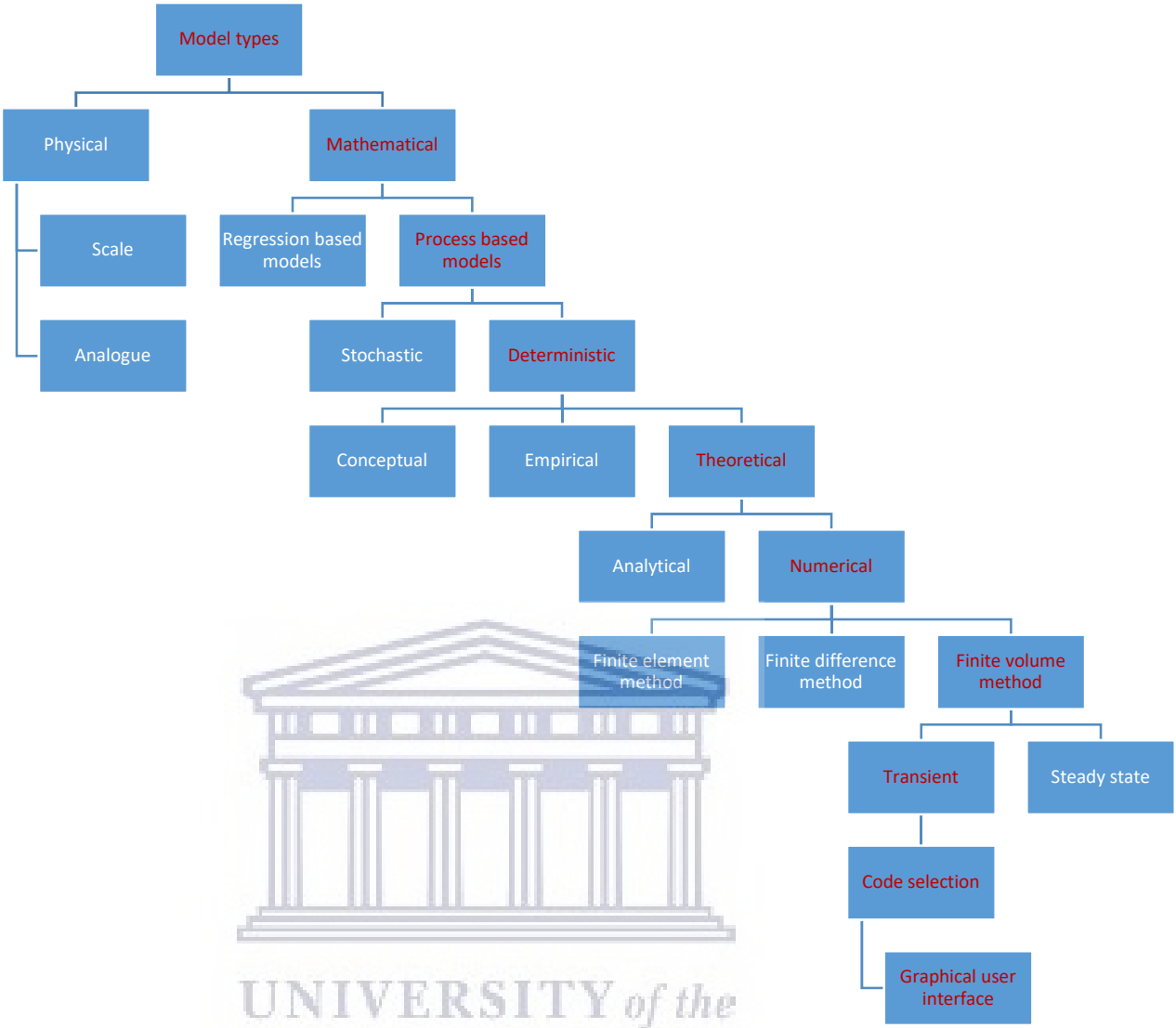

Figure 14: A hierarchy model decision tree indicating the model selection process

Model types

There are two main types of models, namely physical and mathematical models. Physical models are actual physical natural replicas scaled down to a laboratory size that may represent a single or group of entities (Essink, 2000; Kresic, 2007), whereas mathematical models use partial differential equations to describe hydrogeological processes. Mathematical models were chosen for this study as they require and produce quantitative results, enabling an easier and objective comparison of backfilling scenarios.

Mathematical models

Mathematical models can be categorized into regression-based models or process-based models depending on their equations (Clarke et al., 2002). Regression-based models recognise that hydrological events depend on chance, whereas process-based models describe the

hydrological phenomena based on the perceived processes in operation (Clarke et al., 2002). Process-based models are based on a theoretical understanding of relevant hydrogeological processes, provide a useful framework to incorporate specific responses to altered environmental conditions (Clarke et al., 2002) and thus deemed suitable for this thesis.

Process-based models

Process-based models can be either stochastic or deterministic. Stochastic models assume random variability in the simulated output data and assume that variables have distributions in probabilities (Barnett et al., 2012). Whereas, deterministic models do not assume random variability in the simulated output, because it is generated from numerous defining input parameters. In other words, deterministic models assume that future processes are determined by parameter values and initial conditions, free from random variability and law of probability. This is favourable as it defines cause-and-effect relations, giving the model credibility to the changes in flow and transport properties in this study.

Deterministic Models

Deterministic models are categorised into: empirical, conceptual and physical models (Table 8)(Kresic, 2007).

Empirical models are object orientated models which use information based on observation and experiment, without considering the features and processes of the hydrological system (Essink, 2000; Devia et al., 2015). Hence, these type of models are often called data-driven models, as it involves mathematical equations derived from data series and not from the physical processes of the system itself (Devia et al., 2015). Empirical models are often considered as 'lumped' models, meaning they neglect the spatial distribution of input variables and regard the catchment as a homogenous whole unit (Kapangwiri, 2009; Pathak et al., 2018;). These models are often used for inaccessible areas or where little or no data is available for calibration (Essink, 2000).

Conceptual models are used to improve our understanding of the real world and make predictions based on this. Generally, these types of models describe all the component hydrological processes within a system, in an attempt to add physical relevance to variables which are used in mathematical equations (Devia et al., 2015). Consideration is often given towards the physical processes which act upon input variables to produce output variables (Devia et al., 2015).

Theoretical models mathematically idealize the real world using variables which are a function of both space and time (Devia et al., 2015). These models describe hydrological processes by solving partial differential equations incorporating the laws of conservation of mass, momentum and energy (Essink 2000; Kapangaziwiri 2009). Theoretical models are often regarded as 'distributed' models meaning that their inputs are divided into elementary unit areas accounting for spatial and temporal variability (Essink, 2000). As theoretical models strongly depict the natural characteristics based on spatiotemporal input parameters, they are advantageous for this study.

Table 8: Summary of the differences between the three types of deterministic models (Data sourced from Essink 2000; Devia et al., 2015)

Empirical Model	Conceptual Model	Theoretical based model
Involves mathematical equations. Derives values from observation and experiment.	Includes semi-empirical equations with a physical basis.	Based on spatial distributions. Evaluation of parameters describing physical characteristics.
Little consideration of features. No consideration of physical laws.	Parameters are derived from field data and calibration.	Requires data about the initial state of model and morphology of catchment. Considers physical laws.
Lumped model	**Semi-distributed**	**Distributed**
Can be generated on other catchments	Requires hydrological and meteorological data	Can be generated on other catchments, may encounter scale related problems

Theoretical Models

Theoretical models are well suited for this study because they consider physical laws. The fundamental relationship between flow and solute transport models are based on the 'law of conservation of mass', meaning that the change in storage of water or solute mass within a volume is equivalent to the difference between mass in and mass out (Barnett et al. 2012). This principle is expressed in the form of partial differential equations that govern water flow and solute transport, which can be solved analytically or numerically (Kresic, 2007).

Analytical models use partial differential equations and numerous assumptions to obtain an exact simplified solution. A characteristic of analytical models is to solve only one equation at a time, which results in a solution specific to a point or line of points. Analytical solutions are fast at problem-solving if the system is homogenous, isotropic and has an infinite extension (Essink 2000). However, analytical solutions are limiting to natural scenarios due to probable

heterogeneity and spatial boundaries. Conversely, numerical models are better at site representation, as they use partial differential equations to account for spatial and temporal variabilities. Numerical models subdivide space and time into discrete intervals called 'cells' or 'elements', whereby each cell solves a basic groundwater flow equation considering its water balance (OhioEPA, 2007; Barnett et al., 2012b). These points may be placed in the centre of the cell or between adjacent cells. The basic differential equation is substituted with an algebraic expression, which is solved numerically. The solutions to the head and solute concentrations are calculated at specified points, making it more representative of the hydrogeological system as it accounts for heterogeneity and temporal changes (Freeze and Witherspoon, 1967), which is preferred for this study.

Numerical methods

Three main numerical methods should be considered when constructing a model: the Finite Difference Method (FDM), Finite Element Model (FEM) and Control Volume Finite Difference (CVFD) (Table 9) (Kumar, 2019). The FDM is the most used, as they are easy to understand and are well documented. The FDM grid is created using structured, rectilinear grids, however, is not as efficient in refining areas around the area of interest. FEM uses a finite element (triangular) mesh to represent the model domain, allowing for efficient refinement around an area of interest and adaptability to variable stratigraphy. This model is well suited for anisotropic and heterogeneous conditions; however, layers need to be continuous and the model does not guarantee mass conservation. CVFD formulation enables a cell to be connected to an arbitrary number of cells, allowing for infinite possibilities in cell geometry (Waterloo Hydrogeologic, 2018). As cells may be discretized in various geometric shapes, the grid can be refined around the area of interest without adding any new cells. CVFD models do not require continuous layers and remain mass conservative (Waterloo Hydrogeologic, 2018). In addition, CVFD models are more versatile and attain all the advantageous functions of FDM and FEM, thus it has been chosen for this study.

Table 9: Summary of the differences between the finite element, finite difference and finite volume models

Finite difference model	Finite element model	Control volume finite difference model
Rectangular grid structure	Triangular grid structure	The rectangular, triangular and Voronoi grid structure
Average at refining area of interest	Good at refining area of interest	Excellent at refining area of interest

Same horizontal discretization in all layers	Same horizontal discretization in all layers	Same or different horizontal discretization in all layers.
Continuous layers	Continuous layers	Continuous layers or discontinuous layers allowed

Temporal discretisation

A model's temporal behaviour may either be a steady state or transient state. The behaviour of a steady-state system is 'fixed with respect to an external of absolute time reference'(Paul et al., 2001), whereas a transient model adapts its behaviour to known execution times, aperiodic input arrival times, and internal state via dynamic scheduling techniques (Paul et al., 2001). Lubczynski and Gurwin (2005) declare that transient flow models are more representative of a real system than steady-state models are in exploring groundwater behaviour, as they incorporate spatiotemporal variations and have a higher degree of freedom. This is suited for this study as it examines the changes in physicochemical properties between coal ash, mine spoils and geology through time.

Numerical models are typically executed using computer-based software. The computation of the numerical models requires computer code that gives the computer instructions to solve partial differential equations for flow and solute transport. When selecting a code, Anderson and Woessner (2002) suggest considering the following factors: 1) Has the accuracy of the code been verified against one or more analytical solutions?; 2) Does the code include water balance computations?; 3) Has the code been used in other fields of studies?; and 4) Does the code have a proven track record?

Code selection

In order to understand the changes in the hydrogeological flow regime, a groundwater flow code is needed. Commonly used groundwater flow codes are tabulated below (Table 10) alongside their respective capabilities.

Table 10: Description of commonly used groundwater flow codes

GW Flow Code	Capabilities
FEFLOW	• Flexible mesh and includes time-varying geometries • Finite element code • Variable saturated flow • License needed
MODFLOW 2005	• Steady and unsteady flow • Flow for irregularly shaped flow system • Confined, unconfined, both • Hydraulic conductivity and transmissivity may be anisotropic

	• Storage coefficient heterogeneous • Open source software
MODFLOW-LGR	• MODFLOW-2005 with local grid refinement
MODFLOW-NWT	• Upstream weighting (UPW) Package based in Layer property flow • (No wetting and rewetting function) • Asymmetric matrix only
MODFLOW-USG	• For unstructured grid • Nested grid and various grid shapes • Sub-discretize layers • Underlying control volume finite difference (CVFD) • Layer property flow • Cell connected to an arbitrary number of cells • Includes the Groundwater Flow (GWF) Process-based in MODFLOW-2005 • Newton-Raphson formulation based on MODFLOW-NWT which improves convergence and rewetting of cells. • Allows for time-variant materials (TVM) • Sparse Matrix Solver (SMS) provides several methods for resolving nonlinearities, symmetric and asymmetric linear solutions. • Public domain
MODFLOW-SURFACT	• Desaturation and resaturation of cells • Accurate delineation and tracking of water table position • Prevent water table build up beyond a specific recharge-ponding elevation • Adaptive time stepping • Model unsaturated water and air • Newton-Raphson formulation increases robustness • License needed

FEFLOW is a finite-element subsurface flow code, which has a long-standing record since its development in 1979 by the Institute for Water Resources Planning and Systems Research Inc. Trefry and Muffels (2007) conducted a review stating that FEFLOW is suitable to handle saturated and unsaturated flow in complex groundwater modelling applications. However, it is not user-friendly in setting up spatial co-ordinates and experiences difficulty when simulating time steps over long periods.

The MODFLOW codes are comparable since its development in 1978 under FORTRAN 77 (American National Standards Institute) (Pathak et al. 2018). It was developed by McDonald and Harbaugh of the US Geology Survey, which used the finite-difference method to describe the movement of groundwater flow. Since its release in 1988, MODFLOW has become the industrial standard worldwide for groundwater modelling due to its flexible modular structure,

complete coverage of hydrogeological processes and public domain free availability (Barlow and Harbaugh, 2006). Examples of MODFLOW applications include recharge estimation (Mahesh, 2004); quantifying river leakage (Sarda, 2006); assessing the effects of effluent discharge on groundwater quality (Rajamanickam and Nagan, 2010); and investigating the effects of stream-aquifer fluctuations on aquifer stream (Chen and Chen, 2003). The US Geology Survey has updated this code several times including MODFLOW-88 (Harbaugh and McDonald, 1988); MODFLOW-96 (Harbaugh and McDonald, 1996); MODFLOW-2000 (Harbaugh et al., 2000) and MODFLOW-2005 (Harbaugh, 2005). The 2005 version of the MODFLOW family is adapted to compute saturated-unsaturated flow processes. MODFLOW-LGR is an adaptation of MODFLOW-2005 which is suited for enhancing local grid refinement, giving detail to smaller areas within a larger model. MODFLOW-NWT is a Newton formulation for MODFLOW-2005 which is intended for solving problems involving drying and rewetting non-linearities of the unconfined groundwater flow equation (Niswonger et al. 2011). This function is of great significance as it allows for successful model convergence during dry and wet cycles. The MODFLOW-NWT formulation is incorporated in the newer versions of MODFLOW called MODFLOW-USG and MODFLOW-SURFACT. This functionality is essential in a mining scenario due to the dewatering of the pit during its operational phase, and water level recovery during the post-closure phase. Additionally, both codes are well suited for spatial and temporal variabilities expressed using Time Variant Materials (TVM) and Adaptive Time Stepping (ATS) functions. Time-variant materials allow for a physical change in storage and hydraulic conductivity per time step, this caters for this study as it accounts for changes in hydraulic conductivity of the CCR backfill. Adaptive time stepping allows for automatic time step adjustments that enables effective model convergence. Whilst both MODFLOW-USG and MODFLOW-SURFACT have extensive functionality suited for this study's objectives, MODFLOW-USG has the advantage of simulating complex geometries using the unstructured control volume finite difference (CVFD) grid and solvers, whereas MODFLOW-SURFACT uses a structured finite difference code. An added advantage to MODFLOW-USG is that it is available in the public domain, whereas MODFLOW-SURFACT requires a license. Thus, MODFLOW-USG is chosen as a suitable flow code for its functionality and support.

The simulation of solute concentrations and plume migrations require solute transport codes. Commonly used groundwater transport codes are tabulated below (Table 11) alongside their respective capabilities.

Table 11: Descriptions of commonly used transport codes

GW Transport Code	Capabilities
FEFLOW	• Variable fluid density mass and heat transport
FEMWATER	• Simulate density-driven coupled flow and contaminant transport in saturated and unsaturated zones.
MF2K-GWT	• 3D groundwater flow and solute transport model with MODFLOW 2000
SEAWAT	• Simulate 3D variable-density groundwater flow with multi-species solute and heat transport • Viscosity variations from the viscosity (VSC) package.
MT3D	• Modular three-dimensional transport model • Transport model for the simulation of advection, dispersion, and chemical reactions of contaminants in groundwater systems.
MT3D-USG	• An updated version of MT3DMS. • Unsaturated-zone transport • Transport within streams and lakes, including a solute exchange with groundwater • Route solute through dry cells that may occur in the Newton-Rhapson formulation (MODFLOW-NWT) • Has a chemical reaction package that has the ability to simulate interspecies reactions and parent-daughter chain reactions
MODFLOW-SURFACT	• Includes solute transport, multiphase transport and NAPL dissolution and volatilization • Includes vapour flow

The numerical code FEMWATER was developed in the early 1990's with an interest in adopting a three-dimensional (3D) variably saturated model for wellhead protection using irregular geometries (Lin et al. 1997). This code also allows for variable fluid density mass and heat transport, effectively modelling saline intrusions and allowing for multi-species reactive transport simulations (Insigne & Kim 2010). FEFLOW is a similar code to FEMWATER as it simulates variable fluid density mass and heat transport, additionally allowing for multi-species reactive transport simulations (Trefry & Muffels 2007). The MF2K-GWT code is an enhanced version of MODFLOW-2000 that incorporates the additional capability to simulate solute-transport processes and compute changes in concentration (Langevin et al., 2010). SEAWAT is a coupled version between MODFLOW-2000 and MT3DMS, that is designed to simulate variable-density and variable viscosity solute transport (Langevin et al., 2010). MT3DMS (Zheng and Wang, 1999) does not allow for variable viscosity and density flow but is the leading code for analysing contaminant migration in groundwater. It is the newer version of

MT3D developed in the 1990's and is designed to work directly with the flow code MODFLOW-88 and MODFLOW-96 (SSG, 2005). MODFLOW-USG is a newer code, which incorporates the transport code of the widely used MT3DMS. Additionally, it computes solute transport for unstructured grid cells and solves solutes through dry cells. MODFLOW-SURFACT is just as capable and is commonly used by the mining industry. It allows for multiphase solute transport, vapour flow and NAPL dissolution and volatilization. These are advanced multiphase functions in MODFLOW-SURFACT and are not necessary for this study as it will only be assessing solute concentrations in the liquid phase. The aforementioned codes simulate physical solute transport from advection, dispersion and diffusion reactive processes, which are based on the law of conservation of mass (Freeze and Cherry, 1979).

Of all the discussed numerical flow and transport codes, MODFLOW-USG, MODFLOW-SURFACT and MT3DMS are deemed suitable for this study. These codes agree with Anderson and Woessners' (2002) consideration guidelines as the MODFLOW suite is the most widely used set of groundwater codes in the world and is the standard for litigation purposes in the United States (USGS, 2018). All the chosen codes have been verified by analytical solutions and include water balance computations allowing for field-based water budget comparisons. These codes have also been extensively used in diversified fields such as mining, water resource management and groundwater-surface water interactions as tabulated in Table 12 below.

Table 12: Groundwater modelling codes reference studies

Field	Article
Water Resource Management	• Feinstein et al., 2016 – *A Semi-structure MODFLOW-USG model to Evaluate Local Water Sources to Wells for Decision Support* • Lux et al. 2016 – *Evaluation and optimization of multi-lateral wells using MODFLOW unstructured grids [MODFLOW-USG]* • *Larry M, et al., 2010 – Comprehensive Optimal Management of Integrated Aquifer and Surface Water Resource Systems [MODFLOW-SURFACT]* • Woods and Cook, 2015 - *Modelling salt dynamics on the River Murray floodplain in South Australia: Modelling approaches [MT3D-USG]* • Dommisse 2015 – *Mathematical modelling of solute transport in a heterogeneous aquifer [MT3D-USG]*
Mine water management	• Krčmář and Sracek, 2014 – *MODFLOW-USG: the New Possibilities in Mine Hydrogeology Modelling (or What is Not Written in the Manuals)* • Doherty, 2001 – *Improved Calculations for Dewatered Cells in MODFLOW [MODFLOW-SURFACT]* • Roemer, 2017 – *In-situ mobilization of arsenic in the subsurface using ferrous chloride [MT3D-USG]*

Groundwater-surface water interactions	• Black, 2017 – *The need for improved representation of groundwater-surface water interaction and recharge in cold temperate- subarctic regions* [MODFLOW-USG] • Panday and Huyakorn, 2008 - *MODFLOW SURFACT: A State-of-the-Art Use of Vadose Zone Flow and Transport Equations and Numerical Techniques for Environmental Evaluations*

Graphical user interface (GUI)

In aims of analysing model output and visually displaying the code, Graphical User Interfaces (GUI's) are used. GUI's are pre- and post-processing packages for the modelling code that facilitate the model design and parameter inputs. The most widely used Windows-based GUI's are (Zhou & Li 2011): Processing Modflow (Chiang and Kinzelbach, 2001), Visual Modflow (Waterloo Hydrogeological, 2018, Groundwater Modelling Systems (GMS) (Brigham Young University, 2000) and Groundwater Vista's (Rumbaugh and Rumbaugh, 2005). The different GUI's with their processing codes are tabulated (Table 13) below.

Table 13: Graphical User Interfaces (GUI's) and codes

Graphical User Interface	Processing codes
Visual MODFLOW	MODFLOW-2000, 2005, NWT, MODFLOW-USG, MODFLOW-LGR, SEAWAT, MT3DMS, RT3D, MODPATH, Zone Budget, PEST v.12.3
Groundwater Modelling Software (GMS)	MODFLOW 2000, MODPATH, MT3DMS/RT3D, MODFLOW-UG, SEAM3D, FEMWATER, PEST, UTEXAS, MODAEM and SEEP2D
Groundwater Vistas (GW Vistas)	MODFLOW, MODFLOW-SURFACT, MODPATH, MT3D, MODFLOW-USG and PEST. Now available with GW3D visualization and Remote Model Launch
Processing Modflow (PMWiN)	MODFLOW, MODPATH, PMPATH, MT3D, RT3D, MOC3D, PEST and UCODE
Model Muse	MODFLOW-2005, MODFLOW-LGR, MODFLOW-LGR2, MODFLOW-NWT, MODFLOW-CFP, MODFLOW-OWHM, MT3DMS, SUTRA, PHAST, MODPATH, ZONEBUDGET and Well Footprint

Groundwater Modelling Software, Groundwater Vistas and Visual Modflow are suitable GUI's for processing the MODFLOW-USG and MT3DMS-USG code. Of these three options, GW Vistas was selected based on its support, familiarity and sophisticated user interface.

3 CONCEPTUAL MODEL DEVELOPMENT

This chapter describes the various components that contribute to developing conceptual models. Conceptual models are realistic representations of the natural system that consider the hydrogeological processes in an attempt to form the basis to which numerical models are designed (Devia et al., 2015). Components used to construct the conceptual model are discussed in the following subsections and are assimilated into six conceptual backfill scenarios.

3.1 Study Site: Witbank Coalfield

The study region is located within the Mpumalanga province, South Africa; which holds the bulk of coal reserves and mines (Figure 15). The majority of the coal from Mpumalanga is sourced from the Witbank and Highveld coalfields, together accounting for approximately 75% of South Africa's production (Ratshomo and Nembahe 2013). Of these two coalfields, the Witbank Coalfield has the longest withstanding mining history, producing the highest quantity of coal in South Africa to date (Hancox and Gotz 2014). In 2001, this coalfield had 71 operational collieries accounting for 155 Mt of Run Of Mine (ROM) production (SACSMM, 2001). Based on its active past, the Witbank Coalfield now hosts a large array of abandoned shallow coal mines. Moreover, it remains economically important as it currently supplies over 50% of South Africa's saleable coal (Hancox and Gotz, 2014) and is a major source of coal to several Eskom Power plants in surrounding areas (e.g. Kendal, Matla, Kriel, Duvha, Arnot, Hendrina and Komati) (Zelenková et al., 2009). The close proximity between coal-fired power plants and opencast coal mines are favourable as CCRs are produced nearby and may be cost-effectively transported to the potential backfilling mine.

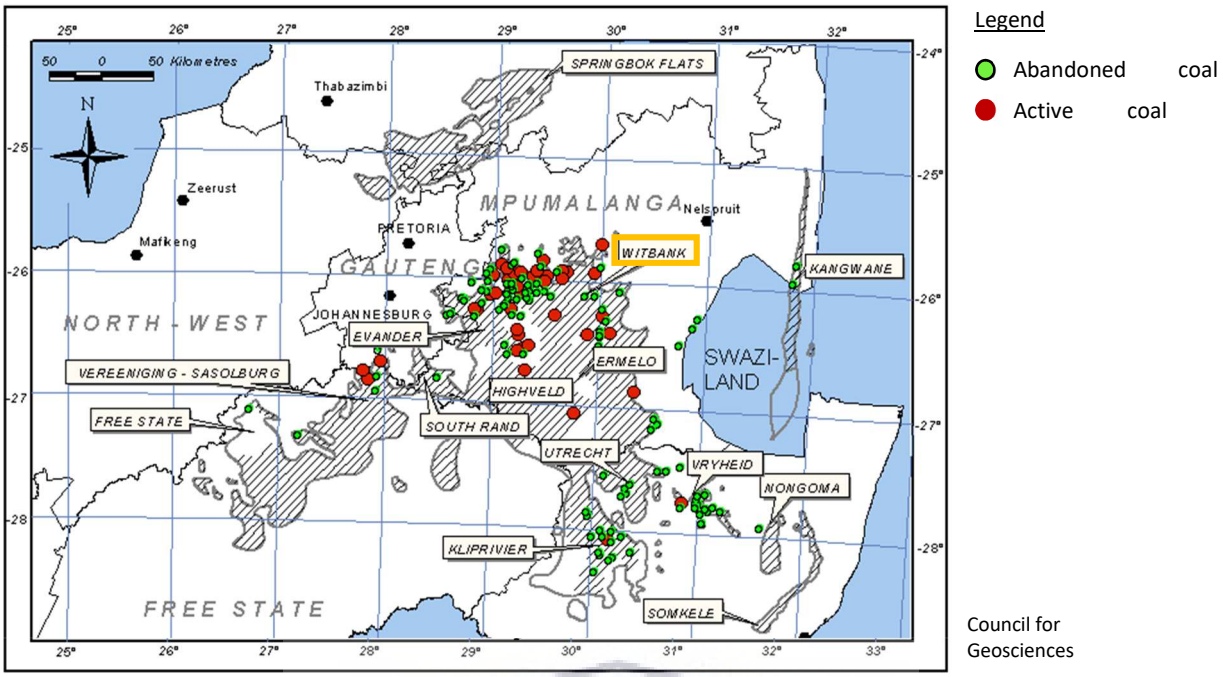

Figure 15: Coalfields of South Africa (Sourced from the Council of Geosciences, 2003)

3.2 Climate

The Witbank Coalfields are located within the Mpumalanga Highveld region which is characterised by hot and rainy summers with cold dry winters (Viljoen, 2015). During the summer months (from September to April), rainfall predominantly occurs in the late afternoon in the form of rain showers and thunderstorms (Viljoen, 2015) with temperatures ranging from 12 - 25ºC (Bethal Monitoring Station; Weather SA, 2017). During the winter months (from June to August) precipitation mainly occurs in the mornings in the form of frost (Viljoen, 2015), reaching lower temperatures between 1 - 18ºC (Weather SA, 2017). Long-term averages of historical climate data are represented in Figure 16 below.

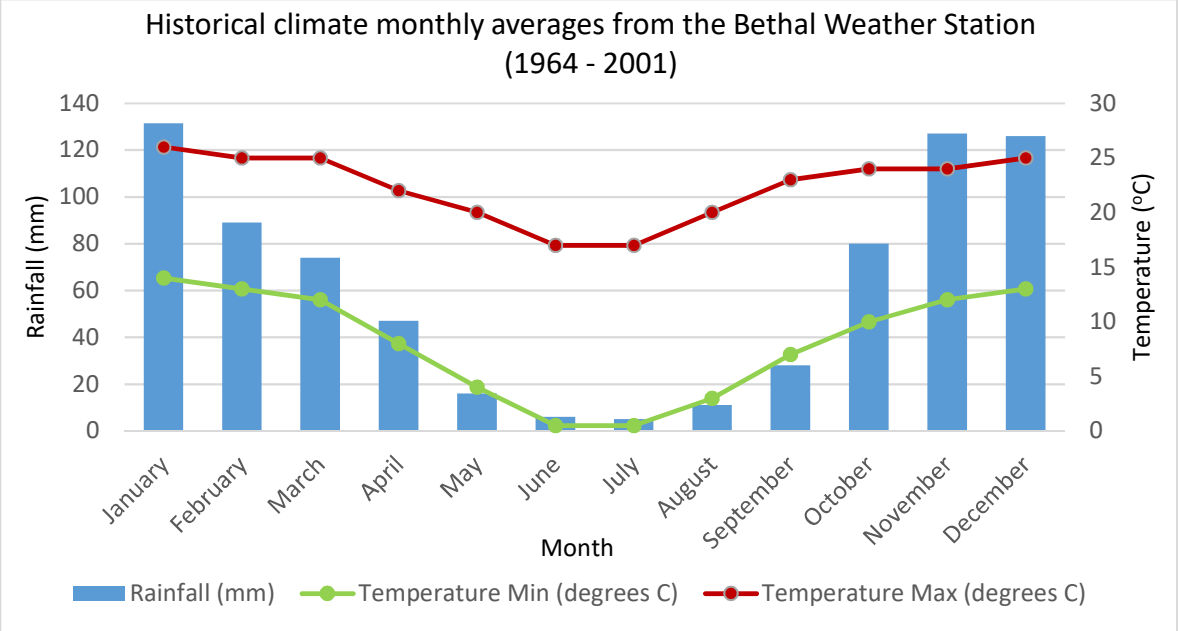

Figure 16: Historical climate data (Data sourced from Climate Information Platform, 2001)

The mean annual precipitation of the study area is 688 mm/annum, whereas the mean annual evaporation is approximately 2.5 times greater than the annual rainfall. As evaporation is greater mean precipitation, it is assumed that a mine void in this region has the potential to become a 'terminal' sink, provided that the rebounded water level is lower than the pre-mining groundwater level (Mpetle and Johnstone, 2018).

3.3 Geology

South African coal occurs within the sedimentary layers of the Karoo Supergroup (McCarthy 2011; Cairncross 2001), that were deposited between 300 – 180 million years ago (Visser, 1986). The sedimentary part of the Karoo Supergroup comprises four main lithostratigraphic units, which from the base up are: the Dwyka, Ecca, Beaufort and Stormberg Groups (Table 14) (Johnson et al., 1996). Although these groups cover approximately 60% of the country (McCarthy 2011; Cairncross 2001), only the Ecca Group that is found in the provinces of Mpumalanga, Free-state and Kwa-Zulu Natal attain suitable conditions for coal formation (Ratshomo & Nembahe 2013). The Ecca Group comprises sediments deposited in shallow marine and fluvial-deltaic environments where coal was accumulated as peat in marshes and swamps that were laid down by large river deltas of the Karoo Sea (Dutoit, 1954). The Ecca Group is subdivided into three formations, namely the Pietermaritzburg, Volksrust and Vryheid formations (Table 20)(SACS, 1980). The Pietermaritzburg Formation consists almost entirely of siltstone and mudstone (Du Toit, 1954), whereas the Volksrust and Vryheid formations

contain coal. The Volksrust Formation consists of siltstone, mudstone, intercalated shale and bright coal (Cadle et al., 1990), whereas Vryheid Formation consists of interbedded sandstones, carbonaceous shale layers, siltstones and thick coal seams (Cairncross and Cadle, 1987). The majority of economically extracted coal in South Africa lies within the Vryheid Formation where it is the thickest in the south and where the basin is the deepest (Whateley, 1980a; Stavrakis, 1989; Cadle et al., 1990). Dolerite dykes and sills commonly intrude this formation and are often responsible for the devolatilization of the coal adjacent to the dolerite intrusions (Viljoen, 2015).

Table 14: Stratigraphy of the Karoo Basin (data sourced from Cadle et al., 1990; Hancox and Gotz, 2014)

Supergroup	Group	Formation
Karoo Supergroup	Stormberg	
	Beaufort	
	Ecca Group	Pietermaritzburg
		Volksrust*
		Vryheid*
	Dwyka Group	

*Economical coal layers

3.4 Coal Seams

South African coal reserves predominantly (96%) consists of bituminous coal (World Energy Outlook 2011), primarily used for electricity generation (Eskom, 2016). Bituminous coal is classified as lower grade coal due to its low calorific value (Eskom, 2016). Lower grade coal produces less heat, thus large volumes are needed to produce electricity, resulting in higher ash volumes (Jordaan, 1986; Jeffrey, 2005; Eskom, 2016).

The structure of South Africa's coal seam horizons is generally undeformed, thick and close to the surface. Approximately a quarter of this coal is between 15 – 50 m below the surface, with the remaining, between 50 – 200 m below the surface (Eberhard, 2011).

The Witbank Coalfield has five main coal seams, successively numbered from oldest (No. 1) to youngest (No. 5) (Cairncross, 1986). These five coal seams are categorized into three main sequences, named No. 2, No. 4 and No. 5(Cairncross, 1986) (Figure 17). A summary of Witbank's coal seam sequence is presented in Table 15 below.

Table 15: Thickness, grade, purpose of economically viable coal seams (Data sourced from Jeffrey, 2005; Hancox and Gotz, 2014)

Coal Seam (No.)	Thickness (m)	Grade	Purpose	Economic Importance
5	0 - 2	Low	Blending coke Cooking coal Chemical feedstock	Low
4	2.5 – 6	Low	Feedstock for Power stations	Medium
2	4.5 – 20	High	Metallurgical coal Export steam coal	High

Coal seam sequence No. 5 is the uppermost coal seam (youngest) with a thickness ranging from 0.5 - 2m (Hancox and Gotz, 2014) (Figure 17). This seam is extensively eroded being bright in colour. Often used as a blending coke, lower quality coking coal and chemical feedstock.

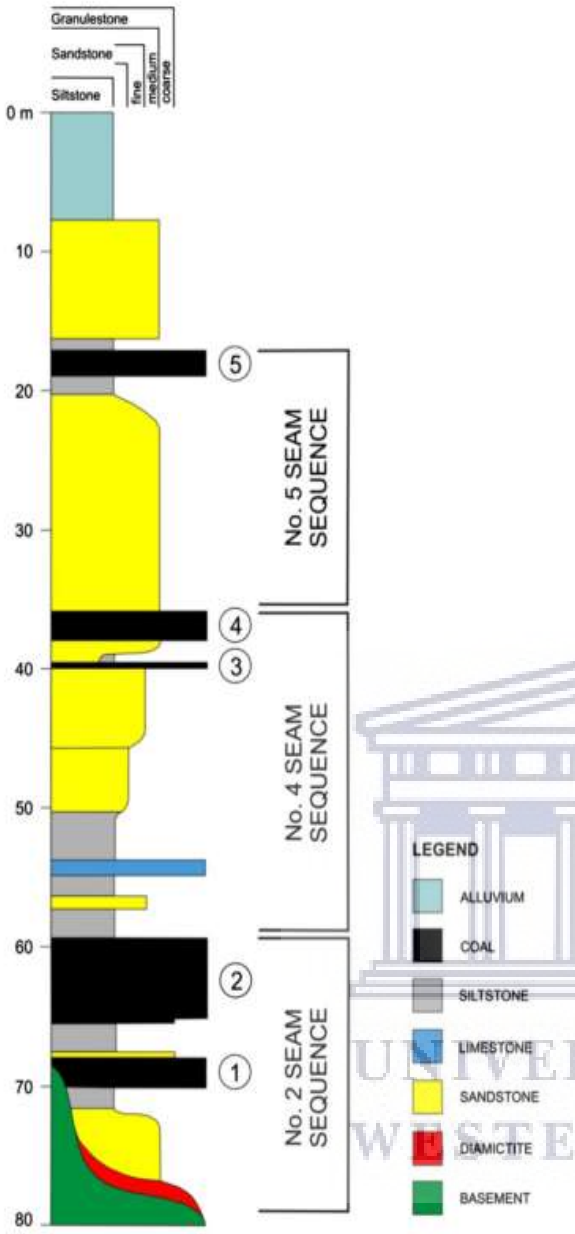

Coal seam sequence No. 4 is the second uppermost coal seam, which ranges in thickness between 2.5 – 6.5m thick (Hancox and Gotz, 2014; Jones and Wagener, 2016). This coal seam is commonly categorized into No. 4 upper and No. 4 lower seams, separated by sandstone and or siltstone partings (Hancox & Gotz 2014). This coal seam is primarily used as feedstock for power stations.

Coal seam sequence No. 2 is the lower (oldest) coal seam which ranges in thickness between 4.5 - 25m (Glasspool, 2003; Jeffrey, 2005). This coal seam is the most economically important, hosting an estimated 70% of the coal resource with very high quality (Jeffrey, 2005). This coal is used for the production of low ash metallurgical coal and export steam coal.

Figure 17: Generalised stratigraphic column of coal seams within the Vryheid formation in the Witbank Coalfield. Redrawn from Cairncross and Cadle (1998*)*

3.5 Hydrogeology

The natural hydrogeological characteristics of an area indicate the occurrence, distribution and movement of groundwater through geological formations. Witbank consists of three distinct hydrogeological zones, namely the: unconfined primary aquifer, semi-confined aquifer and confined aquifer (Hodgson and Krantz, 1998; Zelenková et al., 2009).

The *primary unconfined aquifer* is a shallow weathered aquifer, primarily restricted to the soil (soft overburden) horizon with a limited vertical depth (Viljoen, 2015). Although it has a limited vertical depth, it has extensive lateral exposure to atmospheric conditions. The main source of recharge into this aquifer is directly linked to rainfall and surface water runoff that infiltrates to the aquifer through the unsaturated (vadose) zone (Geo Pollution Technologies, 2016). Sedimentary hydrogeology indicates that recharge into this aquifer is relatively high, up to 3% of the mean annual precipitation (Kirchner et al., 1991; Vermuelen and Usher, 2006). High recharge rates in the weathered zone (comprised of transported colluvium and in-situ weathered sediments) form a water table which falls within a few metres below the surface (Zelenková et al., 2009). This aquifer undergoes diffuse recharge, which is a widespread movement of water from land surface to the water table as a result of precipitation over large areas infiltrating and percolating through the unsaturated zone. The vertical movement of water is faster than the lateral, as vertical water is assisted by the influence of gravity (Geo Pollution Technologies, 2016). Groundwater flow patterns in this aquifer usually follow the topography, draining towards topographic lows.

The *semi-confined aquifer* is a fractured aquifer, comprising consolidated sediments of the Ecca Group within the Karoo Supergroup. The fractured Ecca aquifer consists of un-weathered sandstone, shale and coal beds (Zelenková et al., 2009; Geo Pollution Technologies, 2016). Fractures in this aquifer primarily control groundwater movement, as the pores of the Ecca sediments are well bonded together, restricting the flow of water (Zelenková et al., 2009). Preferential recharge occurs along secondary structures, such as fractures, faults, dykes and joints. These structures are better developed in competent rocks, producing high water-yielding properties. The water-yielding capacity is governed by secondary porosity, which is the porosity attributed to secondary structures rather than the rock itself (Zelenková et al., 2009). Although initial yields of these secondary structures may be high, it has limited storage which may prove unsustainable. Excluding secondary structures, it is important to note that the coal seams in this aquifer often contain the highest hydraulic conductivity (Hodgson & Krantz 1998).

The *confined aquifer* is a deep aquifer consisting of dolerite intrusions in the form of dykes and sills. These intrusions can serve as both aquifer or aquiclude, meaning that it may either act as a permeable or impermeable medium. This variability in function either allows water to pass through or inhibit it, making the yield of this aquifer highly variable. Sufficient information about the confined aquifer geology such as its weathering, size and fracturing conditions give a further indication an indication of its yield capacity (Shangoni Aquiscience 2013).

An example are thick unbroken dykes that inhibit the flow of water to perpendicular dykes, thereby forming compartmentalised water zones. Whereas, the baked and thick contact zones are generally highly conductive parallel to the dykes, which successfully interconnect both vertical and horizontal strata into a single aquifer (Geo Pollution Technologies, 2016).

The three aforementioned hydrogeological zones indicate an overall summary of the general geohydrology of the Witbank area and it is important to note that these characteristics may vary depending on localised conditions.

3.6 Conceptual backfilling scenarios

The aforementioned literature contains hydrogeological information of a realistic study site located within the Witbank Coalfield. Understanding the hydrogeological parameters of the aquifer, such as its permeability, storage, hydraulic head, lithology, climatology and hydrogeology are essential in planning or designing suitable ash disposal sites (Libicki et al., 1985). Libicki et al., (1982) identifies three broad ash disposal types, (which are classified in accordance to their spatial relation of coal ash) namely: over-terrain, unsaturated and saturated disposal sites.

Over-terrain sites (also known as a dry cover) are distinguished by the disposal of coal ash above the land surface as an ash monolith (Figure 18). The use of this type of site is potentially beneficial as it has the dual benefit of limiting oxygen and water ingress from atmospheric conditions whilst affording some protection against the resuspension of mine spoils due to the wind (Johnson and Hallberg 2005). Although this type of disposal method is proven to be an effective AMD reduction technique, the focus of this study is to backfill opencast coal mine pits, thus only underground (saturated and unsaturated) ash disposal sites are of interest.

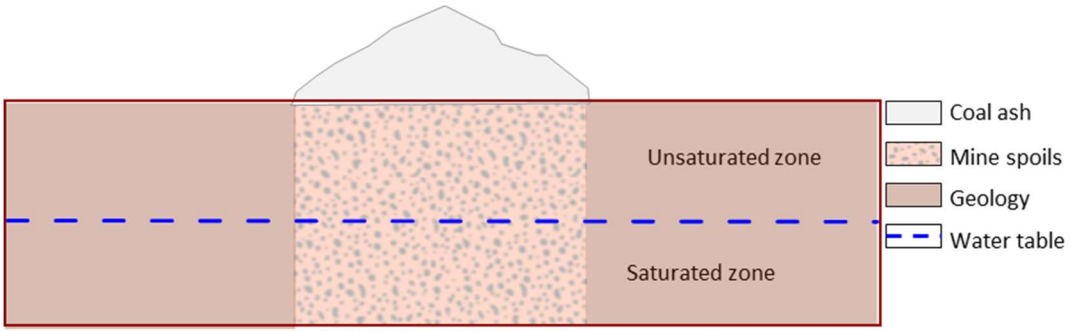

Figure 18: Over terrain ash disposal site (sourced from Bittner and Kondziolka, 2017)

Unsaturated disposal sites are sites that dispose of ash below the terrain, but above the groundwater table (Libicki, 1985; October, 2011). Ash monoliths are disposed of in a section of the pit that does not intersect the water table and the ash remains unsaturated due to it being isolated from contact with continuous groundwater through flow (Figure 19). The ash monoliths are not directly in contact with the groundwater table but may potentially collect moisture from precipitation.

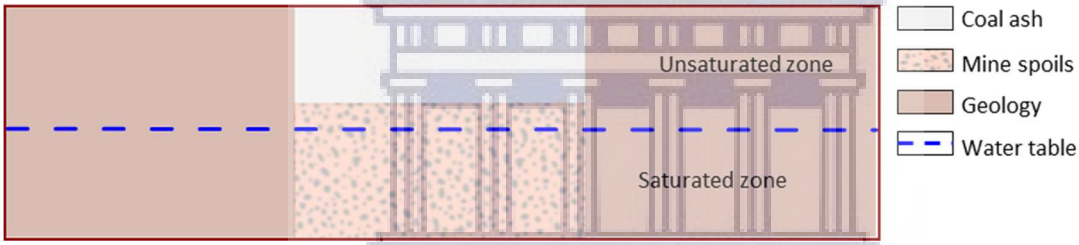

Figure 19: Unsaturated ash disposal site (sourced from Bittner and Kondziolka, 2017)

Saturated disposal sites are sites that dispose of ash below the terrain level and below the groundwater table (Libicki, 1985). Ash monoliths, in these sites, are disposed of in a section of the pit intersecting the water table (Figure 20). Therefore, coal ash is continuously saturated by lateral groundwater inflow, filling the soil pores with water until the moisture content equals porosity (Bear and Cheng 2010).

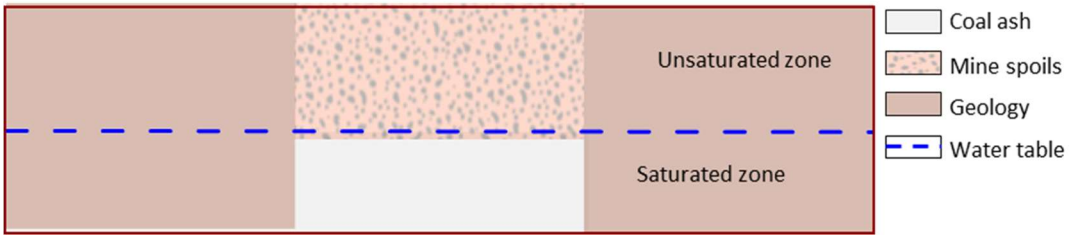

Figure 20: Saturated disposal site (sourced from Bittner and Kondziolka, 2017)

Using coal ash as a structural fill has the benefit of preventing AMD formation provided it is placed in a way that inhibits water or oxygen availability within the mine spoils (USEPA,

1994). The most efficient and practical technique is to limit oxygen ingress within the mine spoils by keeping them saturated at all times (Aubertin et al. 2016; Kuyucak 2012). The United States Environmental Protection Agency (USEPA) found that the placement of mine spoils below the water table experienced a slow diffusion of oxygen, which impeded AMD production within mine spoils (USEPA 1994).Conversely, when mine spoils were placed above the water table, they experienced an influx of water flow and oxygen in joints that accelerated AMD production. Mine spoil saturation may be achieved through the method of 'waterflooding', which involves placing reactive mine spoils underwater to prevent oxidation (Ouangrawa et al., 2010). An additional method is to raise the water table ('water table elevation'), which is achieved by modifying the water balance on site, either by increasing the water retention of mine spoils or decreasing the lateral flow (Ouangrawa et al., 2010). These two methods are practical applications to consider in opencast coal mines.

3.7 Conceptualized CCR backfill scenarios

The conceptualization of the fictitious site was developed by synthesising information on the study site, climate, geology, coal seam locality and hydrogeological properties from literature (Chapter 3). This provides a realistic representation of a typical opencast coal mine located within the Witbank Coalfields, Mpumalanga. The designs of suitable ash disposal sites incorporated both saturated and unsaturated ash disposal methods, in the aims of preventing AMD formation. In consideration of these concepts, the following six practical CCR backfilling scenarios were conceptualised:

1. Backfill with mine spoils only/no ash;
2. Ash backfilled below the water table;
3. Ash backfilled above the water table;
4. Ash backfilled in the middle of the pit up to the surface topography;
5. Ash backfilled down-gradient of the mine pit up to the surface topography; and
6. Ash backfilled in the middle of the pit up to the weathered zone.

Conceptual models demonstrating the opencast mining process prior to backfilling are presented in Figures 21 – 24 below. These pre-mining/mining stages illustrate the hypothesised changes to groundwater levels, geology and recharge before backfilling commences. The six aforementioned conceptualised backfill scenarios are presented from Figures 25 – 30 below.

Pre-mining phase:

This stage indicates the natural conditions of the anticipated mine pit prior to opencast coal mining (Figure 21). The depth (30 m), width (300 m) and length (300 m) is volumetrically equivalent to a volume of 2 700 000 m^3. The pit is located within the geology of the Karoo Supergroup that intercepts the top weathered zone for 10 meters and the underlying unconfined aquifer for 20 meters. The static water level of the pit was averaged at *c.*16 metres below ground level (mbgl) with a natural recharge of 3%.

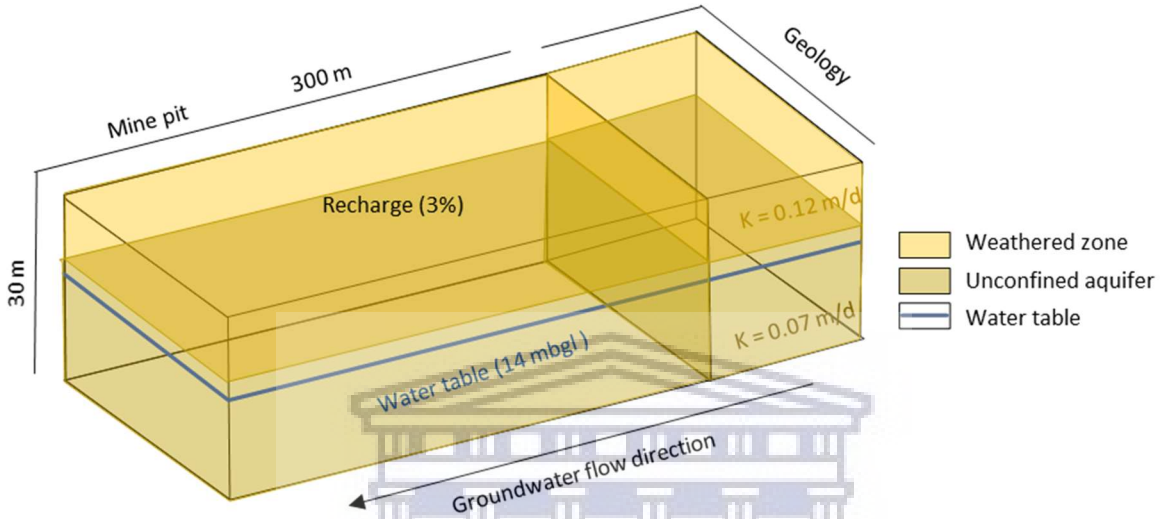

Figure 21: A conceptual model of the pre-mining stage

Operational phase:

During this stage, the coal pit is actively mined out, following a conventional opencast strip-mining procedure (referred to in Section 2.3.4). This procedure involves mining out consecutive sections of the pit, by blasting the overburden, removing it and setting it aside. The accumulated overburden/mine spoils are then backfilled into former voids as successive mining continues. An illustration of this process is displayed in Figures 22 to 24 below.

The conceptual model presented in Figure 22 below, illustrates the initial active mining stage, which creates a void from the initial blasting and removal of overburden rock. The void is subject to high water inflows (averaged at 70% of rainfall) (Hodgson and Krantz, 1998), creating hydraulic head difference that directs water from the surrounding unconfined aquifer into the pit. The pit is dewatered whilst the mine actively mines out the coal seam.

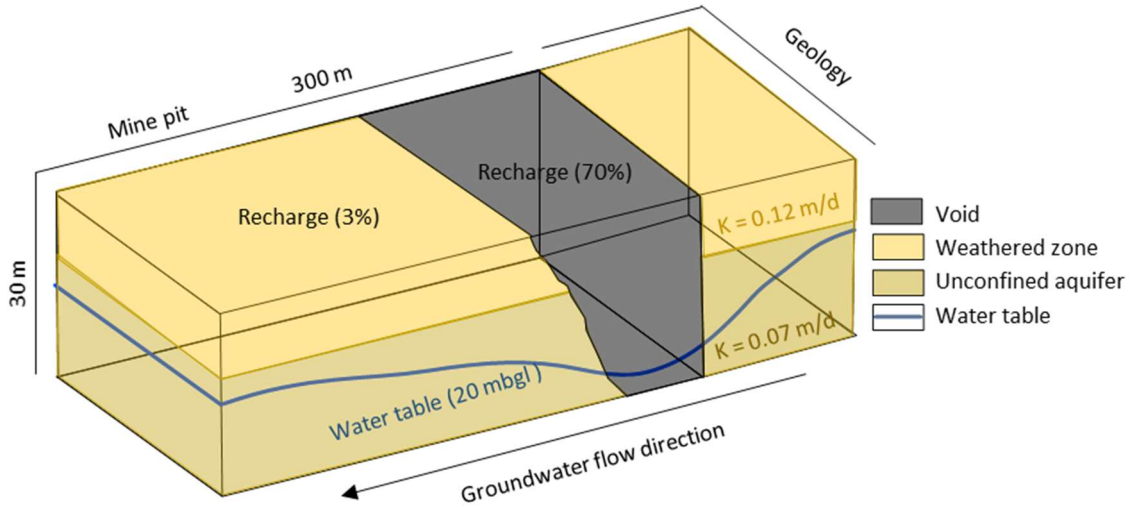

Figure 22: A conceptual model of the initial active mining stage

This conceptual model illustrates the second successive void space created by the removal of overburden rock that is backfilled into the initial void space (Figure 23). Both the mine spoils and the void space have a higher hydraulic conductivity in contrast to the surrounding geology, creating a hydraulic head difference, which directs the water table from the surrounding unconfined aquifer into the void. The water directed towards the void is dewatered whilst the mine actively mines out the coal seam.

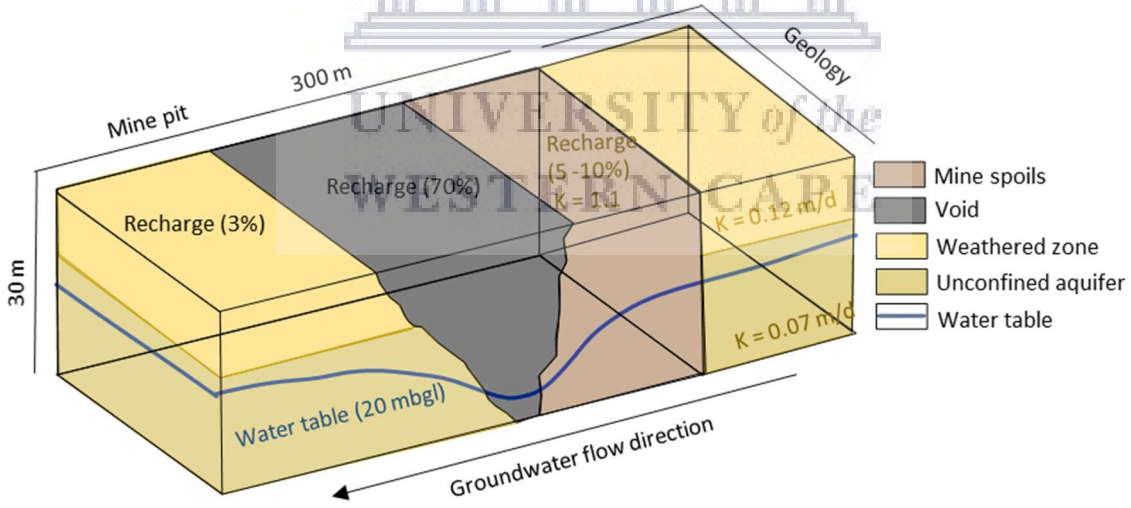

Figure 23: A conceptual model of the second successive active mining stage

This conceptual model illustrates the last remaining void space created by the removal of overburden rock backfilled into the former two void spaces (Figure 24). Both the mine spoils and the void space have a higher hydraulic conductivity in contrast to the surrounding geology, directing the water table from the surrounding unconfined aquifer into the pit. The pit is dewatered whilst the mine actively mines out the coal seam.

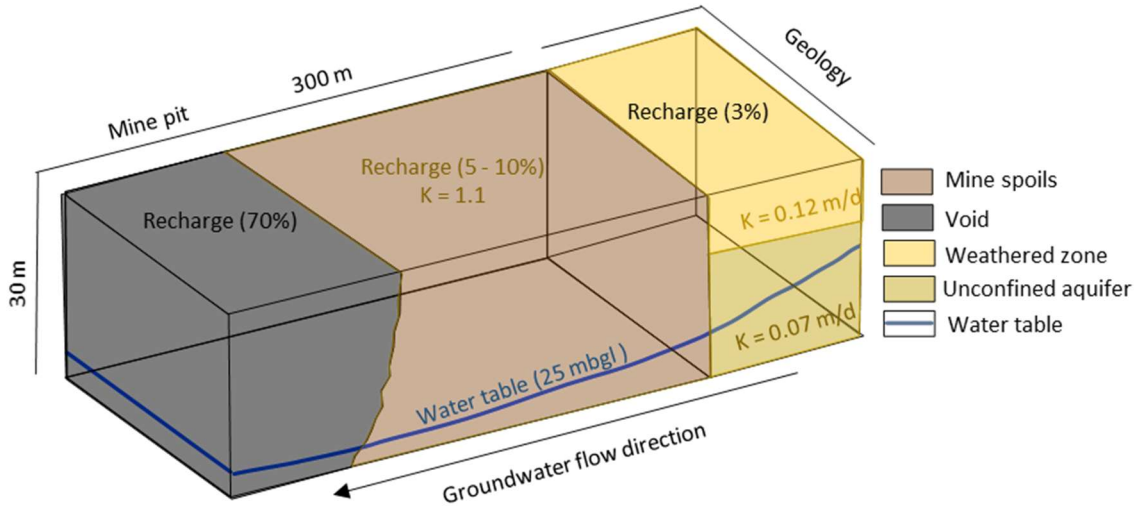

Figure 24: A conceptual model of the third successive active mining stage

Backfilling with coal ash and mine spoils are determined by the following six conceptualised scenarios' (Figures 25 – 30).

Scenario 1 (baseline scenario) illustrates the conditions of a typical opencast coalmine backfilled with mine spoils only (Figure 25). The mine spoils have a higher hydraulic conductivity and recharge rate in comparison to the surrounding geology, directing water from the surrounding aquifer into the pit. The groundwater is expected to permeate through the mine spoils with ease, following the hydraulic flow direction. This scenario is expected to have high concentrations of AMD, due to elevated infiltration rates and oxygen ingress through the sulphide-rich mine spoils, prompting the formation of AMD.

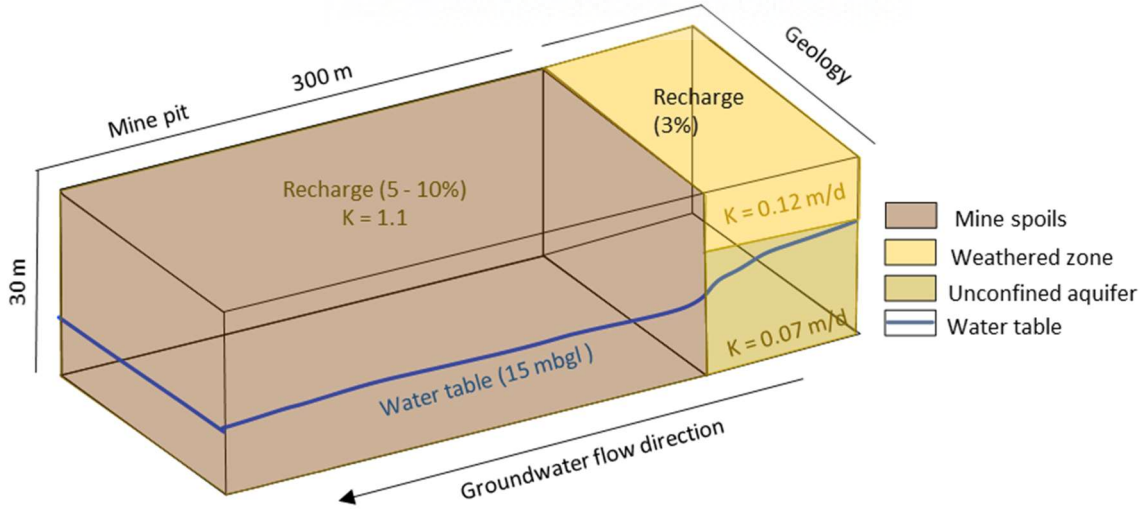

Figure 25: Scenario 1 - A conceptual of model showing baseline scenario backfilled with mine spoils only

Scenario 2 illustrates a conceptual model of the pit backfilled with a coal ash monolith below the water table (Figure 26). Groundwater travelling into the pit follows the hydraulic flow direction. The groundwater table is expected to mimic Scenario 1 as it does not alter the flow regime and has the same recharge. In addition, similar groundwater quality to be expected (to Scenario 1), as the sulphide-rich mine spoils experience similar saturation and oxygenation levels.

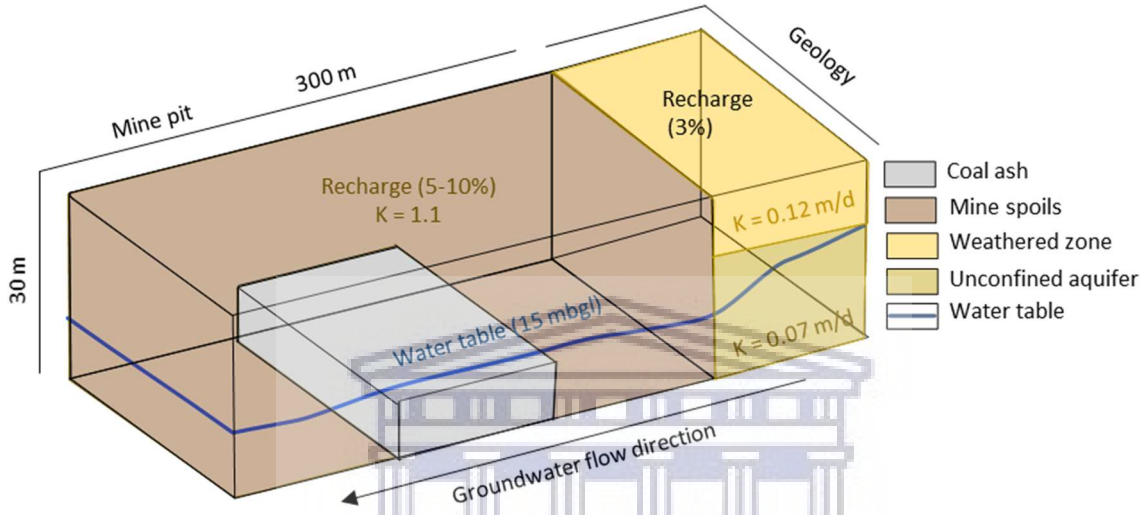

Figure 26: Scenario 2 - A conceptual model of the backfilled CCR monolith below the water table

Scenario 3 illustrates a conceptual model of the pit backfilled with coal ash above the water table (Figure 27). Over time, the ash monolith is expected to decrease in hydraulic conductivity, which will decrease percolation and infiltration rates of rainfall. Consequently, this will reduce the amount of precipitation entering the pit via precipitation/recharge. The volume of groundwater baseflow entering the pit from the surrounding aquifer is expected to be similar to Scenario 1, as the placement of the ash monolith similarly does not intercept the water table. The water table is expected to remain the same if groundwater baseflow from the surrounding aquifers is the dominant water inflow process, conversely the water table is expected to decrease slightly if recharge is the dominant water inflow process. Groundwater quality is expected to improve marginally, if recharge is the dominant inflow process, as the ash monolith reduces oxygen ingress and the infiltration of sulphide-rich mine spoils.

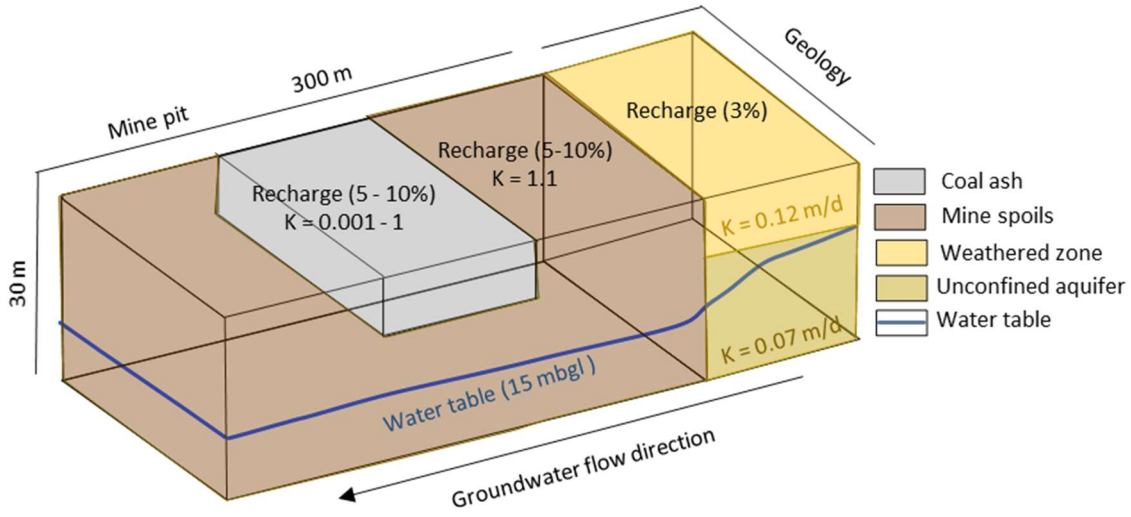

Figure 27: Scenario 3 - A conceptual model of the backfilled CCR monolith above the water table

Scenario 4 illustrates a conceptual model of the middle of the pit backfilled with coal ash up to the surface topography (Figure 28). The backfilled ash monolith is expected to decrease in hydraulic conductivity over time, reducing its permeability. As the groundwater baseflow from the surrounding aquifer enters the pit, it is intercepted by the low permeability of the ash, inhibiting the flow of water and raising water levels up gradient of the ash monolith. In addition, the low permeability of ash monolith may produce a perched water table. Groundwater quality is expected to improve as groundwater levels are expected to rise, increasing mine spoil saturation and decreasing oxygenation.

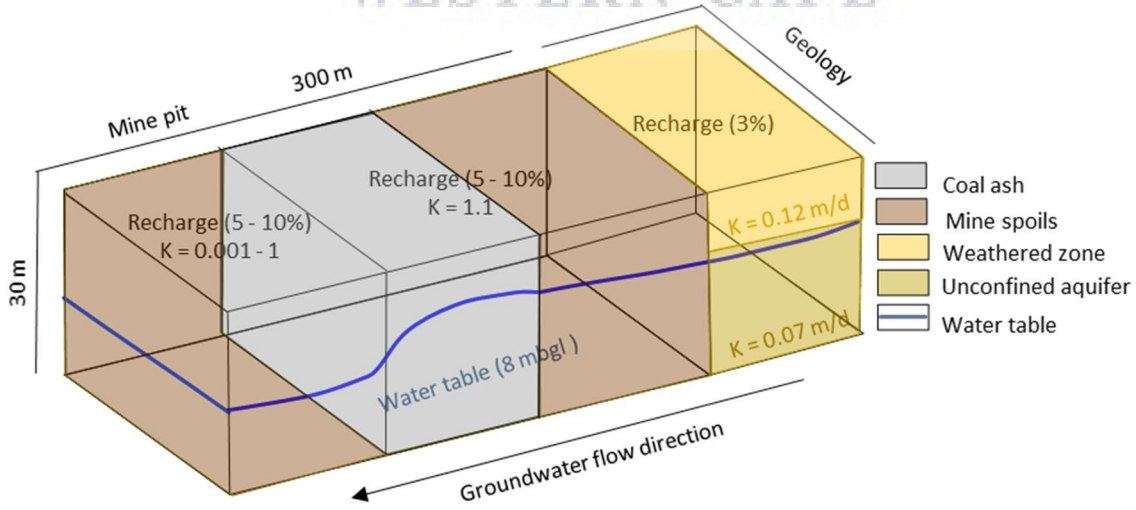

Figure 28: Scenario 4 – A conceptual model of the backfilled CCR monolith to the surface in the middle of the pit

Scenario 5 illustrates a conceptual model of the down-gradient portion of the pit backfilled with coal ash up to the surface topography (Figure 29). The backfilled ash monolith is expected to decrease in hydraulic conductivity over time, reducing its permeability. Groundwater baseflow entering the pit from the surrounding aquifer, is intercepted by the low permeability ash monolith, which inhibits the flow of water out of the pit. The obstructing ash monolith retains water within the pit, raising water levels over a large area. The effect of raised water levels is expected to improve groundwater quality, by limiting mine spoil oxygen ingress, which reduces the formation of AMD.

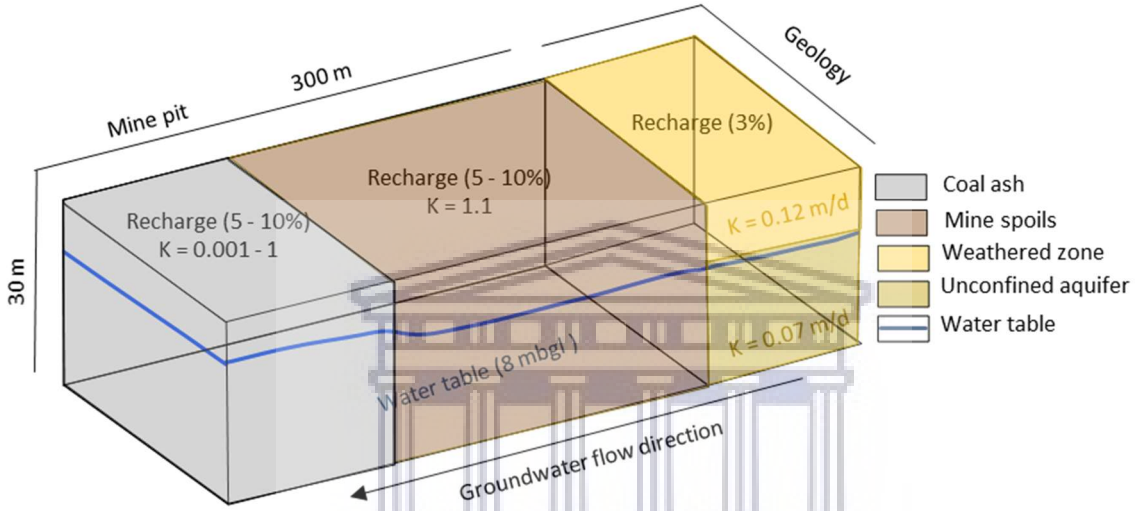

Figure 29: Scenario 5 - A conceptual model of the backfilled CCR monolith backfilled down-gradient of the mine pit

Scenario 6 illustrates a conceptual model of the pit backfilled with coal ash from the base of the pit to the weathered zone (Figure 30). The water table is intercepted by the ash monolith in the middle of the pit, which due to its low permeability inhibits the flow of water to up to the weathered zone boundary (*c.*10 mbgl). The restricted water in the upper portion of the pit, prompts a water level rise up to the top of the ash monolith (*c.*12 mbgl), where the water is expected to flow over, around or through the ash monolith to the lower portion of the pit. Recharge into the pit is expected to be similar to that of Scenario 1, as the ash monolith is placed beneath the surface and not in direct contact with precipitation. A slight improvement is expected in groundwater quality, due to the rise in water levels up-gradient of the ash monolith. This limits mine spoil oxygen ingress, thus reduces the formation of AMD.

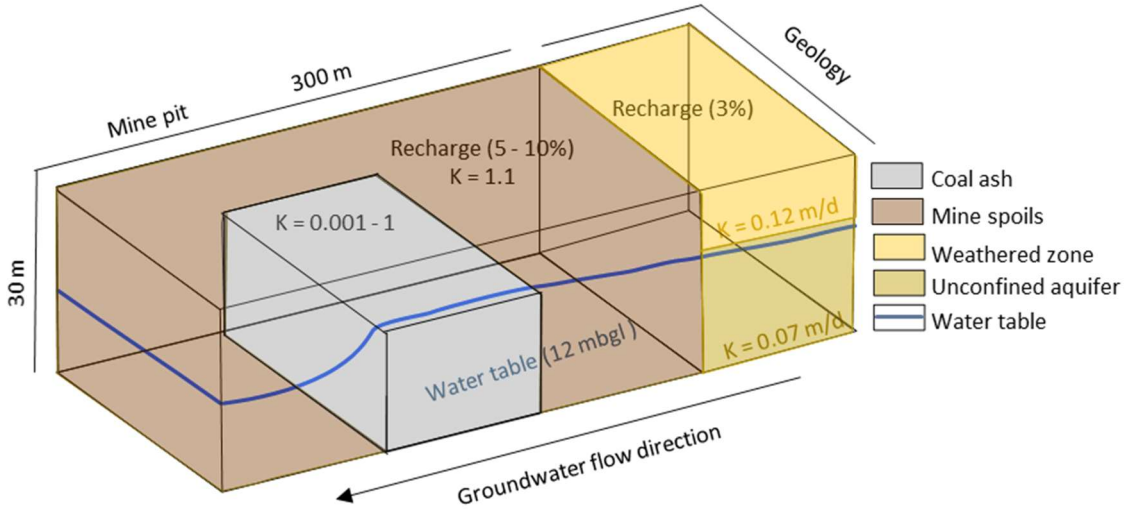

Figure 30: Scenario 6 - A conceptual model of the backfilled CCR monolith placed from the pit base up to the weathered zone

4 NUMERICAL MODELLING

Numerical groundwater modelling is a computer-based representation of the hydrogeological system. It provides a simplified version of the natural system, which utilises governing equations to incorporate data and simulate the hydraulic properties or geochemical properties. This chapter describes the construction and input variables used to create numerous flow and transport models, simulating future responses in the hydrogeological system under the influence of various backfilling conditions.

4.1 Model objectives

The aim of the model is to predict the hydrogeological responses under various fly ash backfilling scenarios in an opencast coal mine. Numerical flow and transport models were constructed for each of the hypothesised scenarios to achieve the following outputs:

- *Flow models:* simulate the hydraulic head, rate and direction of water movement through the subsurface. This allows one to establish or identify changes to the groundwater flow regime, evaluate groundwater flow directions and analyse water table recovery rates.
- *Transport models:* simulate the advection, dispersion and chemical reactions of solutes in groundwater systems. This allows one to predict the concentration, movement of contaminants and identify contaminant plumes under various scenarios.

The modelling results indicates the hydrogeological responses for the various scenarios, providing an understanding of whether coal ash backfilling will have a positive, negligible or negative impact on groundwater resources.

4.2 Model dimension and code selection

The groundwater model was formulated in three-dimensions (3D) in order to simulate groundwater movement in both the horizontal and vertical planes. The model was constructed using Groundwater Vistas Version 7 (GWV 7), a pre- and post- processing package for the modelling code MODFLOW-USG. MODFLOW-USG (Panday et al., 2013) advanced version and the xMD solver for unstructured grids was used in the simulation of hydrogeological responses for the various coal ash backfilling scenarios.

MODFLOW-USG is based on an underlying control volume finite difference (CVFD) formulation in which a cell can be connected to an arbitrary number of adjacent cells. MODFLOW–USG includes a Groundwater Flow (GWF) Process, based on the GWF Process in MODFLOW–2005. MODFLOW–USG provides a framework for tightly coupling multiple

hydrologic processes. The tight coupling occurs through the formulation of a global conductance matrix that includes the cells for all processes. The framework allows individual MODFLOW–USG processes to add to the global conductance matrix in order to represent fluxes between cells within a process as well as with cells of other processes. The global conductance matrix can be symmetric or asymmetric and is unstructured, indicating that an individual cell may have an arbitrary number of connections with other cells. The CVFD formulation accommodates this unstructured framework of tightly coupling flow processes as well as of allowing flexibility in cell geometry and connectivity within processes. Following is the general form of a CVFD balance equation for cell n:

$$\Sigma_{m\in n}\, C_{nm}\,(h_m - h_n) + HCOF_n\,(h_n) = RHS_n$$

Where:

- C_{nm} is the inter-cell conductance between cells n and m
- h_n and h_m are the hydraulic heads at cells n and m
- $HCOF_n$ is the sum of all terms that the coefficients of hn in the balance equation for cell n, and
- RHS_n is the right-hand-side of the balance equation.

4.3 Model extent and boundary conditions

Boundary conditions are partial differential equations, which simulate the way in which the considered domain interacts with its environment (Anderson and Woessner, 2002). In other words, they express the conditions of known water flux, or known variables, such as the hydraulic head. Different boundary conditions result in different solutions; thus, it is important to select suitable boundary conditions that simplify the actual hydrogeological conditions. There are three principal types of boundary types in MODFLOW which can be specified either as: a specified head (Dirichlet; specified flux) or Neumann; or mixed (Cauchy) boundary conditions.

For the numerical models constructed, two types of boundary conditions were incorporated, namely:

- The *General-Head boundary*: This boundary simulates head-dependent flux boundaries that is always proportional to the difference in head. This allows the model to compute general hydraulic head gradients across the model with realistic outcomes.
- The *Drainage boundary:* This boundary simulates head-dependent flux boundaries. If the head in the cell falls below a certain threshold, the flux from the drain to the model

cell drops to zero. The drain boundary is used to simulate dewatering and mining excavations during the operational phase as well as decant post-closure.

A summary of the real-world local boundaries adapted to model boundary conditions are presented in Table 16 below:

Table 16: Identification of real-world local boundaries and the adopted model boundary conditions

Boundary	Boundary Description	Boundary Condition
Top	Higher hydraulic conductivities in the weathered zone and unconfined aquifer	Recharge rates
Bottom	Lower hydraulic conductivities in the deep fractured aquifer	No flow boundary
South	Local flow gradient	General head boundary representing upper flow in the second layer
North	Local flow gradient	General head boundary representing lower flow in the third layer
East, West	Local catchment boundary	No flow conditions
Mine Pit	Operational mine floor	Drain boundary used to dewater the mine during the operational phase
Mine water decant	Water flow from mine after rebound	Drain boundary used to specify decant elevation of recovered mine water level

4.4 Spatial discretization

The compilation of the finite-difference grid using Groundwater-Vistas graphic user interface consists of eight layers with a total of 80 000 cells (100 x 100 x 8 layers). Given that this is a generic model, all hydrogeological layers are flat (weathered, primary unconfined aquifer, semi-confined aquifer and confined aquifer). The bottom elevation is 80 mbgl which incrementally increases by 10 m elevation differences. The mesh size is relatively comprehensive with 10m cells over an area 1 km^2. The total model area spans 1 000 000 m^2 with a 90 000 m^2 square opencast pit in the centre (Figure 31). In addition, a 10 m groundwater flow gradient was simulated across the model from north to south (Figure 32) using a general head boundary between the second and third layers (20 – 30 mbgl).

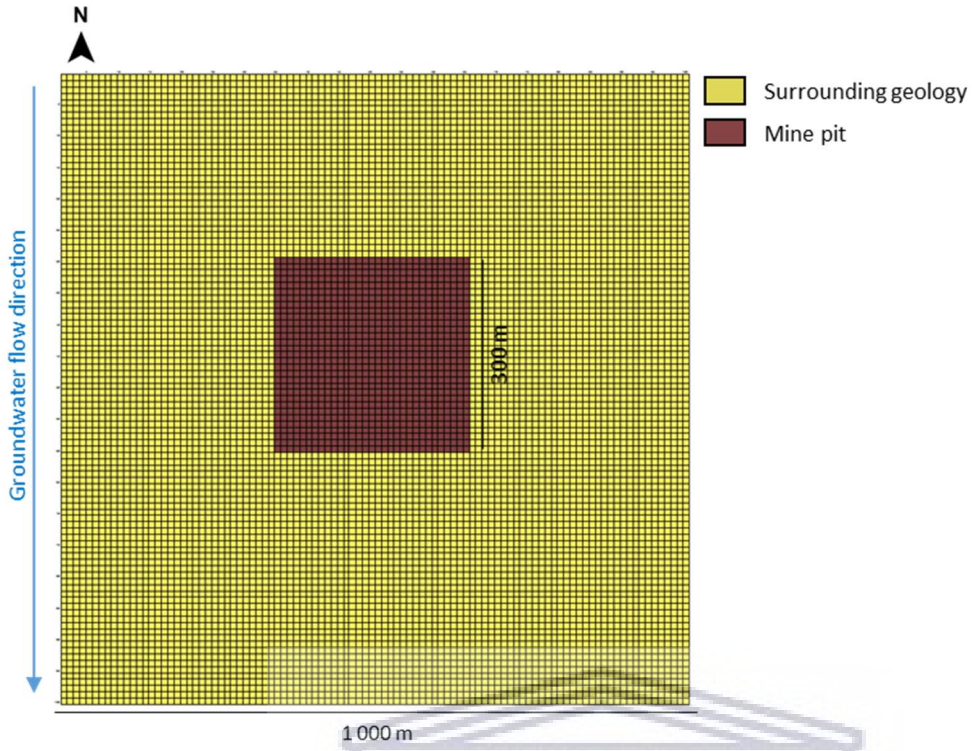

Figure 31: An aerial display of the finite difference grid

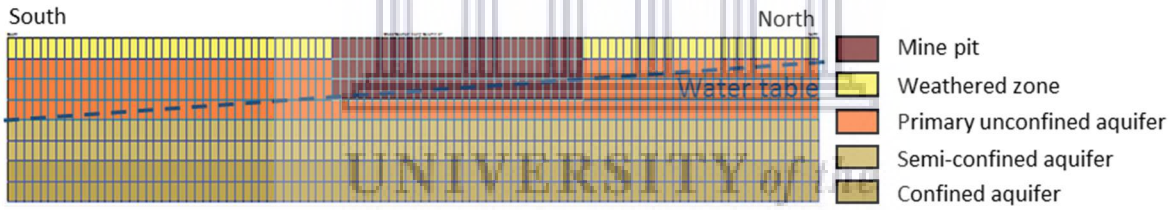

Figure 32: A north-south cross section of the finite difference grid

4.5 Temporal discretization

Several different time periods were modelled to simulate the entire mine-cycle. This was achieved by incorporating the following stages: pre-mining, mining and post-mining. The mining operational phase lasts for a period of 5 years, whereas the post-mining phase lasts for a period of 105 years. These time frames were chosen in order to monitor long-term (100 years) environmental impacts. A summary of the periods alongside their corresponding mining phase is provided in Table 17 below.

Table 17: A summary of short and long-term modelling periods.

Mining phase	Time period (years)	Cumulative period length (years)
Pre-mining	0 (1 day)	0
Operational	1	1

	1	2
Operational (backfill phase 1)	1	3
Operational (backfill phase 2)	1	4
Operational (backfill phase 3)	1	5
Closure	5	10
Post-closure	5	15
	5	20
	10	30
	10	40
	10	50
	55	105

4.6 Input parameters

The simulation of the various models requires mathematical input to describe the flow and transport processes that occur. As the model is based on a fictitious site, all quantitative data is derived from secondary sources. These secondary sources include co-researchers, field and laboratory analysis, hydrogeological reports, journals, articles and theses. The quantitative input data is sub-divided into three major categories, namely; study site properties, coal ash properties and mine spoil properties. These properties are described in the sub-chapters below.

4.6.1 Study site input parameters

This study aims to specify the flow and transport processes of CCR backfilling, rather than examine an actual site response, thus theoretical models are simulated. Therefore, study site properties are an indication of generalised geological properties that occur within the Witbank Coalfields. As previously discussed in Chapter 3.5, the Witbank Coalfields comprise of three main hydrogeological units being; the primary unconfined, semi-confined and confined aquifers. A weathered zone is present at the surface, comprising exposed rock that has been chemically and physically altered due to natural conditions. A summary of the study site input parameters along with their corresponding subscripted authors are presented in Table 18 below.

Table 18: Hydrogeological zone properties.

Hydrogeological Zone	Layer	Thickness (m)	K (m/day)	Specific Storage (1/m)	Specific Yield (m^3/m^3)	Porosity (m^3/m^3)	Precipitation (mm/a)	Recharge (mm/a)

Weathered zone	1	10	0,12 (9)	0,002 (4)	0,02	0.05 (1,2)	688 (5,10)	21 (5,9,6)
Primary unconfined aquifer	2-4	3 x 10	0,07 (5,9)	0,001 (1,4,7)	0,01	0,03 (2,3)	n/a	n/a
Semi-confined aquifer	5-6	2 x 10	0,05 (5)	0,001 (1,4,7)	0,01	0,03 (2,3)	n/a	n/a
Confined Aquifer	7-8	2 x 10	0,004 (9)	0,001 (1,2,4,7)	0,01	0,03 (2,3,7)	n/a	n/a

Input data is derived from the following sources: (1) Hodgson and Krantz, 1998; (2) van Bart, 2008; (3) SLR, 2011; (4) Steyl, 2011; (5) Shangoni Aquiscience, 2013; (6) Du Toit, 2014; (7) Delta H, 2015; (8) Ma et al. 2015; (9) GPT, 2016; and (10) Weather SA, 2017

Anthropogenic activities such as mining and excavations alter the natural hydrogeological properties. For example, temporary mine voids increase recharge rates depending on their floor slope and the degree to which these structures are filled with water. General rainfall into voids within the Mpumalanga region is averaged at 70% (Hodgson and Krantz, 1998).

4.6.2 Coal ash input parameters

The hydraulic properties of coal ash have been extensively discussed in Chapter 2.3.2, forming the basis of model input parameters. A summary of coal ash input parameters with their corresponding subscripted authors are presented in Table 19 below.

Table 19: Hydraulic input parameters of coal ash

Hydrogeological Zone	Layer	Thickness (m)	K (m/day)	Specific Storage (1/m)	Specific Yield (m^3/m^3)	Porosity (m^3/m^3)	Recharge (m/day)
Coal ash	1-3	0 – 30	0.001 – 0.1 (1,2)	0.008	0.1 (2)	0.1 (1)	0.01 – 0.0002 (3)

Coal ash input derived from the following authors (1) October, 2011; (2) Johnson, 1967 and (3) GPT, 2014.

From the aforementioned hydraulic conductivity properties reported in Chapter 2.3.2, coal ash values from Mpumalanga have been highlighted based on its contextual relevance. Two main studies conducted by October (2011) and co-researcher Johnson (2018) have formed the basis to which hydraulic conductivity values of coal ash in Mpumalanga were derived. These studies focus on two types of coal ash from the Tutuka and Kendal Power stations. These two power

stations are of relevant importance as they are in close proximity of existing opencast coal mines and have an abundance of coal ash which needs to be disposed of. October (2011) and Johnson (2018) studies were suitable based on the availability of data as well as experimental design. It is of importance to note that the hydraulic conductivities of coal ash change through time, based on the factors listed in Chapter 2.3. These hydraulic changes are accounted for in the model by using the function of 'time variant materials' within the MODFLOW-USG code. The changes in the hydraulic conductivity and recharge rates of coal ash are presented in Table 20 below.

Table 20: Changes in ash hydraulic conductivity and recharge for corresponding mining phases

Mining Stage	Hydraulic Conductivity (m/d)	Recharge (%)
Pre-mining	n/a	3 (1)
Backfill	0.8	10 (1)
10 years post-backfill	0.1 (2,3)	10 (1)
15 years post-backfill	0.01 (2,3)	8 (1)
100 years post-closure	0.001 (3)	5 (1)

Coal ash input derived from the following authors (1) Hodgson and Krantz (1998); (2) October, 2011; (3) Johnson, 2018.

4.6.3 Mine spoil input parameters

The hydraulic properties of mine spoils have been elaborated on in Chapter 2.3.2, forming the basis of numerical model input data. A summary of the mine spoils hydraulic properties is presented in Table 21 below. It is given that limited data has been published on the specific yield and storage of mine spoils within Mpumalanga, thus estimates of these values are gathered from mine spoils comparison to the coarse gravel textural classes.

Table 21: A summary of the hydraulic input parameters of mine spoils alongside subscripted authors

Hydrogeological Zone	Layer	Thickness (m)	K (m/day)	Specific Storage (1/m)	Specific Yield (m^3/m^3)	Porosity (m^3/m^3)	Recharge (m/day)
Mine Spoils	1-3	0 – 30	1.1 (4,5)	0.02 (1)	0.2 (1,2)	0.25 (6,3)	0.01 – 0.0002 (3)

Input data was derived from the following sources: (1) Johnson, 1967; (2) Moran, et al., 1978; (3) Hodgson and Krantz, 1998; (4) Buczko et al., 2001; (5) Hawkins, 2004; and (6) Fourie, 2007.

Mine spoils contain pyrite minerals that contribute towards forming sulphate (interchangeably as known as AMD) when exposed to sufficient amounts of air and water (USEPA, 1994; Brick, 1998; Simate and Ndlovu, 2014). Sulphate was the source of contamination within the model and was simulated as a non-reactive solute (solute does not partake in chemical reactions which grow or decay over time). Non-reactive solutes were modelled to determine the maximum concentrations both spatially and temporally and were governed by the transport processes of advection and dispersion.

The model simulated a period of 105 years, comprising five years of active operation/backfill which includes mine excavation, dewatering and backfilling (both CCR and mine spoils). Thereafter, the model predicted impacts of groundwater flow and contamination for 100 years post-closure. A summary of the recharge rates and concentrations of mine spoils respective to each scenario mining stages are presented in Table 22 below.

Table 22: Recharge and sulphate concentrations of mine spoils per mining phase

Mining Stage	Recharge (%)	Concentration (g/m^3)
Pre-mining	3	0
Backfill	10	3500
10-year post-backfill	10	3500
15-year post-backfill	8	2000
100-year post-closure	5	2000

4.6.4 Model assumptions, limitations and exclusions

Several simplifications, assumptions and approximations were made in developing the flow and transport models. As these models were constructed using a generic modelling approach, an idealized representation of the flow system was created. The water table was assumed to be between 20 – 30 mbgl, creating a 10 m hydraulic flow descent based on mean water levels found in literature. The opencast mining pit floor was assumed to be 30 mbgl based on estimations of the targeted coal seam depth. In addition, the mine pit is assumed to be within the unconfined aquifer unit based on the strata within which the coal seam was embedded.

It was assumed that the horizontal (Kx) hydraulic conductivity input parameters (such as the geology, coal ash and mine spoils) correlated with the vertical values (Ky) at any given location, however the diagonal values (Kz) differed by an order of magnitude less. The hydraulic conductivity values were also homogenous over each geological layer. The confined

aquifer layer did not account for potential fractures acting as a groundwater conduit; therefore it was generalised to be homogenous with low hydraulic conductivity values.

Rainfall values were based on long term rainfall averages, accounting for the recharge values utilised. Specific storage values were assumed to be an order of magnitude less than specific yield values. Lastly, the simulation of AMD was computed as a non-reactive solute, therefore AMD solutes remained constant whilst following the fluid regime as it did not partake in chemical reactions.

5 RESULTS AND DISCUSSION

This chapter presents and discusses the results of the numerical models and risk assessments. Results from the flow models are depicted as hydrographs displaying the changes in water levels and recovery rates. Aerial and cross-sectional graphs were used to present the results of the solute transport models, displaying the changes in contaminant concentrations and contaminant plume migrations. The risk assessment contextualises the risks associated with each scenario to determine whether CCR backfilling will have a positive, negligible or negative impact on the environment.

5.1 Groundwater flow

To understand the hydrogeological flow regime of the mine pit, volumes (m^3/day) of water leaving the pit are quantified over the entire assessment period (Figure 33). All scenarios initially undergo five years of mine dewatering, contributing towards large volumes of water leaving the pit. Once dewatering has ceased and the pumps have stopped, the water table gradually rises as the mine is filled with water from adjacent aquifer inflows and rainfall infiltration. The water table took between 30 - 40 years to recover (depending on the scenario), hence it is during this period that lower volumes of water left the pit due to the hydraulic head difference flowing towards the pit. Once the water table had recovered, groundwater gradually flowed out of the pit into the surrounding aquifer or towards the mining decant point (drain). The general trend is that all scenarios attained similar decant water volumes of 12 m^3/d over time, differing in water table recovery periods.

Water table recovery periods were identified as the year that water flowing out of the pit was constant. Scenario 1, 2 and 3 experienced a water table recovery period of 35 years before pit outflow volumes began to stabilize. Scenarios 4 and 6 obtained a 40-year water table recovery,

whereas Scenario 5 demonstrated a water table recovery of 45 years.

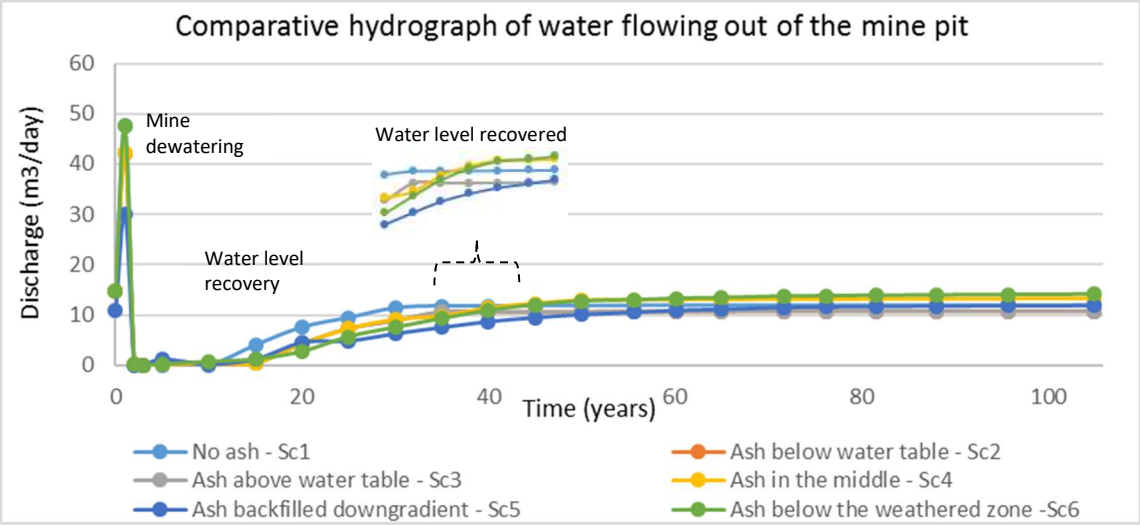

Figure 33: Comparative discharge hydrographs of water flowing out of the pit

To understand the changes in water levels that occurred within the mining pit, north-south cross-sectional line graphs (Figures 33 to 38) are presented below, which display the simulated water levels per layer over 100 years post-closure. In the aim of visually enhancing the contrast between backfilling with no ash versus scenarios that backfill with coal ash, a red line was overlaid on all the graphs to represent the simulated water level of Scenario 1. Water levels in Layer 2 were chosen as the representative water level, as it best represents natural water levels in the pit based on baseline water levels.

Scenario 1 involved backfilling with mine spoils only (Figure 34). The results displayed simulated water levels of 12.39 mbgl upon entering the pit (located at 700 m on the x-axis of the cross-section found in Figure 32) and 13.98 mbgl when exiting the pit (400 m), creating a hydraulic difference of 1.59 m within the pit with an average water level of 12.91 mbgl. Additionally, water levels for this scenario took a period of 35 years to recover. Water levels found in this scenario correlate with literature-based values and thus serve as a baseline comparison to the proceeding water levels.

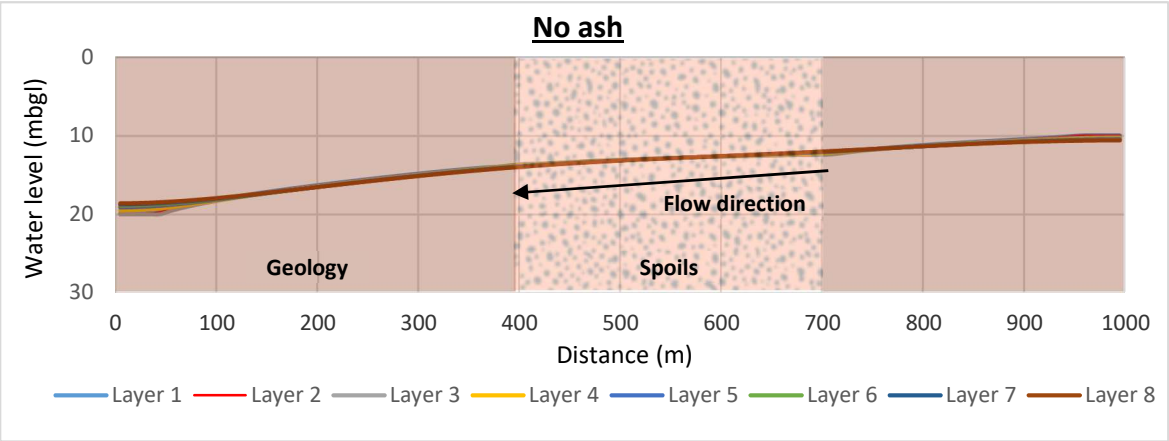

Figure 34: Scenario 1 - Simulated water levels

Scenario 2 involved backfilling with coal ash below the water table (Figure 35). The results display simulated water levels of 12.10 mbgl upon entering the pit and 13.98 mbgl when exiting the pit, creating a hydraulic flow difference of 1.88 m with an average water level of 12.79 mbgl within the pit. These water levels are similar to Scenario 1, displaying a slight water level increase of 0.29 m, equating to a minor difference of 1.65%. The results from this particular scenario indicated a negligible effect on water levels and recovery rates, providing no evident changes to the hydrogeological flow regime. The water levels, similarly, to Scenario 1, required 35 years to recover.

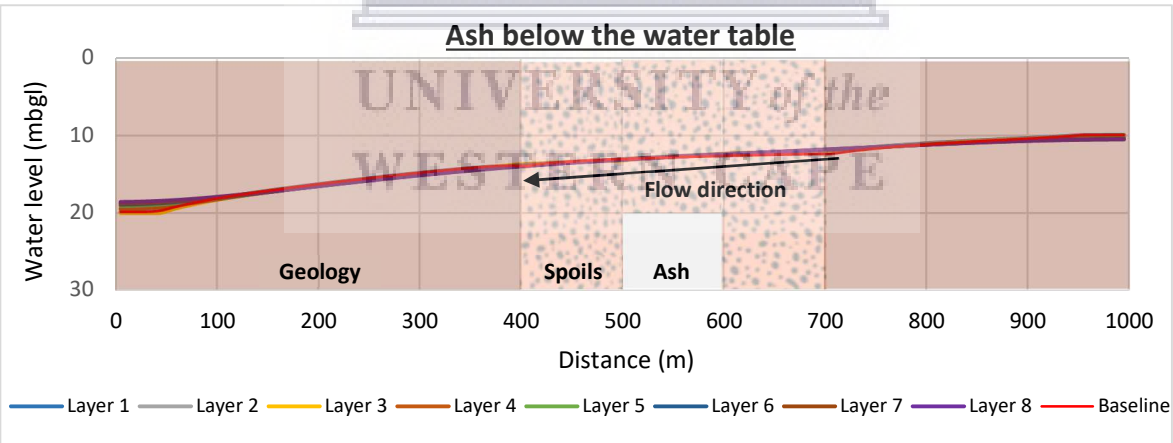

Figure 35: Scenario 2 - Simulated water levels

Scenario 3 involved backfilling with coal ash above the water table (Figure 36). The results display simulated water levels of 12.38 mbgl upon entering the pit and 13.98 mbgl when exiting the pit, creating a hydraulic flow gradient of 1.59 m within the pit. These water levels are effectively equivalent to that of scenario 1 (0.005% difference). The one particular exception to that of Scenario 1 was the perched water levels within the ash monolith, experienced in layer 1 (located between 500 – 600 m). This was due to the low permeability of the ash which encapsulates recharge to form a lens of saturated material in an unsaturated zone. In addition,

this scenario also took a period of 35 years were required for the water table to recover (as in Scenarios 1 and 2).

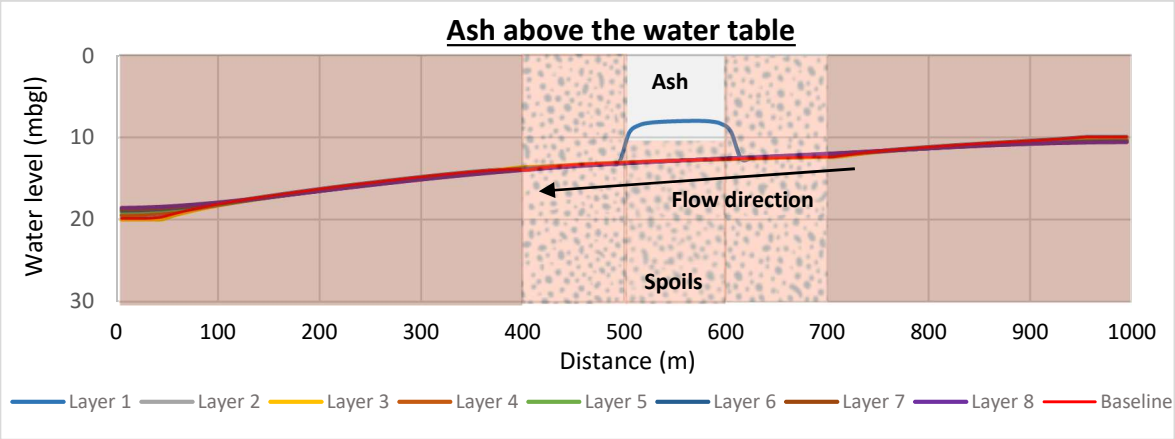

Figure 36: Scenario 3- Simulated water levels

Scenario 4 involved backfilling with coal ash from middle of the pit up to surface topography (Figure 37). The results display simulated water levels of 11.09 mbgl upon entering the pit and 13.99 mbgl when exiting the pit, creating a hydraulic flow difference of 2.90 m within the pit. Groundwater entering the pit continued to flow for 100 m (between 700 - 600 m) within the mine spoils, experiencing a water level increase of 1.37 m, equating to a 10.98% increase in water levels up-gradient of the ash monolith. Down-gradient of the ash monolith, the lower portion of the pit experiences a minor 3.17% water level increase. The ash monolith obtained a perched water table, trapping recharge to form a lens of saturation. A period of 40 years was needed for the water table to recover.

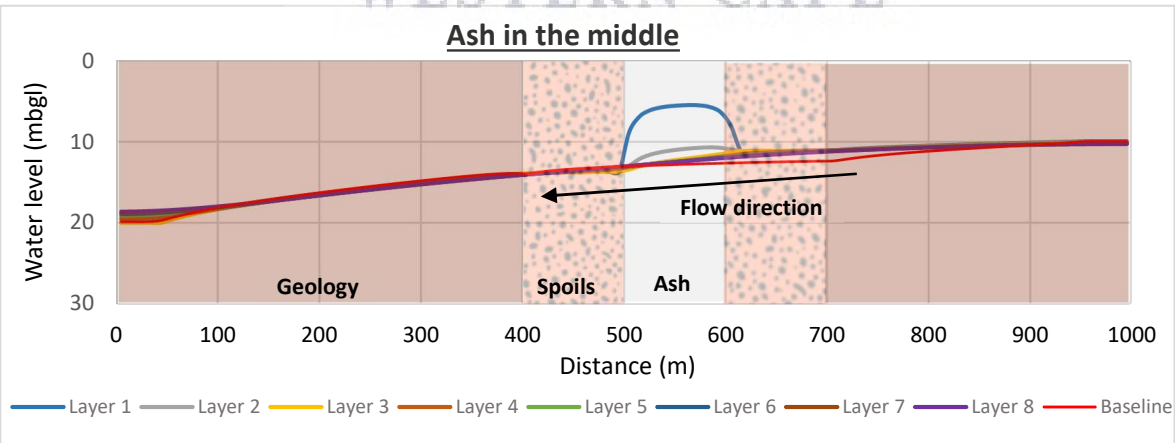

Figure 37: Scenario 4 - Simulated water levels

Scenario 5 involved backfilling with coal ash down-gradient of the pit up to the surface topography (Figure 38). The results display simulated water levels of 11.00 mbgl upon entering

the pit and 14.00 mbgl when exiting the pit, which created a hydraulic flow difference of 3.00 m within the pit. Groundwater entering the pit experienced a 12.05% rise in water levels in the up gradient of the ash monolith, due to the low permeability of the ash which acts as a hydraulic barrier. A perched water table occurred in ash due to slow vertical water flow from recharge. Additionally, water levels for this scenario took a period of 25 years to recover, which was 10 years faster than the baseline scenario. The faster water level recovery implies quicker mine spoil saturation, limiting oxygen ingress, thus reducing AMD formation.

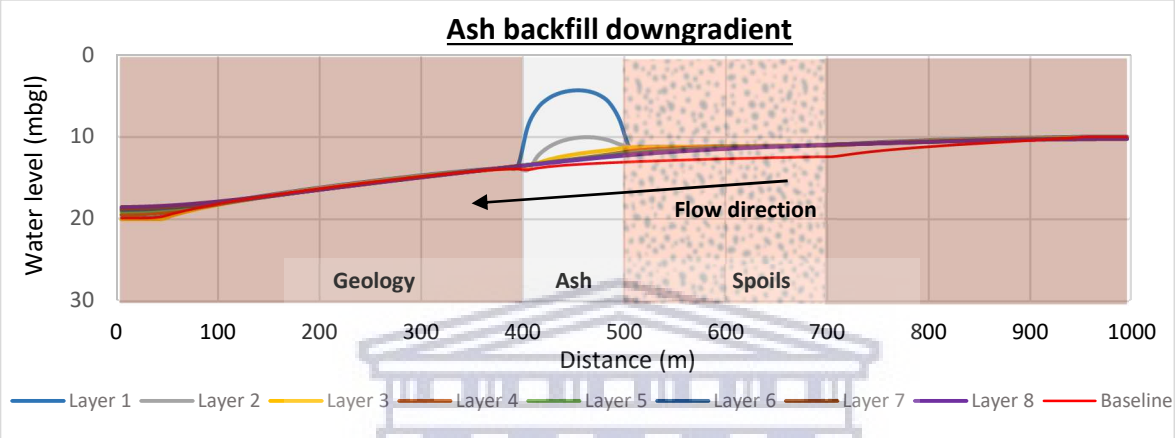

Figure 38: Scenario 5 - Simulated water levels

Scenario 6 involved backfilling with coal ash from the pit floor to the weathered zone (Figure 39). The results display simulated water levels of 11.01 mbgl upon entering the pit and 13.99 mbgl when exiting the pit, which created a hydraulic head difference of 2.98 m within the pit. Groundwater entered the pit and continued to flow for 100 m within the mine spoils, experiencing a 1.45 m water level rise, equating to an increase of 11.58% due to the low permeability ash monolith located within the unconfined aquifer. A perched groundwater level was simulated within the ash. Once the groundwater had passed through or around the ash monolith it continued to flow down-gradient towards the lower portion of the pit, experiencing a minor 2.96% water level increase. Additionally, water levels for this scenario took a period of 40 years to recover, which is five years slower than the baseline scenario.

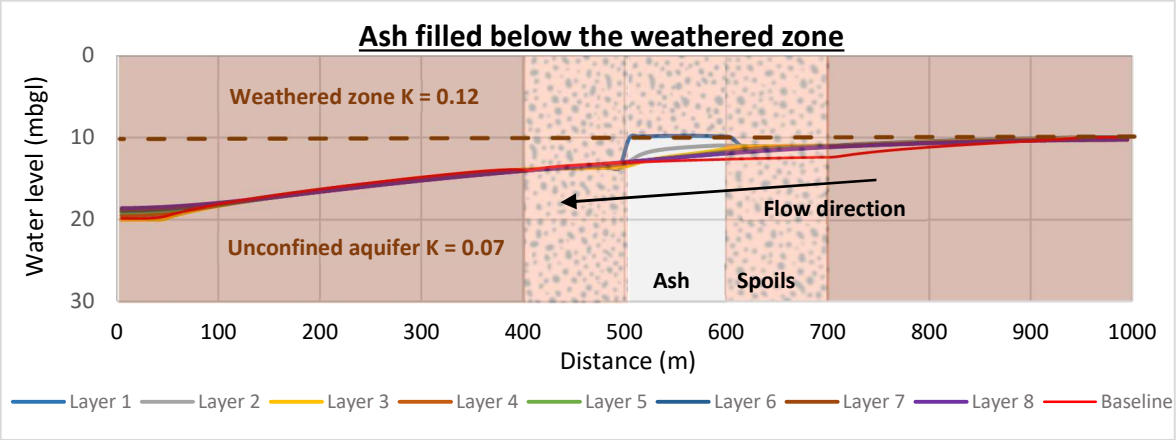

Figure 39: Scenario 6 –Simulated water levels

In summary, the simulated flow models (Figures 33 - 38) indicated that Scenarios 2 and 3 showed no significant effect on mine pit water levels as compared to Scenario 1 (Base Case). This is attributed to the fact that the placement of coal ash in these scenarios did not intercept the water table, thus had a negligible influence on the hydrogeological flow regime. Contrastingly, the results from Scenarios 4, 5 and 6 induced a water table elevation of 1.37 m, 1.52 m and 1.45 m respectively, equating to a 10.97, 12.05 and 11.58% rise in pit water levels. The water level increase evident from these three scenarios indicated that the placement of coal ash intersecting the groundwater regime successfully acted as a hydraulic barrier, consequently raising the water table. The rise in water levels is assumed to be a favourable result as it would potentially increase the volume of saturated mine spoils, reducing oxygen ingress, potentially reducing AMD formation. This study goes onto fulfilling a gap in knowledge by understanding which types of ash disposal scenarios produce a water table rise and have an effect on the hydrogeological flow regime.

5.2 Solute-transport

5.2.1 Salt load and concentrations

To understand the magnitude of potential contamination, salt loads per various scenarios were quantified. Salt loads depict the number of sulphate salts (AMD) produced per volume of water leaving the pit, equating to:

$$Salt\ load = Concentration\ x\ Volume\ flux$$

Salt loads per various backfilling scenarios alongside their respective decant water volume rates are presented in Figure 40 below.

The scenario outcomes displayed high discharge water volumes within the first three years as a result of active opencast mining. During the active stage, large volumes of water were pumped from the pit due to mine dewatering. Pumped water volumes of 314.59, 375.38 and 243.90 m^3/d were calculated for the first, second and third year respectively. Once the pumping stopped (post-closure), the water table gradually began to rebound as the mine filled up with water from adjacent aquifer inflows and rainfall infiltration. Water table recovery took a period of 30 - 40 years (depending on the scenario) to recover. Salt (sulphate) was produced, however, the salts did not migrate because the groundwater hydraulic head difference flowed towards the pit. Once the water table had recovered, groundwater began to flow out of the pit and into the surrounding aquifers, creating an apparent increase in salt load over time. The general increase in salt load was apparent from 30 years onwards, gradually increasing over time with stabilised discharge volumes.

By comparing backfill scenarios, it is evident that Scenarios 1 and 2 produced the highest salt loads, reaching a maximum of 238.02 and 227.39 g/m^3 respectively at 100 years post-closure. Scenario 3 had the third highest salt load concentration, reaching a maximum of 163.69 g/m^3, reducing salt loads by 31.23%. Scenarios 4 and 6 were similar with 101.75 and 119.70 g/m^3, which reduced salt load concentrations by 57.25% and 49.71% respectively. Scenario 5 displayed the lowest salt load leaving the pit, with a maximum cumulative salt load of 49.26 g/m^3. This is significantly lower than Scenario 1, as the placement of the ash monolith successfully contained the plume within the pit, reducing solutes leaving the pit by 79.30%.

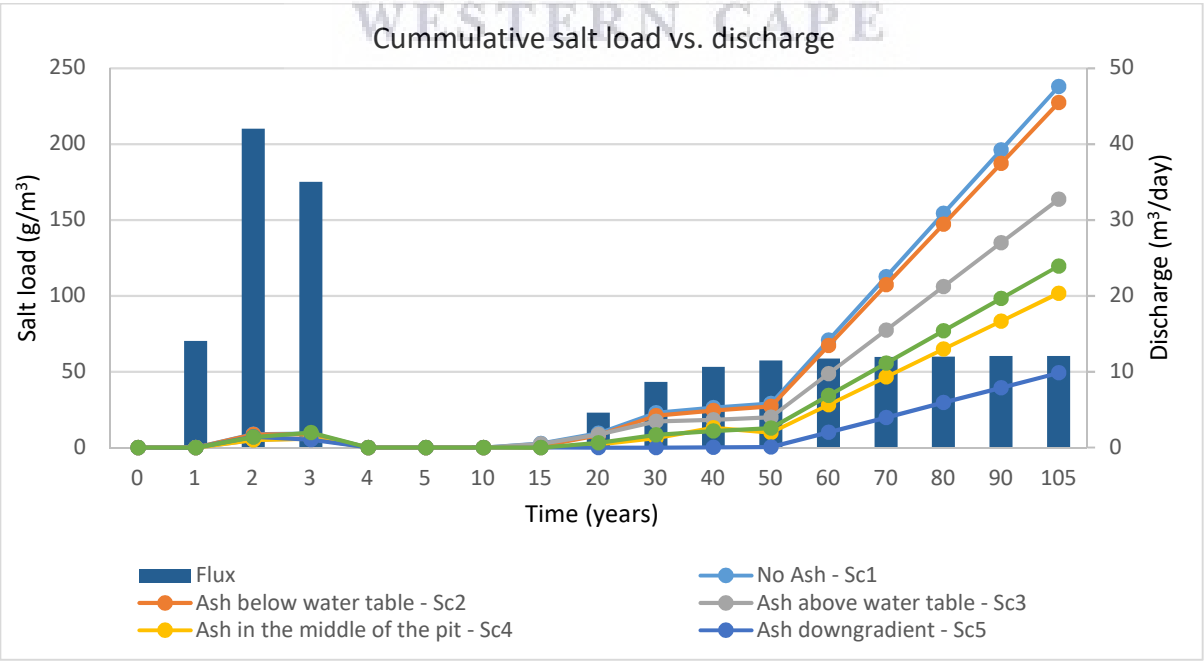

Figure 40: Salt loads vs water outflow flux rates per scenario

The accumulation of salt load concentrations within the pit for 100 years post-closure are presented as line graphs below (Figure 40– 45). The line graphs are superimposed by graphical conceptualisations of the various backfill scenarios to visually assist with its interpretation and should be noted that it is not drawn to scale.

Scenario 1 comprised of backfilling with mine spoils only (Figure 41). This scenario displayed moderate concentrations within the mine pit, accumulating in accordance with the hydraulic flow direction. Low concentrations of 151.49 g/m^3 were displayed at the upper boundary (700 m) of the pit, whereas high concentrations peaking 330.53 g/m^3 were found at the lower boundary (400 m). This scenario served as a baseline to proceeding scenarios.

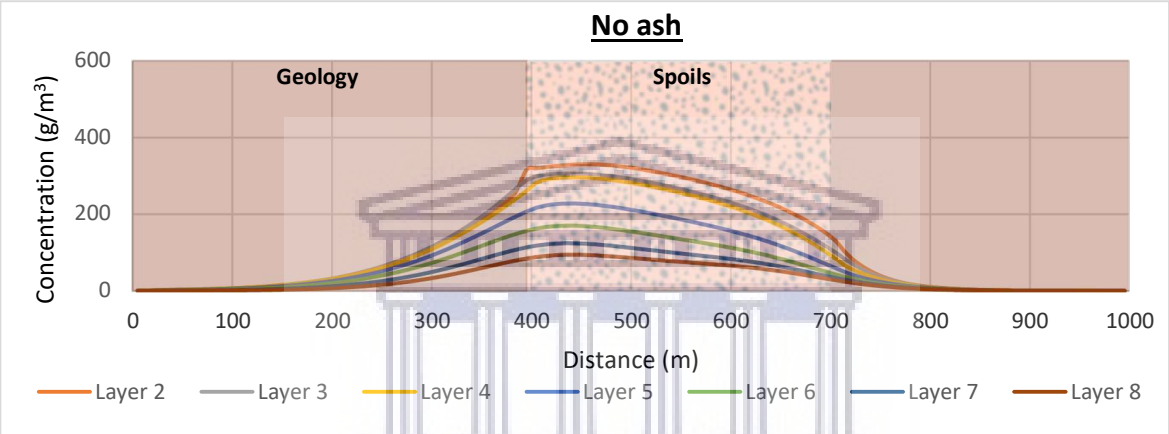

Figure 41: Scenario 1 - Concentrations of backfilling with mine spoils only

Scenario 2 involved backfilling with ash below the water table (Figure 42). Simulated concentrations were similar to that of scenario 1, displaying an increase of 6.15 - 12.60%. These concentrations range between 160.81 to 372.18 g/m^3 at the upper and lower boundaries of the pit respectively.

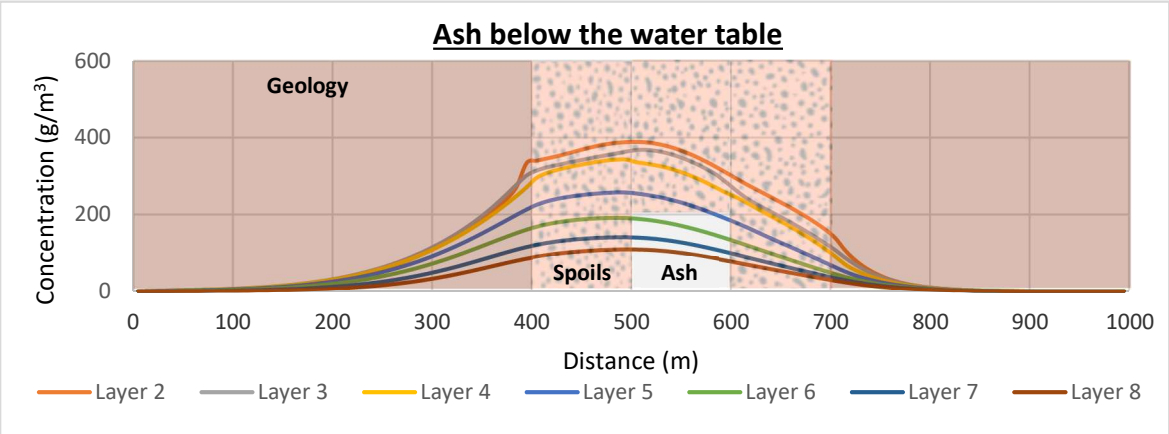

Figure 42: Scenario 2 - Concentrations of backfilling with CCRs below the water table

Scenario 3 comprised of backfilling with CCRs above the water table (Figure 43). Simulated results displayed elevated concentrations in the upper and lower portions of the pit, with significantly lower concentrations underlying the ash monolith. Concentrations reached 189.93 g/m^3 in the upper boundary of the pit, decreasing to a low of 100.97 g/m^3 at 540 m (underneath the ash monolith), and peaking at 273.56 g/m^3 in the lower boundary of the pit. This scenario displayed an averaged 35.01% decrease in pit concentrations, in comparison to Scenario 1.

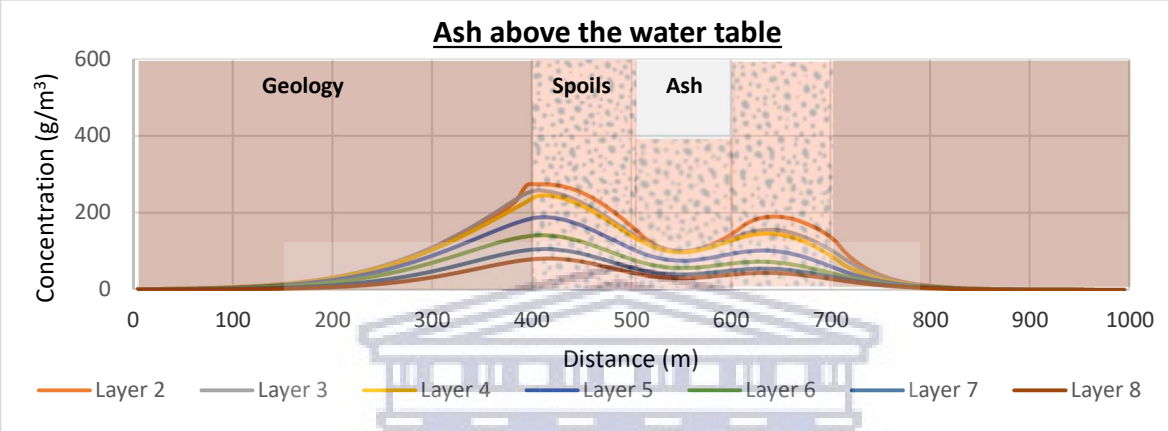

Figure 43: Scenario 3 - Concentrations of backfilling with CCRs above the water table

Scenario 4 involved backfilling with CCRs in the middle of the pit to the surface (Figure 44). Simulated results displayed elevated concentrations in the upper and lower sections of the pit, with significantly lower concentrations underlying the ash monolith. Concentrations reached 239.28 g/m^3 in the upper boundary of the pit, decreasing to a low of 37.49 g/m^3 (within the ash monolith), and peaking at 307.85 g/m^3 in the lower boundary of the pit. These solute pit concentrations displayed improvement to that of scenario 1, decreasing by 30.49%.

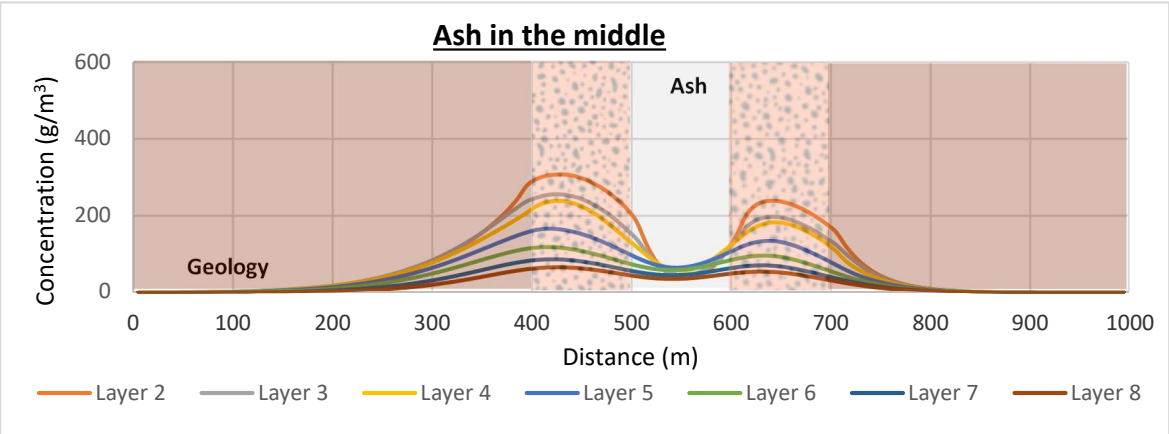

Figure 44: Scenario 4 - Concentrations of backfilling with CCRs in the middle of the pit to the surface

Scenario 5 comprised of backfilling with CCRs in the down-gradient portion of the pit (Figure 45). This scenario obtained the highest in-pit concentrations, peaking at 563.15 g/m^3 within the pit. These in-pit concentrations were significantly higher to that of scenario 1, displaying a 70.13% increase in concentration.

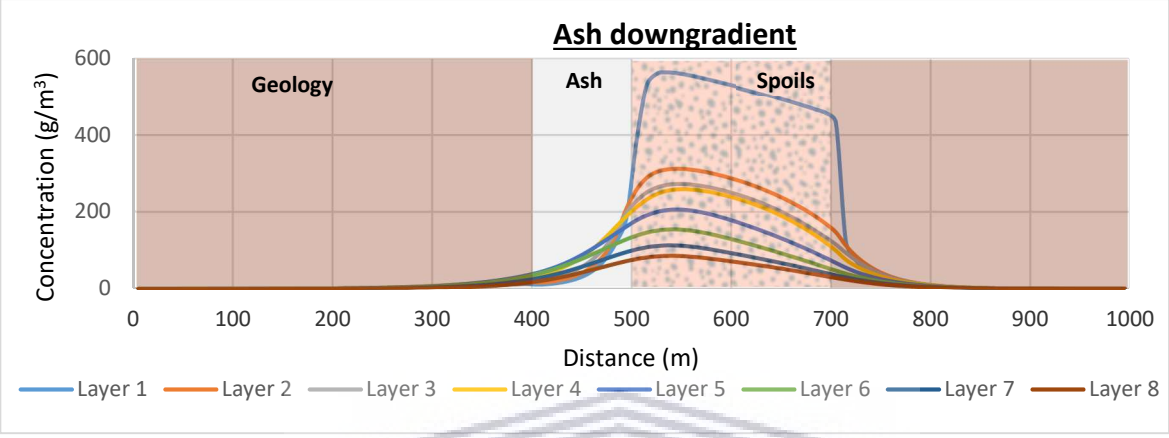

Figure 45: Scenario 5 - Concentrations of backfilling with CCRs down-gradient to the surface

Scenario 6 involved backfilling with CCRs from the pit-floor up to the weathered zone (Figure 46). Simulated results displayed considerably elevated concentrations on either side of the ash monolith. Groundwater reached concentrations of 239.67 g/m^3 in the upper portion of the pit, thereafter, flowing with the hydraulic flow direction and intercepting the ash monolith (backfilled up to the weathered zone at 10 mbgl). This interception directed the water above (via the weathered zone) or around (via the unconfined aquifer) the ash monolith, towards the lower portion of the pit which reached a concentration of 554.72 g/m^3. These in-pit concentrations were higher than that of Scenario 1, displaying a 43.02 – 49.87% increase in concentration.

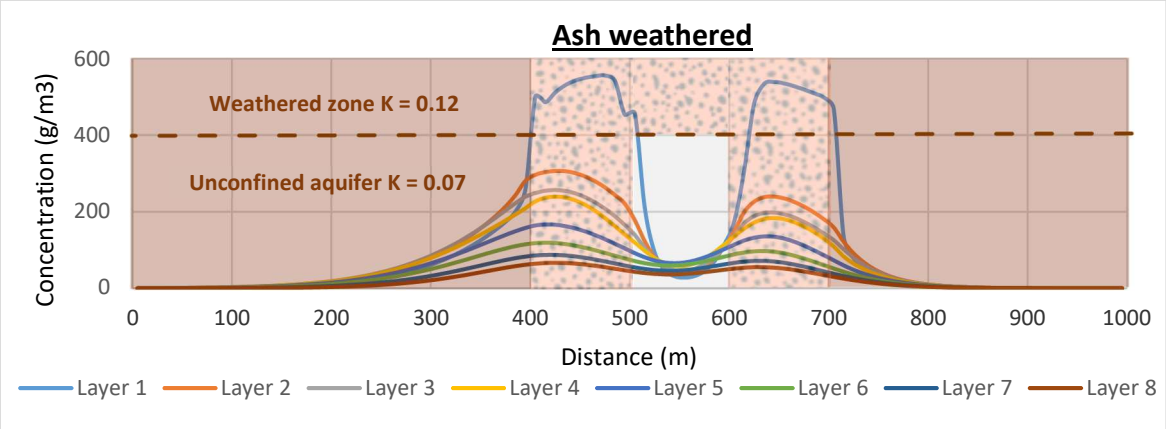

Figure 46: Scenario 6 - Concentrations of backfilling with CCRs from the pit floor to the weathered zone.

In summary, it is evident that all scenarios which backfilled with CCRs all reduced the quantity of salt loads leaving the pit. Scenario 1 was unfavourable as it had the greatest salt load concentration and Scenario 3 obtained similar concentrations (-4%). Scenarios' 2, 4 and 6 considerably reduced the salt loads by 31, 57 and 50% respectively. Scenario 5 displayed the greatest reduction of 79%. The reduction in salt loads leaving the pit, was favourable as it lessened the degree of contamination. The quantity of salt loads leaving the pit, was also dependent on the concentrations retained within the pit. Scenarios 5 and 6 displayed elevated concentrations of 70% and 50% respectively, implying that accumulation of solutes was a result of the plume being retained, which is regarded as a favourable outcome to limit plume migration.

5.2.2 Plume migration

Solutes or salts travel in groundwater to form contaminant plumes. A network of six monitoring boreholes were located within the vicinity of 100 m and 200 m east, west and south to monitor plume concentrations at 100 years post-closure (Figure 47). To gain a visual understanding of the configuration of the contaminant plumes per scenario, for 100 years post-closure, aerial representations alongside their respective conceptual models are presented from Figures 47 – 52 below.

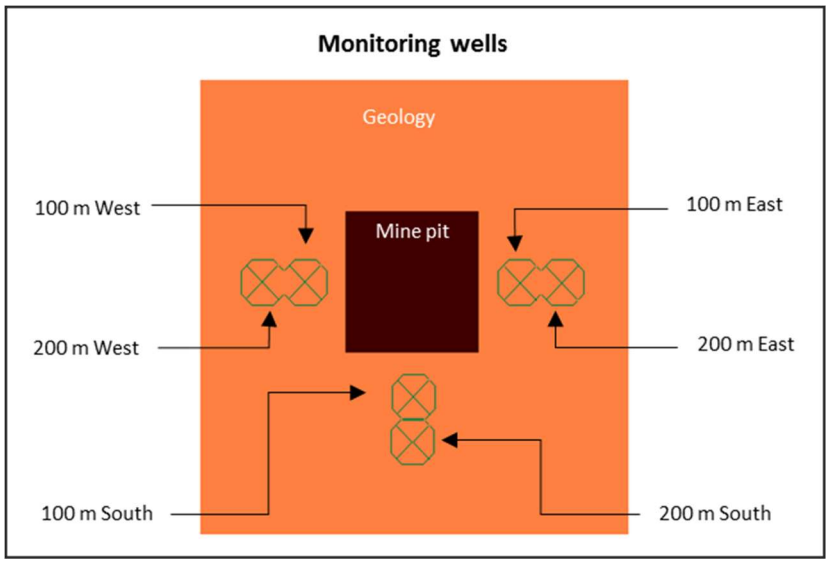

Figure 47: Monitoring boreholes

Scenario 1 (Figure 48) displayed a southward extending contaminant plume, that travelled down-gradient into the unconfined aquifer. The plume extended for *c.*200 m southwards, with concentrations of 270.29 and 171.81 g/m^3 for 100 m and 200 m southwards respectively. Monitoring boreholes placed at the east and west of the mine exhibited low concentrations of 11.08 and 8.54 g/m^3 respectively. The high concentrations of contaminants recorded at the listed boreholes display the contaminants moving southwards out of the pit. These concentrations and plume migrations served as the baseline to which subsequent scenarios were compared against.

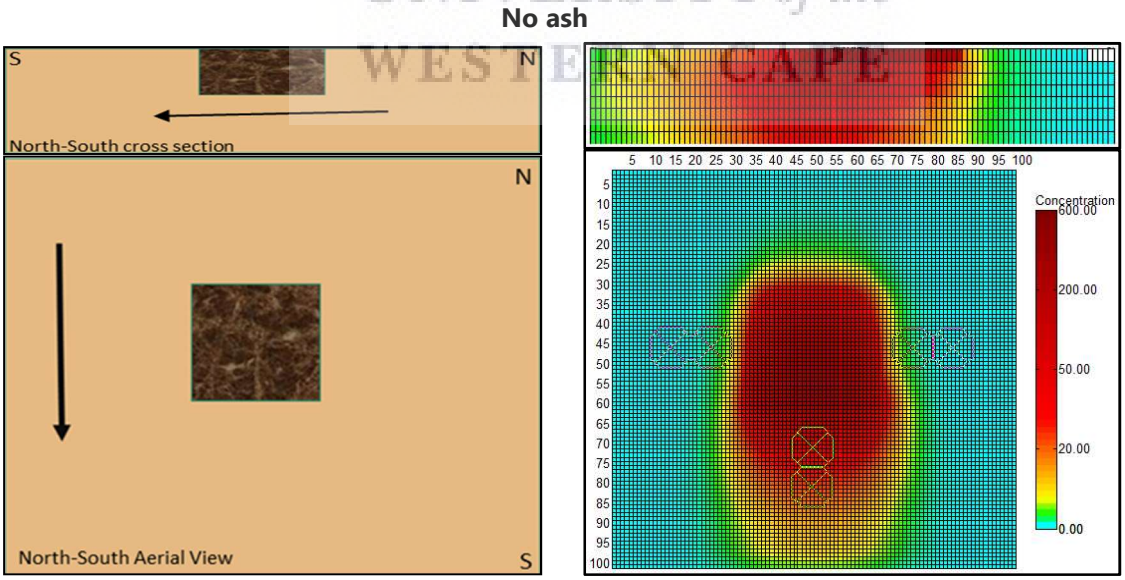

Figure 48: Scenario 1: Contaminant plume from backfilling with mine spoils only.

Scenario 2 (Figure 49) displayed a similar southward extending contaminant plume to Scenario 1, that travelled down-gradient into the unconfined aquifer. The plume extended for *c.*200 m southwards, with concentrations of 290.66 and 171.81 g/m^3 for 100 m and 200 m southwards respectively. Displaying a slightly higher concentration of *c.*20 g/m^3 at 100 m south and a similar concentration at 200 m south. Monitoring boreholes placed at the east and west of the mine exhibited exceptionally low concentrations of 9.95 and 7.95 g/m^3 respectively.

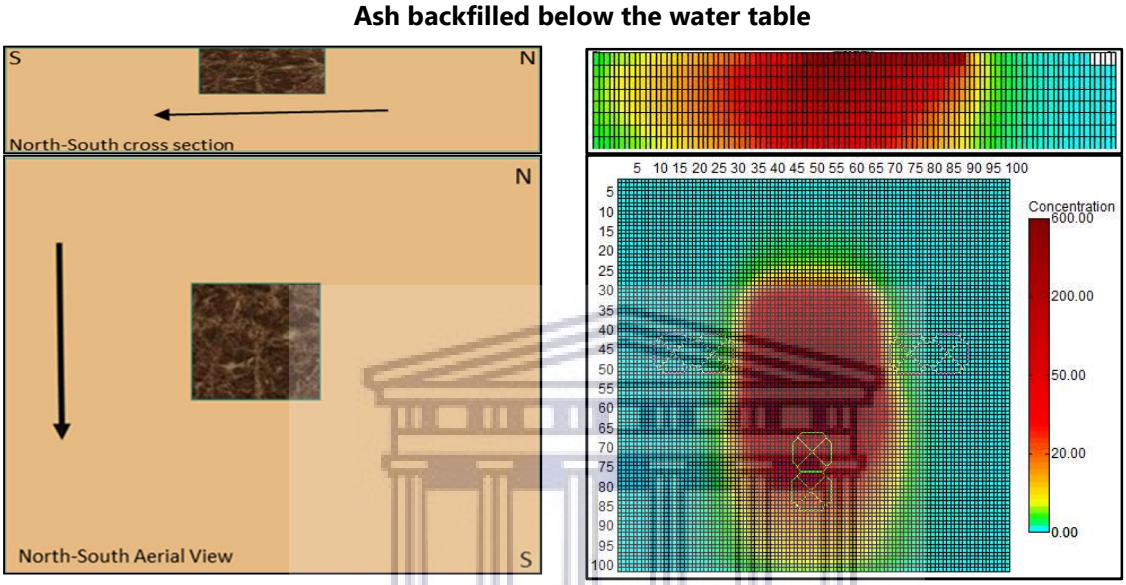

Figure 49: Scenario 2: Contaminant plume from backfilling with CCRs below the water table.

Scenario 3 (Figure 50) displayed a similar southward extending contaminant plume to Scenario 1, that travelled down-gradient into the unconfined aquifer. The plume extended for *c.*200 m southwards, with concentrations of 222.33 and 142.07 g/m^3 for 100 m and 200 m southwards respectively. This southwards plume reduced concentration by 13% in comparison to Scenario 1. The monitoring boreholes placed at the east and west of the mine exhibited low concentrations of 7.23 and 5.65 g/m^3 respectively.

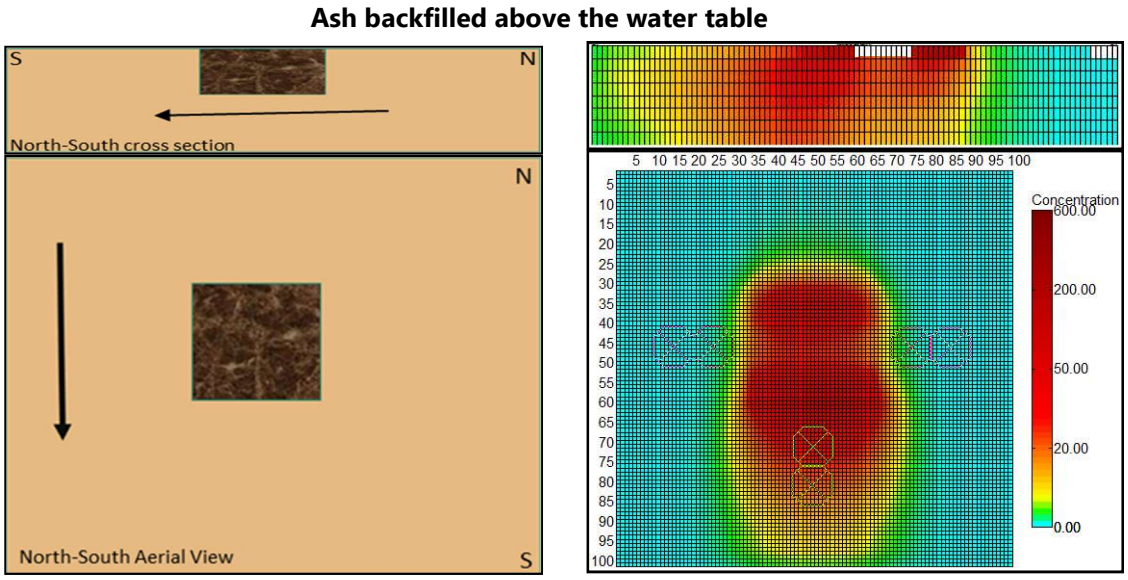

Figure 50: Scenario 3: Contaminant plume from backfilling with ash above the water table.

Scenario 4 (Figure 51) displayed a southward extending contaminant plume. The plume migrated approximately 180 m southwards, obtaining concentrations of 225.13 and 128.09 g/m^3 for 100 m and 200 m south respectively. Monitoring boreholes on the east and west of the pit displayed very low concentrations of 13.16 and 12.52 g/m^3 respectively. Indicating that the contaminant plume entering the surrounding aquifer encountered a 22% reduction in concentration.

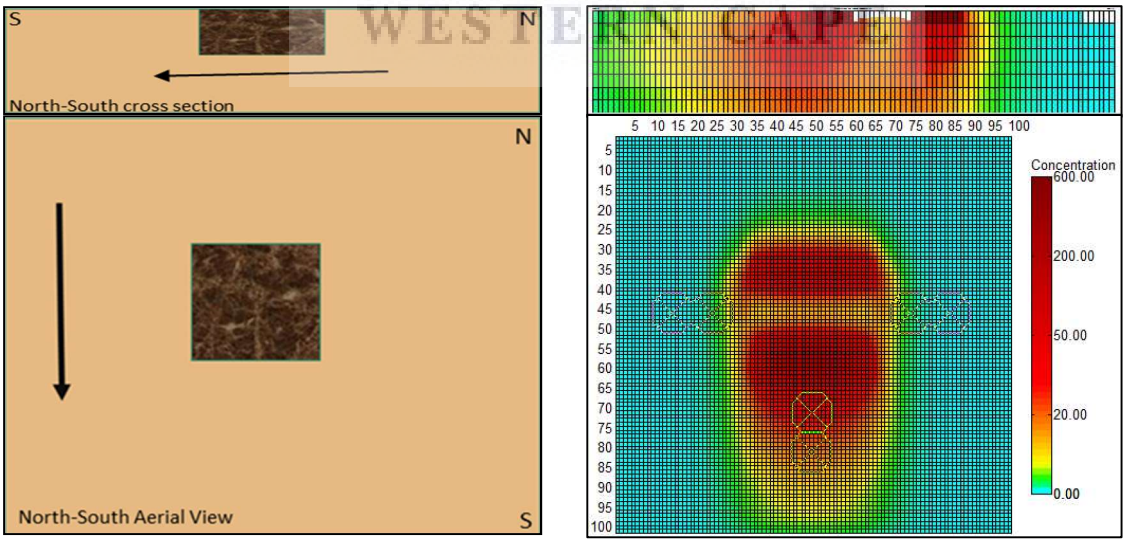

Figure 51: Scenario 4: Contaminant plume from backfilling with ash in the middle of the pit.

Scenario 5 (Figure 52) was the only scenario that did not display a southward extending contaminant plume. Instead, the majority of contaminants were contained within the pit and migrated into the aquifer as seepage at the lower east and west of the pit, creating a minor 50 m east and west contaminant plume. The monitoring boreholes located at 100 m east and west of the pit obtained concentrations of 45.30 and 41.32 g/m^3 respectively, having the highest concentrations within these boreholes amongst the scenarios. The monitoring boreholes located at 100 m and 200 m south displayed the lowest concentrations of 50.55 and 25.61 g/m^3 respectively, indicating that the contaminant plume moving southwards into the surrounding aquifer experienced an 84% reduction. This scenario offered a significant improvement in down-gradient water quality.

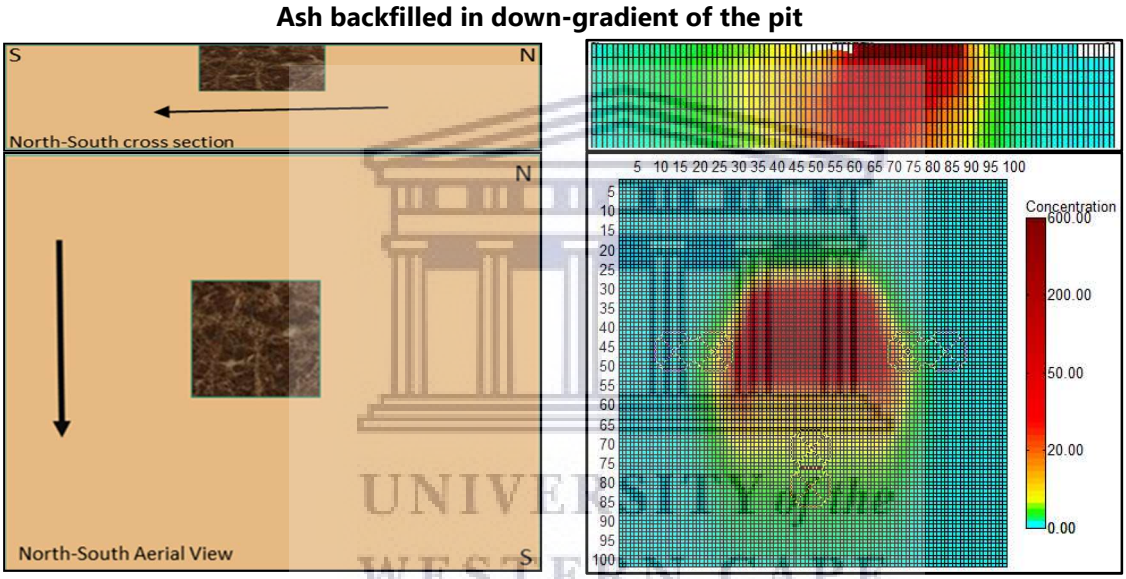

Figure 52: Scenario 5: Contaminant plume from backfilling with ash down-gradient of the pit.

Scenario 6 (Figure 53) had a moderate southwards extending plume, similar to that of Scenario 4. The contaminant plume migrated approximately 150 m south with concentrations of 225.92 and 129.17 g/m^3 for 100 m and 200 m south respectively. The monitoring boreholes on the east and west of the pit displayed very low concentrations of 14.61 and 13.96 g/m^3 respectively, indicating that the contaminant plume entering the surrounding aquifer encountered a 21% reduction in concentration.

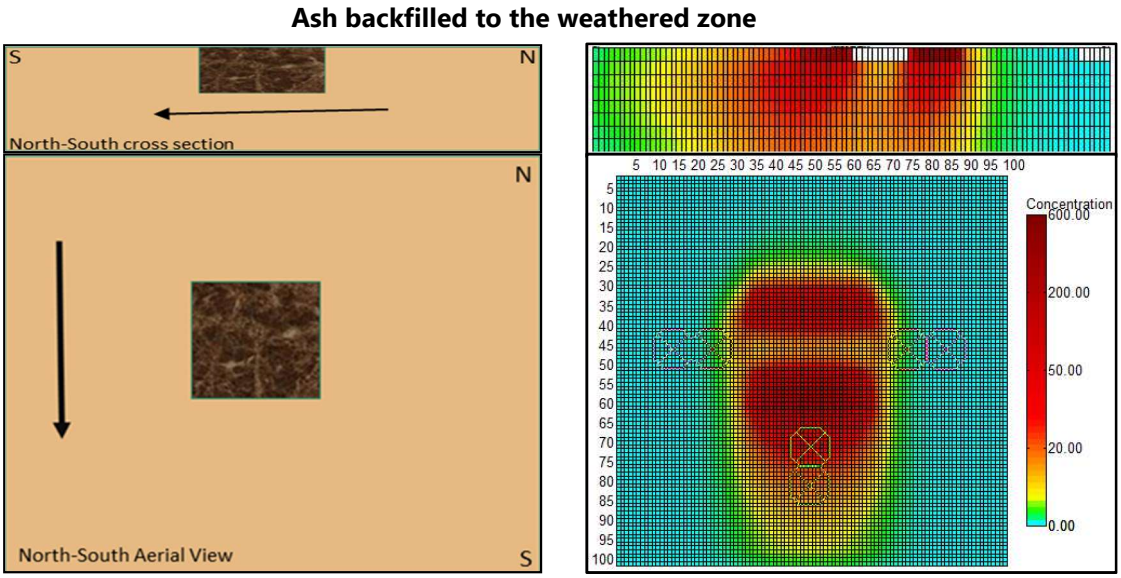

Figure 53: Scenario 6: Contaminant plume from backfilling with ash below the weathered zone.

In summary, all scenarios displayed a 150 – 200 m southwards extending plume, with the exception of Scenario 5 which displayed a 100 m east and west contaminant plume. Scenario's 1 and 2 produced the greatest contaminant plume, with equally high concentrations of 171 g/m3 at the 200 m South monitoring borehole. Suggesting that Scenario 2 did not offer a significant improvement to groundwater quality. Scenario 3 displayed the third highest contaminant plume concentration of 142 g/m^3 at 200 m south, offering a 13% improvement in groundwater quality. Scenario's 4 and 6 exhibited similar contaminant plume configurations and concentrations of 128 g/m^3 at 200 m south, which offered a 21 - 22% reduction in plume concentrations. Scenario 5 exhibited the lowest contaminant plume with negligible down-gradient concentrations and minor 100 m east and west plume migrations. Monitoring boreholes located at 100 m east and west of the pit displayed low concentrations of 14 g/m^3, whereas negligible concentrations of 0.6 g/m^3 were found in the 200 m east, west and south. Scenario 5 displayed a rapid reduction in concentration over a short distance, indicating that the plume was effectively contained. This implied that Scenario 5 was the only scenario that successfully retained the majority of the plume within the mine pit, offering an 84% improvement to groundwater quality travelling down-gradient.

To make a quantitative comparison of the contaminant plumes per scenario, the concentrations detected at each monitoring borehole are displayed and annotated from Figures 53 – 58 below.

The monitoring borehole located at 100 m South (Figure 54) displayed the highest contaminant concentrations due to its close proximity and interception with the natural groundwater flow

regime. Observed contaminant concentrations commenced at *c.*20 years due to the prolonged water level recovery that directed water towards the pit and away from the monitoring borehole. Once water levels began to recover, concentrations in the boreholes were apparent and gradually increased over time. It was evident that Scenarios 1 and 3 displayed the highest concentrations of 270.29 and 290.66 g/m^3 respectively, whereas Scenarios 2, 4 and 6 displayed similar concentrations of *c.*225 g/m^3 at 100 years post-closure. Scenario 5 displayed significantly lower concentrations of 105 g/m^3, reducing south concentrations by 81% in comparison to Scenario 1.

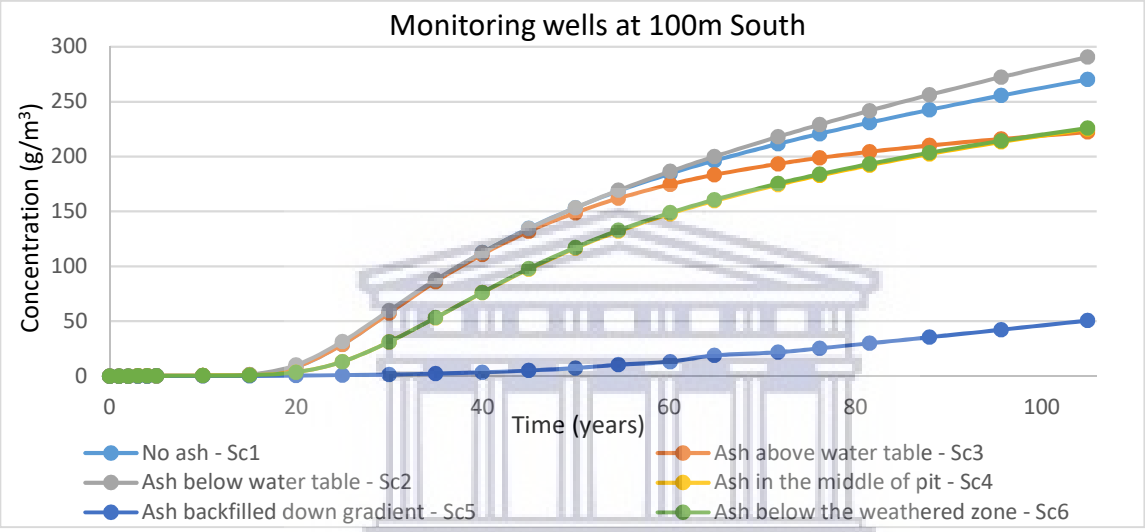

Figure 54: Concentrations at the 100 m South monitoring borehole

The monitoring borehole located at 200 m South (Figure 55) displayed the second highest concentrations due to its interception with the natural groundwater flow. It was evident that Scenarios 1 and 3 attain similarly high concentrations of *c.*170 g/m^3. Scenario 2 obtained the third highest concentration of 142 g/m, whereas Scenarios' 4 and 6 obtained concentrations of *c.*130 g/m^3. Scenario 5 displayed significantly lower concentrations of 25.61 g/m^3, reducing south concentrations by 85% which significantly improved groundwater quality.

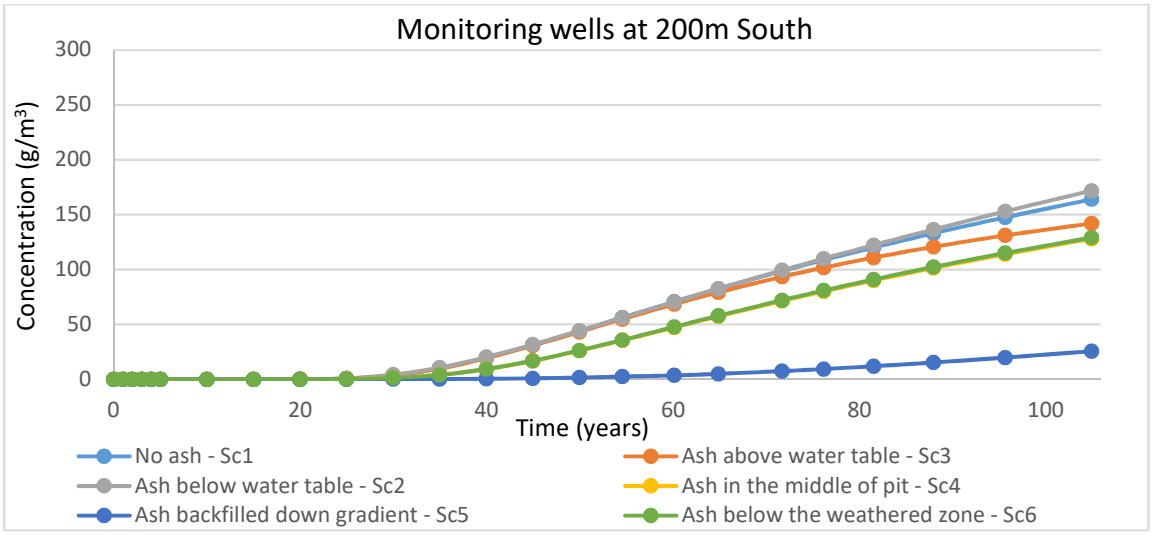

Figure 55: Concentrations at the 200 m South monitoring borehole

The monitoring borehole located at 100 m West (Figure 56) displayed low concentrations. The average concentration for all scenarios was 9.70 g/m^3, with the exception of Scenario 5 that obtained a higher concentration of 41.32 g/m^3 due to its 50 m west contaminant plume.

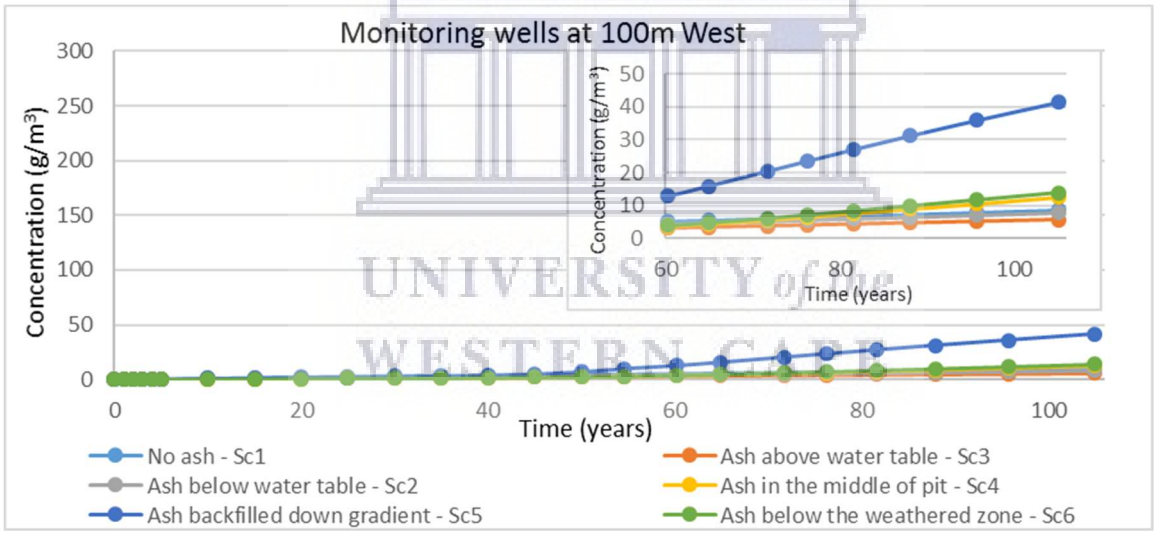

Figure 56: Concentrations at the 100 m West monitoring borehole

The monitoring borehole located at 200 m West (Figure 57) displayed very low concentrations that average 0.11 g/m^3 for all scenarios, except for Scenario 5 which had a slightly higher concentration of 0.54 g/m^3. The significantly low range in concentrations at this monitoring well does not indicate the presence of a contaminant plume.

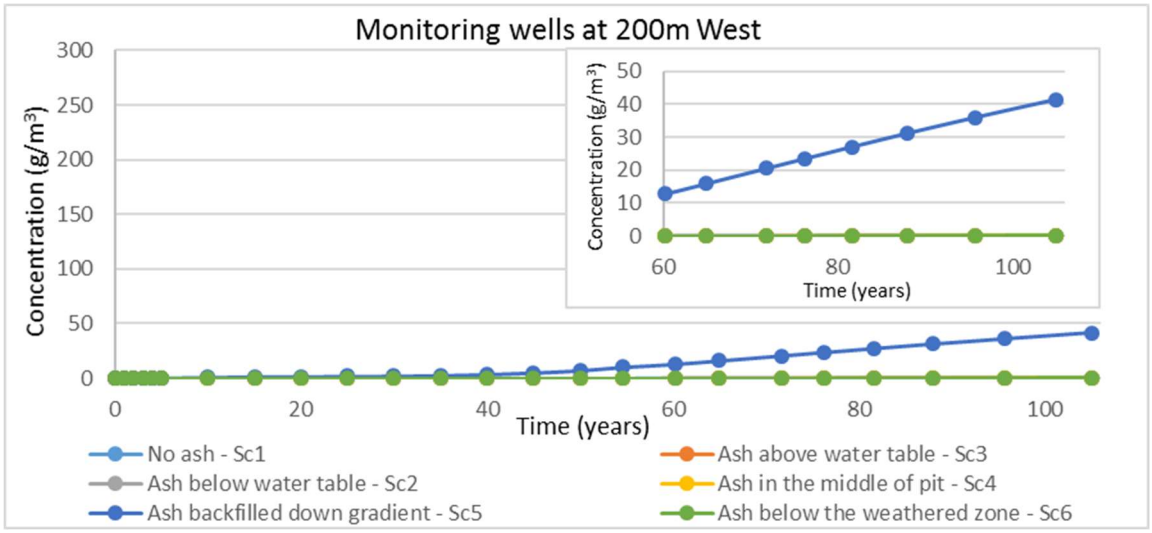

Figure 57: Concentrations at the 200 m West monitoring borehole

The monitoring borehole located at 100 m East (Figure 58) displayed fairly low concentrations. The average concentration for all scenarios was 11.21 g/m^3, with the exception of Scenario 5 that obtained a higher concentration of 45.30 g/m^3 due to its 50 m east contaminant plume.

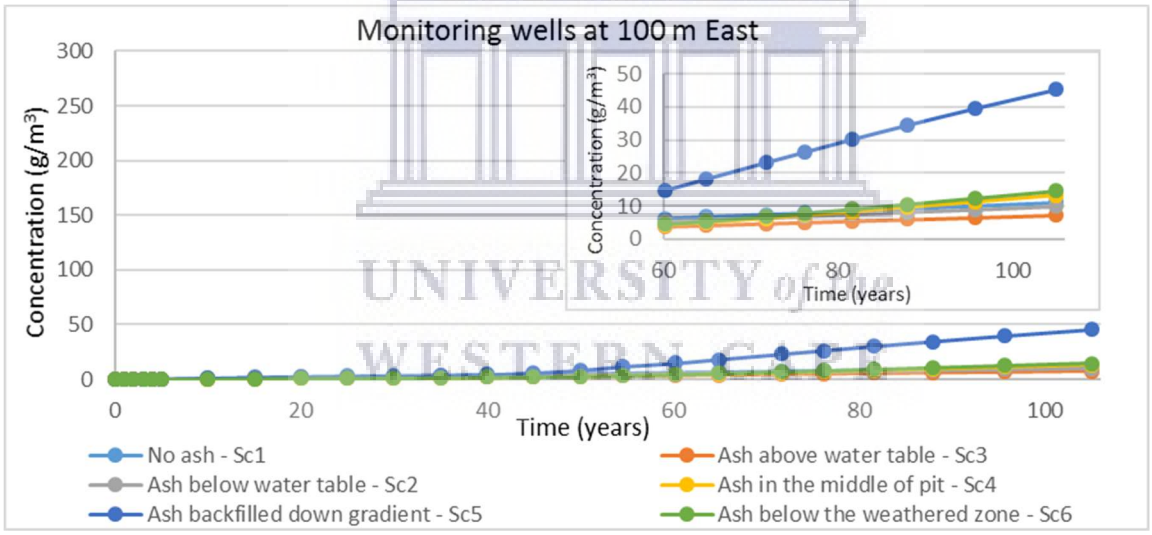

Figure 58: Concentrations at the 100 m East monitoring borehole

The monitoring borehole located at 200 m East (Figure 59) displayed very low/negligible concentrations that averaged 0.16 g/m^3 for all scenarios, with the exception of Scenario 5 which had a slightly higher concentration of 0.69 g/m^3. The significantly low range in concentrations at this monitoring well did not indicate the presence of an eastern contaminant plume.

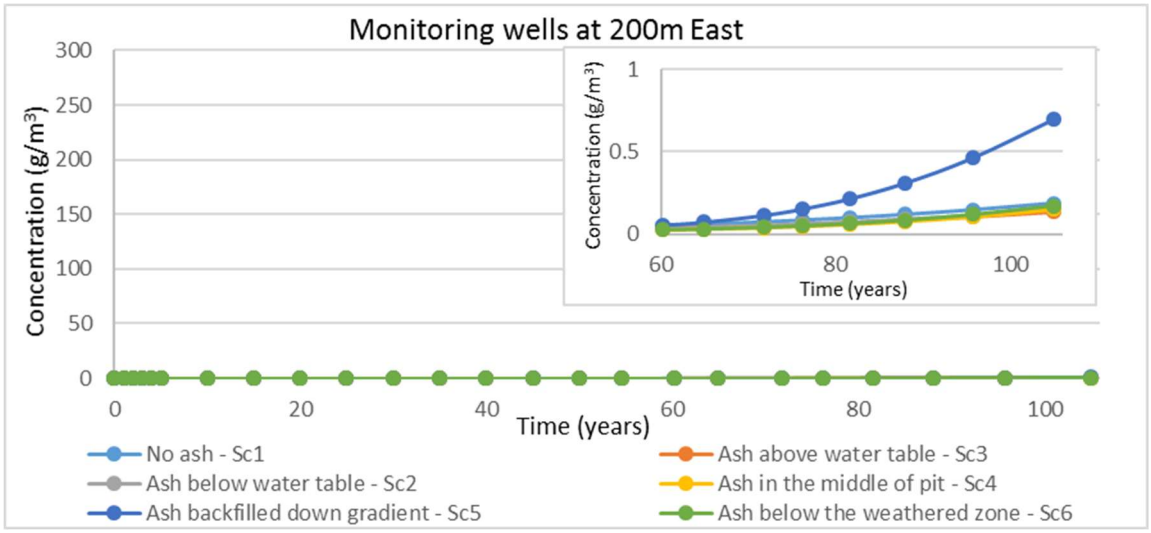

Figure 59: Concentrations at the 200 m East monitoring borehole

5.3 Risk assessment

A risk assessment was conducted to assess the long-term potential risks related to flow regimes, groundwater quality and contaminant plumes associated with each scenario.

Risks were ranked according to magnitude, duration, scale and probability based on the Risk Assessment in terms of Regulation 8 of the Waste Exclusion Regulation (National Environmental Management: Waste Act no. 59 of 2008). The rankings fall within the range of 0 to 5, which is summarised in Table 23 below. Rankings were weighted according to the following equation to assess the magnitude of impact:

$$(Magnitude + Duration + Scale) * Probability = Magnitude\ of\ impact$$

The outcome, being the magnitude of risk, will help assess whether individual backfill scenarios will have a positive, negligible or negative environmental impact. The quantifiable denotation is expressed in Table 24 below.

Table 23: A risk assessment ranking matrix summary (NEM: WA, 2008)

Magnitude: =M	**Duration: =D**
10: Very high/don't know	5: Permanent
8: High	4: Long-term (ceases with the operational life)
6: Moderate	3: Medium-term (5-15 years)
4: Low	2: Short-term (0-5 years)
2: Minor	1: Immediate
0: Not applicable/none/negligible	0: Not applicable/none/negligible
Scale: =S	**Probability: =P**

5: International	5: Definite/don't know
4: National	4: Highly probable
3: Regional	3: Medium probability
2: Local	2: Low probability
1: Site only	1: Improbable
0: Not applicable/none/negligible	0: Not applicable/none/negligible

Table 24: Magnitude of risk matrix(NEM: WA, 2008)

Significance	Environmental Significance Points	Colour Code
High (positive)	>80	H
Medium (positive)	60 to 80	M
Low (positive)	<60	L
Neutral	0	N
Low (negative)	> -60	L
Medium (negative)	-60 to - 79	M
High (negative)	≤ -80	H

Table 25: Risk assessment matrix for Scenario 1

SCENARIO 1: BACKFILLING WITH NO ASH / MINE SPOILS ONLY	ENVIRONMENTAL SIGNIFICANCE						
	M	D	S	P	STATUS	TOTA	CO
Water level Backfilling with only mine spoils contributed towards higher hydraulic conductivities within the pit. Allowing for groundwater to easily permeate through mine spoils, consequently introducing a fast water static water recovery of 35 years. The static water level recovered to a depth of 12.91 mbgl, which is comparably low in respect to the other scenarios implying that a larger volume of mine spoils will remain unsaturated. This is regarded as an unfavourable scenario as mine spoils are exposed to oxygen and precipitation accelerating AMD production.	10	5	1	5	-	-80	H
Salt load Backfilling with only mine spoils, exhibited a high cumulative salt load of 238.02 g/m^3 leaving the pit at 100 years post-closure. This displayed high solute concentrations relative to all scenarios that are attributed to an influx of oxygen and water within the mine spoils accelerating the formation of AMD.	8	5	2	5	-	-85	H
Contaminant plume migration: Backfilling with only mine spoils displayed a southward extending contaminant plume, that travelled down-gradient into the unconfined aquifer. The plume extended for *c.*200 m southwards with high concentrations of 270.29 and 171.81 g/m^3 for 100 m and 200 m southwards respectively. This scenario displayed the highest plume concentrations relative to all scenarios. This highly concentrated contaminant plume moving down-gradient has the greatest potential to threaten biotic components as well as acidify aquifers and streams.	10	5	2	5	-	-85	H
Total environmental risk (water level rise + contaminant concentration + plume migration)				-250			H

Table 26: Risk assessment matrix for Scenario 2

SCENARIO 2: ASH BACKFILLED BELOW WATER TABLE	ENVIRONMENTAL SIGNIFICANCE						
	M	D	S	P	STATUS	TOTAL	CODE
Water level Backfilling with ash below the water table had minor effects on the static water level as the ash monolith did not intercept the water table, causing no disturbance to the flow regime. This scenario allows for groundwater to easily permeate through the mine spoils, giving rise to a fast-static water level recovery of 12.79 mbgl over 35 years. This offered a minor 1.65% increase in static water levels which remained relatively low, therefore a large volume of mine spoils will continue to remain unsaturated, enhancing oxygenation within the mine spoils that accelerates AMD production.	10	5	1	5	-	-80	H
Salt load Backfilling with ash below the water table displayed a high salt load of 227.39 g/m^3. This scenario is similar to Scenario 1, offering a minor reduction of 4% in salt load. Implying that no significant improvement to groundwater quality is made.	8	5	1	5	-	-80	H
Contaminant plume migration Backfilling with ash below the water table displayed a similar southward extending contaminant plume to Scenario 1, that travelled down-gradient into the unconfined aquifer. The plume extended for 200 m southwards with similar concentrations. This highly concentrated contaminant plume moving down-gradient has great potential to threaten biotic components as well as acidify aquifers and streams.	10	5	2	5	-	-85	H
Total environmental risk (water level rise + contaminant concentration + plume migration)					-245		H

Table 27: Risk assessment matrix for Scenario 3

SCENARIO 3: ASH BACKFILLED ABOVE THE WATER TABLE		ENVIRONMENTAL SIGNIFICANCE					
	M	D	S	P	STATUS	TOTAL	CODE
Water level Backfilling with ash above the water table displayed identical groundwater levels to that of Scenario 1 (0.0005% difference), with the exception of layer 1 which had a perched water table within the ash monolith. As groundwater travelled primarily underneath the backfilled ash monolith, it permeated through the mine spoils with ease, giving rise to a fast recovery of static water levels over a period of 35 years. The static water level recovered to a low average of 12.91 mbgl, implying that a larger volume of mine spoils will remain unsaturated. This is regarded as an unfavourable scenario as mine spoils are exposed to oxygen and precipitation accelerating AMD production.	10	5	1	5	-	-85	H
Salt load Backfilling with ash above the water table displayed reasonably high solute salt loads of 163.69 g/m^3 leaving the pit at 100 years post-closure. This scenario undergoes a 31.23% reduction in salt loads leaving the pit, providing a significant improvement to groundwater quality.	8	5	2	5	-	-75	M
Contaminant Plume migration Backfilling with ash above the water table displayed a southward extending contaminant plume, that travelled down-gradient into the unconfined aquifer. The plume extended for *c.*200 m southwards, with concentrations of 222.33 and 142.07 g/m^3 for 100 m and 200 m southwards respectively. The contaminant plume displayed a 13% reduction in concentration which has the potential to threaten biotic components as well as acidify aquifers and streams.	8	5	2	5	-	-75	M
Total environmental risk (water level rise + contaminant concentration + plume migration)					-235		H

Table 28: Risk assessment matrix for Scenario 4

SCENARIO 4: ASH BACKFILLED IN THE MIDDLE OF THE PIT	ENVIRONMENTAL SIGNIFICANCE						
	M	D	S	P	STATUS	TOTAL	CODE
Water level: Backfilling with ash in the middle of the pit raised water levels over a period of 40 years. Groundwater entering the pit experiences a water table rise of 10.98% in the upper portion of the pit. Thereafter, the flow of groundwater is obstructed by the ash monolith in the middle of the pit. Forcing groundwater, it to travel either through or around the ash monolith towards the lower portion of the pit, whereby it experiences 3.17% water table rise. The ash monolith acts as a hydraulic barrier, limiting the volume of water permeating towards the surrounding geology from the upper portion of the pit. This would keep a higher volume of mine spoils saturated over a shorter period, limiting mine spoil exposure to oxygen, consequently reducing the formation of AMD.	6	5	1	5	-	-60	M
Salt load: Backfilling with ash in the middle of the pit displayed a low salt load of 101.75 g/m^3. This scenario offered a significant improvement to groundwater quality by reducing salt loads by 57.25%. Making this scenario the second most favourable in reducing salt loads out of the pit.	6	5	2	5	-	-65	M
Contaminant plume migration: Backfilling with ash in the middle of the pit displayed a southward extending contaminant plume. The plume migrated approximately 180 m southwards, obtaining concentrations of 225.13 and 128.09 g/m^3 for 100 m and 200 m south respectively. This offers a significant environmental improvement, by reducing the contaminant plume by 22%, lowering the potential to acidify aquifers and streams.	6	5	2	5	-	-65	M
Total environmental risk (water level rise + contaminant concentration + plume migration)						-190	M

Table 29: Risk assessment matrix for Scenario 5

SCENARIO 5: ASH BACKFILLED AS A MONOLITH DOWN-GRADIENT	ENVIRONMENTAL SIGNIFICANCE						
	M	D	S	P	STATUS	TOTAL	CODE
Water level: Backfilling with ash to the surface down-gradient significantly raised pit water levels. Groundwater travelled into the pit flows for 200 m downgradient, it was then intercepted the by the ash monolith. The ash monolith acted as a hydraulic barrier, limiting the volume of water permeating towards the surrounding aquifer from the pit. Introducing the fastest pit water level recovery rate of 25 years post-closure and obtaining the highest rise in pit water levels of 12.05%. This kept a larger volume of mine spoils saturated over the shortest period of time, which limited its exposure to oxygen, significantly reducing the formation of AMD.	4	5	1	5	-	-50	L
Salt load: Backfilling with ash down-gradient displayed an exceptionally low salt load of 49.26g/m^3. This scenario offered the greatest improvement to groundwater quality by reducing salt loads by 79.30%. Making this scenario the most favourable, as it attained the lowest quantity of solutes leaving the pit.	4	5	1	5	-	-50	L
Contaminant plume migration: Backfilling with ash down-gradient is the only scenario that exhibited a minor 50 m east and west contaminant plume. This greatly reduced the contaminants migrating down-gradient by 84% offering a significant improvement to groundwater quality, thus has very little potential to threaten biotic components or acidify aquifers and streams.	4	5	1	5	-	-50	L
Total environmental risk (water level rise + contaminant concentration + plume migration)						- 150	L

Table 30: Risk assessment matrix for Scenario 6

SCENARIO 6: ASH BACKFILLED BELOW THE WEATHERED ZONE	ENVIRONMENTAL SIGNIFICANCE						
	M	D	S	P	STATUS	TOTAL	CODE
Water level: Backfilling with ash below the weathered zone partially obstructed the flow regime raising pit water levels. Groundwater entering the pit experienced a water table rise of 11.58%, due to the obstruction of the ash monolith that was placed in the middle of the pit up to the weathered zone. This obstruction forced groundwater to travel, either above or through the ash monolith, towards the lower portion of the pit, whereby it experienced a water table rise of 2.96%. The rise in pit water levels occurred over a period of 40 years, whereby the upper portion of the pit primarily keeps a larger volume of mine spoils saturated, therefore limiting oxygen ingress and reducing the formation of AMD.	4	5	1	5	-	-60	M
Salt load: Backfilling with ash to the weathered zone obtained a moderately low salt load of 119.70 g/m^3 leaving the pit. This scenario offered a salt load reduction of 49.71%, making it the third most favourable scenario at is obtained lower concentrations leaving the pit.	6	5	2	5	-	-65	M
Contaminant plume migration: Backfilling with ash below the weathered zone displayed a moderate southward extending plume with concentrations of 225.92 and 129.17 g/m^3 for 100 m and 200 m south respectively. This scenario reduced contaminant plume concentrations by 21% offering an improvement to groundwater quality, limiting the potential of groundwater and river acidification.	8	5	2	5	-	-75	M
Total environmental risk (water level rise + contaminant concentration + plume migration						-200	M

The magnitude of risk per scenario is ranked by the addition of their environmental significance total, namely:

$$Environmental\ impact\ rank:$$

$$water\ level\ rise\ total + salt\ load\ total + contaminant\ plume\ migration\ total$$

Each scenario is ranked according to the following range values presented in Table 31 below:

Table 31: Magnitude of risk matrix for the comparative risk assessment

Significance	Environmental Significance Points	Colour Code
Low (negative)	≤ - 150	L
Medium (negative)	- 151 to - 209	M
High (negative)	≥ - 210	H

The comparative risk assessment presented in Table 32, indicates that all scenarios fall within three ranks, namely: high, medium and low. Scenarios 1, 2 and 3 were ranked as 'High' negative risk scenarios, as they caused the greatest degradation to groundwater quality. Scenario 1 is the base case and the least favourable scenario, as it obtained a low static water level, high salt load and a large contaminant plume. Scenarios' 2 and 3 are the second and third provided a slight improvement to groundwater quality compared to the base case. Scenarios 6 and 4 showed significant reduction in impacts and were both classified as 'Medium' risk scenarios, as they exhibited raised water levels, a reduction in salt loads and smaller contaminant plumes. These scenarios were ranked as the third and second most favourable backfilling scenarios respectively. Scenario 5, is deemed the most favourable backfilling condition as it exhibited an increase in pit water levels, significantly reduced (84%) salt loads and successfully retained contaminant plume. Scenario 5 improves the mine backfill to a 'Low' negative risk.

Table 32: Comparative risk assessment summary

A COMPARATIVE RISK ASSESSMENT SUMMARY OF ALL SCENARIOS	ENVIRONMENTAL SIGNIFICANCE	
	RANK	COLOUR CODE
Scenario 1 (Mine spoils only): Base case if no mitigation measures are undertaken. Does not prompt a rise in pit water levels, produces high salt load concentrations and easily permits the contaminant plume to migrate down-gradient.	-250	H
Scenario 2 (Ash backfilled below the water table): Did not prompt a significant rise in pit water levels, produces high salt loads and easily permits the plume to migrate down-gradient.	-245	H
Scenario 3 (Ash backfilled above the water table): Does not prompt a rise in pit water levels with a slow recovery, produces relatively high salt loads and permits the plume to migrate down-gradient.	-235	H
Scenario 4 (Ash backfilled in the middle of the pit): Prompts a significant rise in pit water levels, producing relatively low salt loads and inhibits plume migration down-gradient.	-190	M
Scenario 5 (Ash backfilled as a monolith down-gradient): Prompts the greatest rise in pit water levels, producing the lowest salt loads migrating out of the pit and successfully retains contaminants within the pit.	-150	L
Scenario 6 (Ash backfilled below the weathered zone): Prompts a fair rise in pit water levels, producing fairly high salt loads and inhibits plume migration down-gradient to an extent.	-200	M

6 CONCLUSIONS AND RECOMMENDATIONS

This chapter concludes the results, states the main findings and offers an interpretation as to what these findings may imply. Recommendations are stated to better address and understand CCR backfilling for further studies.

6.1 Conceptual scenarios

Six practical CCR monolith backfilling scenarios were conceptualised, which are as follows:

1. No CCRs/mine spoils only (Base Case);
2. CCRs backfilled below the water table;
3. CCRs backfilled above the water table;
4. CCRs backfilled from the middle of the mine pit up to the surface topography;
5. CCRs backfilled down-gradient of the pit up to the surface topography;
6. CCRs backfilled from the middle of the mine pit up to the weathered zone.

These scenarios were designed to provide a theoretical representation of the placement of CCRs under saturated and unsaturated conditions in an opencast coal mine environment. This was used to assess how CCR monolith placements (e.g. from the pit floor to the surface, beneath the surface, intercepting the water table and not intercepting the water table) would impact groundwater quality.

6.2 Hydrogeological flow regimes

Six scenario-based hydrogeological flow regimes were simulated to assess the changes in in-pit groundwater levels. Groundwater level differences were inferred by comparing the Base Case (Scenario 1) against the rest of the scenarios. The comparisons indicated that Scenarios 2 and 3 possessed similar water levels to that of Scenario 1, whereas Scenarios 4, 5 and 6 raised static water levels by 10.9, 12.0 and 11.6% respectively. Scenario 5 obtained the greatest pit water level rise over the largest area, keeping a larger volume of mine spoils saturated. This scenario is deemed favourable as mine spoil saturation is likely to reduce oxygen ingress, consequently limiting the formation of AMD.

In evaluating these scenarios, the general trend is that placing coal ash above or below the water table has a negligible effect on water levels. This is because the placement of coal ash does not obstruct the groundwater flow, thus does not alter the water table. Whereas, scenarios that place coal ash at a position which intercepts the water table, retained or inhibited the flow of water, consequently raising the water table.

6.3 Salt loads and plume migrations

Salt loads and plume migrations were assessed to identify the impact on groundwater quality per scenario. The changes in salt loads and plume migrations from backfilling with coal ash were compared against backfilling with mine spoils only (Scenario 1).

All CCR backfill scenarios reduced the salt loads leaving the mine pit by between 4 - 79%. The highest salt load was observed in the base case scenario (Scenario 1), making it the least favourable scenario as it had the greatest potential to contaminate the surrounding aquifer. Scenario 2 displayed similar salt loads, offering a minor 4% reduction. Scenarios 3, 4 and 6 substantially improved groundwater quality leaving the pit, by reducing salt loads by 31, 57 and 50% respectively. Scenario 5 displayed the lowest salt load of 49 g/m^3, which offered the greatest improvement to groundwater quality leaving the pit by reducing salt loads by 79%. This improvement in groundwater quality was attributed to the placement of the ash monolith (positioned down-gradient up to the surface topography), which acted as a hydraulic barrier and successfully contained the plume within the pit.

The contaminant plume migrated approximately 150 – 200 m down-gradient under all scenarios, with the exception of Scenario 5 which displayed a 100 m lateral contaminant plume. Scenarios 1 and 2 produced the largest contaminant plume, with equally high concentrations observed at the 200 m South monitoring boreholes. This suggests that Scenario 2 did not offer a considerable improvement to groundwater quality. Scenario 3 offered a slight improvement (13%) in groundwater quality, whereas Scenarios 4 and 6 reduced concentrations by 21 - 22%. Scenario 5 demonstrated a minor 100 m lateral contaminant plume, with negligible concentrations down-gradient. The rapid reduction in concentration over a short distance implied that the plume was contained, making this the only scenario that successfully retained the majority of the plume within the mine pit, thus offering an 84% improvement to groundwater quality travelling down-gradient.

6.4 Risk assessment

To evaluate the risks associated with various backfilling scenarios, the changes in water levels, salt loads and contaminant plumes were integrated into a long-term comparative risk assessment. In ranking the risks associated with these factors, it is apparent that the Base Case scenario (Scenario 1) caused the greatest negative groundwater risk, whereas backfilling with CCRs (under any scenario) offers an environmental improvement. Scenarios 2 and 3 are ranked as ‘High’ negative risk scenarios due to their low static water levels, high salt loads and large

contaminant plumes, providing only a slight improvement to down-gradient groundwater quality. Scenarios 6 and 4 are both classified as 'Medium' risk scenarios, exhibiting raised water levels, a reduction in salt loads and smaller contaminant plumes. Scenario 5 was the only 'Low' negative risk scenario, significantly reducing salt loads by 84% and retaining the contaminant plume.

It is thus concluded that all CCR backfilling scenarios provide an environmental improvement to groundwater quality. The beneficial extent is dependent on the placement/design of the CCR monolith in relation to site specific receptors (humans, vegetation, rivers etc.). For example, if the receptors are located down gradient, Scenario 5 would be the most favourable scenario. This is because it retains the contaminant plume within the pit, reducing down-gradient salt loads and plume migrations. However, should receptors be positioned adjacent to the pit (perpendicular to the groundwater flow direction), Scenarios 4 and 6 would be the most favourable because they limit the lateral plume migration. Therefore, it is concluded that each scenario has the potential to provide an improvement (relative to the Base case) and can be beneficially applied under different site conditions.

6.5 Recommendations

This study evaluated pit water levels and contaminant plume migration based on a theoretical site. Thus, it is recommended that a field-based pilot study and site-specific flow model, with the intent of giving an accurate depiction of groundwater level changes, be implemented. Having a specific study site will aid in providing an in-depth understanding of the hydrogeological flow regime and account for groundwater flow diversions towards potential receptors (e.g. rivers and groundwater users).

In addition, it is recommended to couple flow models with geochemical ones in order to represent the processes between the AMD produced from the mine spoils and interactions with the coal ash. Coupling these models is a challenge, as feedback loops are needed between the secondary mineralisation and chemical speciation model to the hydraulic properties to change the flow rates in the ash monolith. In order to achieve this, foreseeable code development may be required for this application.

Implementing these recommendations will provide an in-depth understanding of the flow and geochemical properties of backfilling with CCRs in a site-specific context, which may assist ESKOM in reducing their on-site ash disposal volumes, while providing environmental benefits to groundwater quality backfilling with CCR monoliths into opencast coal mines.

REFERENCES

Ahmaruzzaman, M. (2010). A review on the utilization of fly ash, Progress in Energy and Combustion Science, pp. 327–363. doi:10.1016/j.pecs.2009.11.003.

Akinyemi, S. A. (2011). Geochemical and mineralogical evaluation of toxic contaminants mobility in weathered coal fly ash: as a case study, Tutuka dump site, South Africa. Masters thesis. Cape Town, South Africa: The University of the Western Cape.

Akinyemi, S. a., Akinlua, A. Gitari, W. M., Akinyeye, R. O. and Petrik, L. F. (2011). The Leachability of Major Elements at Different Stages of Weathering in Dry Disposed Coal Fly Ash, Coal Combustion and Gasification Products, 3, pp. 28–40. doi: 10.4177/CCGP-D-11-00005.1.

Alexopoulos, D., Itskos, G., Vasilatos, C., Koukouzas, N. and Stamatakis, M. (2013). Mine wastewater treatment by highly calcareous and siliceous fly ash: a comparative study, 2013 World of Coal Ash (WOCA) Conference.

Anderson, M. P., Wisner, W. W., and Hunt, R. J. (2002). Applied Groundwater Modeling. Madison, USA: Academic Press

Anderson, M.P, and Woessner, W.W. (2002). Applied Groundwater Modeling.2nd Edition. Elsevier Inc Oxford.

American Society for Testing and Materials (ASTM) (2019). Standard specification for coal fly ash and raw of calcined natural pozzolan for use in concrete, ASTM International, West Conshohocken.

Aubertin, M., Bussiere, B., and Bernier, L. (2002). Environment et gestion des rejets miniers. Montreal, QC, Canada: Presses. Int. Polytechnic

Aubertin, M. (2013). Waste rock disposal to improve the geotechnical and geochemical stability of piles. Montreal: 23rd World Mining Congress.

Aubertin, M., ASCE, M., Bussiere, B., Pabst, T., James, M., and Mbonimpa, M. (2016). Review of reclamation techniques for acid generating mine wastes upon closure of disposal sites. Geo-Chicago 2016, pp. 1–16. doi: 10.1061/9780784480137.034.

Aubertin, M., Bussiere, B., James, M., Mbonimpa, M., and Chapuis, R. P. (2011). Analyses of water diversion along inclined covers with capillary barrier effects. Canadian Geotechnical, 46, 1146-1164.

Barnett, B., Townley, L. R., Post, V., Evans, R. E., Hunt, R. J., Peters, L., Richardson, S., Werner, a. D., Knapton, a. and Boronkay, a. (2012). Australian groundwater modeling guidelines, Waterlines Report Series, (82), pp. 1–191. Available at file:///R:/Literature/Angela/hydrogeology methods/Waterlines-82-Australian-groundwater-modeling-guidelines.pdf.

Barlow, P.M., Harbaugh, A.W., (2006). USGS directions in MODFLOW development. Ground Water 44 (6), 771e774.

Bear, J., and Cheng, D. (2010). Modeling groundwater flow and contaminant transport. USA: Springer

Bear, J. 1979. Hydraulics of Groundwater. New York, McGraw-Hill, Book Co.pp. 567.

Benner, S. G., Blowes, D. W., and Ptacek, C. J. (1997). A full-scale porous reactive wall for prevention of acid mine drainage. Groundwater Monitoring and Remediation.

Bittner, A. and Kondziolka, J. (2017). Evaluation of Groundwater Protectiveness of Potential Surface Impoundment Closure Options. Cambridge, MA. Conference proceedings from the 2017 World of Coal Ash.

Black, A. (2017). The need for improved representation of groundwater-surface water interaction and recharge in cold temperate – subarctic regions. Lappeenranta, Finland. Conference proceedings from IMWA Mine Water and Circular Economy 2017, pp. 680–688.

Borm, P. (1997). Toxicity and occupational health hazards of coal fly ash (CFA). A review of data and comparison to coal mine dust, The Annals of Occupational Hygiene, 41(6), pp. 659–676. doi: 10.1016/S0003-4878(97)00026-4.

British Petroleum (2017). BP Statistical Review of World Energy 2017, British Petroleum, (66), pp. 8–11. doi: http://www.bp.com/content/dam/bp/en/corporate/pdf/energy-economics/statistical-review-2017/bp-statistical-review-of-world-energy-2017-full-report.pdf.

Brick, C. (1998). Unpublished notes from Geology 431-Geochemistry. Montana: Missoula, MT: University of Montana.

Brigham Young University, Environmental Modeling Research Laboratory. (2000). Groundwater Modeling System (GMS), GMS 3.1 Tutorials.

Brodie, M. J., Broughton, L. M., and MacG Robertson, A. (1994). A conceptual rock classification system for waste management and a laboratory method for ARD prediction from rock pile. Montreal Canada: Second International Conference on the Abatement of Acidic Drainage.

Buczko, U., Gerke, H. H. and Hüttl, R. F. (2001). Spatial distributions of lignite mine spoil properties for simulating 2-D variably saturated flow and transport, Ecological Engineering, 17(2–3), pp. 103–114. doi: 10.1016/S0925-8574(00)00151-8.

Cadle, AB., Cairncross, B., Christie, AD.M. and Roberts, D.L. (1990). The permo-triassic coal-bearing deposits of the Karoo basin, Southern Africa. Economic geology research unit (WITS), Information circular. No. 218, March 1990. 37 p.

Cairncross, B. (1986). Depositional Environments of the Permian Vryheid Formation in the East Witbank Coalfield, South Africa: A Framework for Coal Seam Stratigraphy, Occurrence and Distribution. Unpublished PhD thesis. Johannesburg, South Africa: The University of Witwatersrand, Johannesburg.

Cairncross, B. (2001). An overview of the Permian (Karoo) coal deposits of southern Africa, Journal of African Earth Sciences, 33 (3–4), pp. 529–562. doi: 10.1016/S0899-5362(01)00088-4.

Cairncross, B., and Cadle, A. B. (1987). A genetic stratigraphy for the Permian coal-bearing Vryheid Formation in the east Witbank Coalfield, South Africa. South African Journal of Geology, 90 (219 - 230).

Cairncross, B., and Cadle, A. B. (1988). Depositional paleoenvironments of the coal-bearing Permian Vryheid Formation in the east Witbank Coalfield, South Africa. South African Journal of Geology, 1(91), 1-17.

Campbell, P. G., and Price, W. A. (1993). How to assess potential biological effects on subaqueous Disposal of Mine Tailings - Literature review and recommended tools and methodologies. Canada. MEND Mine Environment Neutral Drainage

Campbell, R., Botha, L. J. and Beekman, H. E. (2005). Reactive-transport modeling of irrigation effluent in the weathered zone aquifer at the Sasol Goedehoop site, Secunda. Report for the Water Research Commission Project K5/1432.

Carlson, C. L., and Adriano, D. C. (1993). Environmental impacts of coal combustion residues. Journal of environmental quality, 22:227-247.

Chiang, W.H. and Kinzelbach, W., (2001). 3D-Groundwater Modeling with PMWIN: A Simulation System for Modeling Groundwater Flow and Pollution. Springer-Verlag, New York, 346 pp.

Chen, X. and Chen, X. (2003). Sensitivity Analysis and Determination of streambed leakance and Aquifer Hydraulic properties. Journal of Hydrology, Vol.284, pp.270-284

Clarke, R.T., Rother, P., and Raybould, A.F. (2002). Confidence limits for regression relationships between distance matrices: Estimating gene flow with distance. Journal of Agricultural, Biological, and Environmental Statistics, Vol. &, pp. 361-372.

Climate Information Platform (2001). Csag.uct.ac.za. 2001. [online] Available at: <http://www.csag.uct.ac.za/climate-services/cip/> (Accessed 26 March 2020).

Council of Geosciences (2003). Coal fields Republic of South Africa Map.

Deschaine, L., Guvanasen, V., Pinter, J., and Tonwley,L/R. (2011). Optimised Planning for Management of Integrated Surface Water and Groundwater Systems.

`Devia, G. K., Ganasri, B. P. and Dwarakish, G. S. (2015). A review on hydrological models, Aquatic Procedia, 4(Icwrcoe), pp. 1001–1007. doi: 10.1016/j.aqpro.2015.02.126.

Doherty, J. (2001). Improved Calculations for Dewatered Cells in MODFLOW.

Dommisse, J. P. (2015). Mathematical modeling of solute transport in a Heterogeneous aquifer by James Phillip Dommisse. A thesis submitted to the Victoria University of Wellington in partial fulfilment of requirements for the degree of Master of Science.

Donald, S. B., Holl, N., Landine, P., and Welch, D. (1997). Recent hydrogeological developments in uranium mine tailings management in Canada: the Key Lake Experience. Athens, Greece: IAEG International Symposium on Engineering Geology and the Environment.

Du Toit, A. L. (1954). The geology of South Africa. Edinburgh, United Kingdom. 3rd edition, Oliver and Boyd, pp. 611.

Dutoit, G., (2014). Groundwater impact study for the proposed mineral residue deposit expansion, discard retreat plant and briquetting plant project at Anglo American, Goedehoop Colliery. Report compiled for Geovicon Environmental (Pty) Ltd.

Eberhard, A. (2011). The future of South African coal: market, investment and policy challenges. Stanford, United States: Freeman Spogli Institute for International Studies at Stanford University, Working Paper No. 100.

Energy international Administration. (2018). International Energy Outlook Executive Summary, July 2018, pp. 1–3. Available at: https://www.eia.gov/outlooks/ieo/pdf/exec_summ.pdf.

Electric Power Research Institute (2013). Attachment 12 physical and chemical characteristics of wastes special waste landfill permit big sandy plant – ash pond closure Lawrence County, Kentucky. Report on Technical Update - Coal Combustion Products - Environmental Issues.

Electricity Supply Commission (2009). Abridged annual report. Accessed on 15 Jun 2017 from www.eskom.co.za

Electricity Supply Commission (Eskom) (2016). Ash management in Eskom. Accessed on the 9 August 2017 from www.eskom.co.za.

Essink, O. (2000). Groundwater Modeling. Utrecht University Interfaculty Centre of Hydrology Utrecht Institute of Earth Sciences Department of Geophysics. Report no. L4018/GWMI.

Eze, C. P., Nyale, S. M., Akinyeye, R. O., Gitari, W. M., Akinyemi, S. A., Fatoba, O. O. and Petrik, L. F. (2013). Chemical, mineralogical and morphological changes in weathered coal fly ash: A case study of a brine impacted wet ash dump, Journal of Environmental Management, 129, pp. 479–492. doi: 10.1016/j.jenvman.2013.07.024.

Feinstein, D. T., Fienen, M. N., Reeves, H. W. and Langevin, C. D. (2016). A semi-structured MODFLOW-USG model to evaluate local water sources to wells for decision support, Groundwater, 54(4), pp. 532–544. doi: 10.1111/gwat.12389.

Ferguson, K. D., and Erickson, P. M. (1998). Pre-mine prediction of acid mine drainage. Berlin, Heidelberg: Springer-Verlag.

Fetter, C.W. (1994). Applied hydrogeology. 3rd ed. New Jersey: Prentice Hall.

Fourie, P. (2007). The Description of physicochemical processes in coal mine spoils and associated production of acid mine drainage, University of the Free State. Bloemfontein, Free State, South Africa: Msc. Thesis.

Freeze, R. A., and Witherspoon, P. A. (1967). Theoretical analysis of regional groundwater flow. Water Resources Research, 623-634.

Freeze, R. A. and Cherry, J. A., 1979, Groundwater. Prentice Hall, USA, 620 p

Groundwater Consulting Services (2014). Kusile Power Station Hydrogeological Investigation Report. A hydrogeological report submitted for Iliso Consulting, GCS Project Number: 13-427, v 2.

Gitari, M. W., Fatoba, O. O., Nyamihingura, A., Petrik, L. F., Vadapalli, V. R. K., October, A., Nel, J., Dlamini, L., Gericke, G. and Mahlaba, J. S. (2009). Chemical weathering in a dry ash dump: an insight from physicochemical and mineralogical analysis of drilled cores, Journal Environmental Science and Health, 41, pp. 1729–1747.

Gitari, W. M., Petrik, L. F., Etchebers, O., Key, D. L. and Okujeni, C. (2008). Utilization of fly ash for treatment of coal mines wastewater: Solubility controls on major inorganic contaminants, Fuel, 87(12), pp. 2450–2462. doi: 10.1016/j.fuel.2008.03.018.

Gitari, M.W., Fatoba, O.O., Nyamihingura, A., Petrik, L.F., Vadapalli, V.R.K., Nel, J., October, A., Dlamini, L., Gericke, G., and Mahlaba, J.S. (2009). Chemical weathering in a dry ash dump: An insight from physicochemical and mineralogical analysis of drilled cores. Conference proceedings from the World of Coal Ash 2009, May 4-7, Lexington Kentucky, USA. http//www.flyash.info .

Gitari, W. M., Petrik, L. F., Etchebers, O., Key, D. L., Iwuoha, E. and Okujeni, C. (2008). Passive neutralisation of acid mine drainage by fly ash and its derivatives: A column leaching study, Fuel, 87(8–9), pp. 1637–1650. doi: 10.1016/j.fuel.2007.08.025.

Gitari, W. M., Somerset, V. S., Petrik, L. F., Key, D., Iwuoha, E. and Okujeni, C. (2005). treatment of acid mine drainage with fly ash : removal of major, minor elements, SO4 and utilization of the solid residues for wastewater, World of Coal Ash (WOCA).

Glasspool, I. J. (2003). Hypautochthonous-allochthonous coal deposition in the Permian, South Africa, Witbank Ban No. 2; a combined approach using sedimentology, coal petrology and palaeontology. International Journal of Coal Geology, 53, 81-135.

Geo Pollution Technologies. (2004). Geohydrological Report for the Proposed Underground Mining at Brown Shaft 2 Goedehoop North Colliery, Mpumalanga Province.

Geo Polllution Technologies. (2016). Hydrogeological impact study for the proposed Leeuwfontein Colliery, Driefontein section for Geovicon Environmental (Pty) Ltd.

Grobbelaar, R., Usher, B., Cruywagen, L., de Necker, E. and Hodgson, F. (2004). Long-term impact of intermine flow from collieries in the Mpumalanga coalfields, Water Research Commission. doi: WRC Report No. 1056/1/04.

Hancox, P. J. and Gotz, A. E. (2014). South Africa's coalfields - A 2014 perspective, International Journal of Coal Geology, 132, pp. 170–254. doi: 10.1016/j.coal.2014.06.019.

Hans-Wilhelm. (2016). World Energy Resources 2016. World Energy Council, Resources 2016 Summary.

Harbaugh, A.W., E.R. Banta, M.C. Hill, and M.G. McDonald. (2000). MODFLOW-2000, the U.S. Geological Survey Modular Ground-Water Model—User guide to modularization concepts and the ground-water flow processes: U.S. Geological Survey Open-File Report 00-92, 121 p.

Harbaugh, A.W. (2005). MODFLOW-2005, the U.S. Geological Survey modular ground-water model – the Ground-Water Flow Process: U.S. Geological Survey Techniques and Methods 6-A16

Harbaugh, A.W and McDonald, M.G. (1996). User's documentation for MODFLOW- 96 an update to the US Geological Reddy district, Andhra Pradesh using finite difference method. M. Tech thesis Submitted to Osmania University, Hyderabad, India.

McDonald M. D., and Harbaugh, A. W. (1988). A modular three-dimensional finite-difference flow model. Techniques of Water-Resources Investigations of the U.S. Geological Survey, Book 6.

Hardin, C. D. and Daniels, J. L. (2011). Preserving structural fill and mine reclamation as acceptable beneficial reuse of CCRs. Denver, CO, USA. Conference proceedings from the 2011 World of Coal Ash (WOCA) Conference

Hawkins, J. W. (1998). Hydraulic properties of surface mine spoils. Conference proceedings from the American Society of Mining and Reclamation, pp. 32–40. doi: 10.21000/JASMR98010032.

Hawkins, J. W. (2004). Some hydrologic properties of surface mine spoils, pp. 860–878. doi: 10.21000/JASMR04010860.

Haynes, R. J. (2009). Reclamation and revegetation of fly ash disposal sites - Challenges and research needs. Journal of Environmental Management, 90, 43-53.

Heath, R. C. (1983). Hydraulic of wells. Advances in Hydroscience, 281- 442.

Hodgson, F. D. I. and Krantz, R. (1998). Groundwater quality deterioration in the Olifants River Catchment above the Loskop Dam with specialised investigation in the Witbank Sub-Catchment. Bloemfontein: Water Research Commission.

Indiana Department of Environmental Management (IDEM)(2017). Coal Combustion Residuals (Coal Ash). Indianapolis, IN, USA. IDEM Fact Sheet CO0518L, pp. 1–3. Available at: https://www.in.gov/idem/files/factsheet_olq_permits_ccr.pdf.

iLanda Water Services, (2016). Leeupoort Colliery Driefontein mine water balance. Johannesburg, South Africa. Report submitted to Alan Robinson Consulting Civil & Geotechnical Engineers No: 0207-Rep-001 Rev 2.

Insigne, M. S. L. and Kim, G.S. (2010). saltwater intrusion modeling in the aquifer bounded by Manila Bay and Parañaque River, Philippines, Environmental Engineering Research, 15(2), pp. 117–121. doi: 10.4491/eer.2010.15.2.117.

Izquierdo, M. and Querol, X. (2012). Leaching behaviour of elements from coal combustion fly ash: An overview, International Journal of Coal Geology. Elsevier B.V., 94, pp. 54–66. doi: 10.1016/j.coal.2011.10.006.

Jankowski, J., Ward, C. R., French, D., and Grove, S. (2006). Mobility of trace elements from selected Australian fly ashes and its potential impact on aquatic ecosystems. Fuel, 85, 243-256.

Jayaranjan, M. L. D., van Hullebusch, E. D. and Annachhatre, A. P. (2014). Reuse options for coal fired power plant bottom ash and fly ash, Reviews in Environmental Science and Bio/Technology, pp. 467–486. doi: 10.1007/s11157-014-9336-4.

Jeffrey, L. S. (2005). Characterization of the coal resources of South Africa, The Journal of The South African Institute of Mining and Metallurgy, 105(2), pp. 95–102. Available at: http://www.scopus.com/inward/record.url?eid=2-s2.0-16244411695&partnerID=tZOtx3y1.

Jha, A. K., and Singh, J. S. (1991). Spoil characteristics and vegetation development of an age series of mine spoils in a dry tropical environment. Vegetation, 97, 63-76.

Johnson, A.I. (1967). Specific yield - Compilation of specific yields for various materials. Hydrological properties of earth materials. Washington: US Geological Survey.

Johnson, A.G. (2018). Assessing the change in hydro-geochemical properties of fly ash over time when disposed into opencast coal mines in Mpumalanga, South Africa. An unpublished MSc. thesis submitted to The University of the Western Cape, South Africa.

Johnson, D. B. and Hallberg, K. B. (2005). Acid mine drainage remediation options: A review. Science of the Total Environment, 338(1–2 SPEC. ISS.), pp. 3–14. doi: 10.1016/j.scitotenv.2004.09.002.

Johnson, M. R., Van Vauuren, C. J., Hegenberger, W. F., Key, R., and Shoko, U. (1996). Stratigraphy of the Karoo Supergroup in Southern Africa: an overview. Journal of African Earth Sciences, 23, 3-15.

Jones and Wagener. (2016). Anglo operations (Pty) ltd Goedehoop Colliery (Goedehoop Colliery South) undermining of watercourses water use licence application.

Jones, J. R., and Anderson, D. (1994). Relationships among permeability, porosity and grain size measures for unconsolidated materials. North Eastern Geology, 16, 231-236.

Jordaan, J. (1986). Highveld Coalfield in mineral deposits of Southern Africa (pp. 1985-1994). Johannesburg, South Africa: Geological Society of South Africa.

Kapangaziwiri, E. (2009). Introduction to hydrologic models. Presentation for the Department of Natural Resources and the Environment in the Council of Scientific Research (CSIR).

Kasenow, M. (2001). Applied ground-water hydrology and well hydraulics, 2nd Edition. Colorado, USA: Water Resources Publications.

Kikuchi, R. (2006). Alternative By-Products of Coal Combustion and simultaneous SO2/SO3/NOX treatment of coal-fired flue gas: approach to environmentally friendly use of low-rank coal. SpringerLink, 21-32.

Kim, A. G. (2003). Leaching Methods Applied To the Characterization of coal utilization by-products. Pittsburgh, PA. Report for the ORISE Research Fellow, National Energy Technology Laboratory, US Department of Energy pp. 89–96.

Kim, B., and Prezzi, M. (2008). Evaluation of the mechanical properties of class-F fly ash. Waste Management, 28(3), 649-659.

Kirchner, J., Van Kirchner, J., Van der Tonder, G.J. and Lukas, E. (1991). Exploitation potential of Karoo Aquifers, Water Research Commission report no 170/1/91, WRC Report(170), p. 284.

Kockwood, A. and Evans, L. (2012). Ash in lungs. Report submitted by the Senior Scientist and Past President Physicians for Social Responsibility and Emeritus Professor of Neurology, University at Buffalo pp. 150–190.

Kolbe, J. L., Lee, L. S., Jafvert, C. T. and Murarka, I. P. (2011). Use of alkaline coal ash for reclamation of a former strip mine, pp. 1–15. Conference proceedings from the World of Coal Ash (WOCA) Conference - May 9-12, 2011, in Denver, CO, USA http://www.flyash.info.

Kostas, K., Georgios, B. and Ioannis, P. (2000). Hydraulic performance of laboratory PRBs for the decontamination of acidic mine waters, 9th International Mine Water Congress, (2), pp. 347–354.

Krčmář, D. and Sracek, O. (2014). MODFLOW-USG: Die neuen Möglichkeiten für die hydrogeologische Modellierung im Bergbau (oder: Was nicht in den Handbüchern steht), Mine Water and the Environment, 33(4), pp. 376–383. doi: 10.1007/s10230-014-0273-9.

Kresic, N. (2007). Hydrogeology and Groundwater Modeling. 2nd Edition. CRC Press. ISBN-13: 9780849333484

Kumar, C.P. (2019). An overview of commonly used groundwater modelling software. International Journal of Advanced Research in Science, Engineering and Technology. Vol. 6, Issue 1.

Kuyucak, N. (2012). Acid Mine Drainage Prevention and Control Options. Conference proceedings from the International Mine Water Association (IMWA) 2012. www.IMWA.info, pp. 599–606.

Langevin, C. D., Dausman, A. M. and Sukop, M. C. (2010). Solute and heat transport model of the Henry and Hilleke laboratory experiment, Ground Water, 48(5), pp. 757–770. doi: 10.1111/j.1745-6584.2009.00596.x.

Lapakko, K., Lawrence, R. W. (1993). Modification of the net acid production (NAP) test. Proceedings of the 17th Annual British Columbia Mine Reclamation Symposium in Port Hardy, BC, 1993. The Technical and Research Committee on Reclamation

Li, M. G., Aube, B. C., and St-Arnaud, L. C. (1997). Considerations in the use of shallow water covers for decommissioning reactive tailings. Vancouver, Canada: Proceedings of the Fourth International Conference on Acid Rock Drainage.

Libicki, J. (1982). Changes in the groundwater due to surface mining, International Journal of Mine Water, 1(1), pp. 25–30. doi: 10.1007/BF02504605.

Libicki. Y. (1985). Proposal of criteria for selection of dewatering methods in surface mining. Proceedings of the 2nd International Mine Water Association Congress, Granada, pp 105–112

Liblik, V. and Pensa, M. (2003). Alkaline dust for plants, Quality, pp. 193–203.

Lin, H. J., Richards, D. R., Talbot, C. A., Station, W. E., Yeh, G., Cheng, J., Cheng, H. and Jones, N. L. (1997). FEMWATER : A three-dimensional finite element computer model for simulating density-dependent flow and transport in variably saturated media, Transport, (July), pp. 1–143. Available at: http://homepage.usask.ca/~mjr347/gwres/femwref.pdf.

Liu, H., Banerji, S. K., Burkett, W. J. and Vanengelenhoven, J. (2009). Environmental properties of fly ash bricks, WOCA 2009, Lexington, US, pp. 1–18.

Lubczynski, M.W. and Gurwin, J. (2005). Integration of various data sources for transient groundwater modeling with spatio-temporally variable fluxes-Sardon study case, Spain. Journal of Hydrology, 306(1-4): 71-96.

Lux, M., Szanyi, J. and Tóth, T. M. (2016). Evaluation and optimization of multi-lateral wells using MODFLOW unstructured grids, Open Geosciences, 8(4), pp. 39–44. doi: 10.1515/geo-2016-0004.

Ma, C. a, Cai, Q. X., Wang, H., Shao, M. a, Fan, J., Shi, Z. Y. and Wang, F. X. (2015). Modeling of Water Flow in Reclaimed Mine Spoil with Embedded Lignitic

Fragments Using Hydrus-1D', Mine Water and the Environment. Springer Berlin Heidelberg, 34(2), pp. 197–203. doi: 10.1007/s10230-014-0299-z.

Maharana, J. K. and Patel, A. K. (2013). Population structure of Denison's barb, Puntius denisonii (Pisces: Cyprinidae): A species complex endemic to the Western Ghats of India, Journal of Phylogenetics & Evolutionary Biology, 1(1), pp. 1–12. doi: 10.4172/2329-9002.

Mahesh Kumar. (2004). Ground water flow model of north east musi basin, Ranga Reddy district, Andhra Pradesh using finite difference method. M. Tech thesis Submitted to Osmania University, Hyderabad, India.

Mahlaba, J. S., Kearsley, E. P. and Kruger, R. A. (2011). Physical, chemical and mineralogical characterisation of hydraulically disposed fine coal ash from SASOL Synfuels, Fuel. Elsevier Ltd, 90(7), pp. 2491–2500. doi: 10.1016/j.fuel.2011.03.022.

McCarthy, T. S. (2011). 'The impact of acid mine drainage in South Africa, South African Journal of Science, 107(5/6), pp. 1–7. doi: 10.4102/sajs.v107i5/6.712.

Meek, F. A. (1996). Evaluation of acid prevention techniques used in surface mining. Morgantown, West Virginia: West Virginia University and the National Mine Land Reclamation Center.

Mineral Environment Neutral Drainage (1994). Evaluation of alternate dry covers for the inhibition of acid mine drainage from tailings. Ontario, Canada. MEND Project no. 2.20.1.

Menghistu, M. T. (2010).Development of a numerical model for unsaturated/saturated hydraulics in ash/brine systems. A thesis submitted in fulfilment of the requirements for the degree of Doctor of Philosophy in the Agricultural Sciences Department of Geohydrology University of the Free State, Bloemfontein.

Metesh, J. J., Jarrell, T. and Oravetz, S. (1998). Drainage from abandoned mines in remote areas, 2600(202), pp. 1–18.

Midgley, D. C., Pitman, W. V., and Middleton, B. J. (1994). Surface Water Resources of South Africa 1990. WRC Report No 298/1.4/94

Monterroso, C. and Acías, F. M. (1998). Prediction of the acid generating potential of coal mining spoils, International Journal of Surface Mining, Reclamation and Environment, 12(1), pp. 5–9. doi: 10.1080/09208119808944015.

Moran, S. R., Gerald, H., and Cherry, J. A. (1978). Geologic, hydrologic and geochemical concepts and techniques in overburden characterization for mined-land reclamation. North Dakota Geological Survey.

Mpetle, M., and Johnstone. A. (2018). The water balance of South Africa coal mine pit lakes. Conference proceedings of the 11th International Mine Water Association. Pretoria

Mudd G. M., (2002). Solute transport modeling of Latrobe valley ash disposal sites. Unpublished PhD thesis.School of the Built Environment Faculty of Engineering & Science Victoria University.

Munchingami, I. (2013). Non-invasive characterization of unsaturated zone transport in dry coal ash dumps: a case study of Tutuka, South Africa. A thesis submitted in fulfilment of the requirements for the degree of Doctor of Philosophy at the University of the Western Cape, South Africa.

Murarka, I. P. (2006). Use of coal combustion products in mine-filling applications: A review of available literature and case studies. Colorado, CO, USA. A report submitted to Public Service Company of Colorado, DOE award no: 99-CBRC.

National Electricity Regulator. (2004). Electricity Supply Statistics for South Africa. A report submitted by the National Electricity Regulator.

Nhan, C. T., Graydon, J. W. and Kirk, D. W. (1996). Utilizing coal fly ash as a landfill barrier material, Waste Management, 16(7), pp. 587–595. doi: 10.1016/S0956-053X(96)00108-0.

Niswonger, R. G., Panday, S. and Motomu, I, 2011. MODFLOW-NWT, A Newton Formulation for MODFLOW-2005', USGS reports, p. 44.

October, A. (2011). Development of a conceptual model for an ash dump system using hydraulic and tracer test. A thesis submitted in fulfilment of the requirements for the degree of Master of Science at the University of the Western Cape, South Africa.

October, A., Nel, J. M., Reynolds, K., Lasher, C. and Dlamini, L. (2009). Hydraulic and transport properties of ash dumps, 3rd World of Coal Ash, WOCA Conference, May 4, 2009 - May 7, 2009.

Ohio Environmental Protection Agency. (2007). State of Ohio Environmental Protection Agency Division of Drinking and Ground Waters Ground-Water Flow and Fate and Transport Modeling. State Ohio Environmental Protection Agency.

Ouangrawa, M., Aubertin, M., Molson, J., Bussiere, B., and Zagury, G. (2010). Preventing acid mine drainage with an elevated water table: Long term column experiments and parameter analysis. Water, Air and Soil Pollution, 437 - 458.

Panday, S. and Huyakorn, P. S. (2008). MODFLOW SURFACT: A state-of-the-art use of vadose zone flow and transport equations and numerical techniques for environmental evaluations, Vadose Zone Journal, 7(2), p. 610. doi: 10.2136/vzj2007.0052.

Pathak, R., Awasthi, M. K., Sharma, S. K., Hardaha, M. K. and Nema, R. K. (2018). Groundwater flow modeling using Modflow – a review. International Journal of Current Microbiology and Applied Sciences, ISSN: 2319-7706 Volume 7, pp. 83–88. Journal homepage: http://www.ijcmas.com.

Paul, J. M., Suppé, A. J. and Thomas, D. E. (2001). Modeling and simulation of steady state and transient behaviors for emergent socs', pp. 0–5. doi: 10.1145/500001.500062.

Petrik, L. F., White, R. a, Link, M. J., Somerset, V. S., Burgers, C. L. and Fey, M. V. (2003). Utilization of South African fly ash to treat acid coal mine drainage, and production of high-quality zeolites from the residual solids, 2003 International Fly Ash Symposium, 2.

Pilate, A. and Adams, F. (1985). Analysis of air particulate matter and fly ash by spark source mass spectrometry. Fresenius Zeitschrift Fur Analytical Chemistry, pp 295-299.

Prasad, B. and Mondal, K. K. (2008). The impact of filling an abandoned open cast mine with fly ash on groundwater quality: A case study, Mine Water and the Environment, 27(1), pp. 40–45. doi: 10.1007/s10230-007-0021-5.

Qureshi, A., Jia, Y., Maurice, C. and Bjorn Ohlander, B. (2016). Potential of fly ash for neutralisation of acid mine drainage, Environmental Science and Pollution Research, 23(17), pp. 17083–17094. doi: 10.1007/s11356-016-6862-3.

Rajamanickam. R., and Nagan, S. (2010). Groundwater Quality Modeling of Amaravathi River Basin of Karur District, Tamil Nadu, Using Visual Modflow. International Journal of Environmental Sciences, volume 1. pp 91-108

Ram, L. C. and Masto, R. E. (2010). An appraisal of the potential use of fly ash for reclaiming coal mine spoil. Journal of Environmental Management. Elsevier Ltd, 91(3), pp. 603–617. doi: 10.1016/j.jenvman.2009.10.004.

Ratshomo, K. and Nembahe, R. (2013). South African Energy Price Report. A report submitted to the Department of Energy, Pretoria, South Africa, pp. 34. Available at: http://www.energy.gov.za.

Rehm, B. W., Groenewold, G. H. and Morin, K. A. (1980). Hydraulic Properties of coal and related materials, Northern Great Plains, Ground Water, pp. 551–561.

Reynolds-Clausen, K. and Singh, N. (2016). Eskom's revised coal ash strategy and implementation progress. A report submitted to Eskom Holdings SOC Limited.

Robinson, C., Gibbes, B., and Li, L. (2006). Driving mechanisms for flow and salt transport in the subterranean estuary, Geophysics and Resistivity, Vol.33.

Roemer, M. E. (2017). In-situ immobilization of arsenic in the subsurface using ferrous chloride. A Masters thesis submitted to the Faculty of graduate studies of the University of Manitoba.

Roy, M., Roychowdhury, R., Pritam, M., Roy, A., Nayak, B. and Roy, S. (2017). Phytoreclamation of abandoned acid mine drainage site after treatment with fly ash. A report published by IntechOpen, http://dx.doi.org/10.5772/intechopen.69527.

Rumbaugh, J., and Rumbaugh, D., (2005). Groundwater Vistas 5.0, 1996e2005. Environmental Simulation, Inc.

South African Committee for Stratigraphy. (1980). Stratigraphy of South Africa. Part 1 (Comp. L.E. Kent). Lithostratigraphy of the Republic of South Africa, South West, Africa/Namibia and the Republics of Bophuthatswana, Transkei and Venda. Handbook Geology Survey South Africa. 8, 1–690.

South Africa Coal Statistics and Marketing Manual. (2001). South Africa Coal Statistics and Marketing Manual.

Sarda, M. (2006). Groundwater Flow Model of Upper Musi Basin Andhra Pradesh. M. Tech Thesis submitted to Center of Water Resources, IST, JNTUH, 96p

Shangoni Aquiscience. (2013). Geohydrological investigation on the geohydrological investigation on the Farm Droogefontein Portions 26, 46, 47. A report submitted by Restigen Pty Ltd, report no. RES-NGU-13-07-24.

Siddique, R. (2010). Utilization of coal combustion by-products in sustainable construction materials, Resources, Conservation and Recycling. Elsevier B.V., 54(12), pp. 1060–1066. doi: 10.1016/j.resconrec.2010.06.011.

Simate, G. S., and Ndlovu, S. (2014). Acid mine drainage: Challenges and opportunities. Journal of Environmental and Chemical Engineering, 2, 1785-1803.

Simsiman, G. V. (1987). Effect of ash disposal ponds on groundwater quality at a coal-fired power plant. Water Research WATRAG, 21(4), 417-426.

Sing, D. H., and Kolay, P. K. (2002). Simulation of ash-water interaction and its influence on ash characteristics. Progress in Energy and Combustion Science, 28, 267-299.

Sivapullaiah, P.V. and Laksmikamtha, H, (2004). Properties of Fly Ash as Hydraulic Barrier, Soil and Sediment Contamination, 13, pp 489-504

Stavrakis, N., (1989). Sedimentology of the Karoo Coal-measures in the Eastern Transvaal, South Africa. Unpublished PhD Thesis, University of Strathclyde, Glasgow, Scotland, 201 pp

Steyl, G. (2011) Estimation of Representative Transmissivities of Heterogeneous Aquifers. A thesis submitted to the Institute for Groundwater Studies University of the Free State', (November).

Swaine, D. J. (1995). Chapter 11 the formation composition and utilisation of fly ash. Environmental Aspects of Trace Elements in Coal, pp. 204-220, Kluwer Academic Publishers pp. 204–205.

Theis, T. L., and Gardner, K. H. (1990). Environmental assessment of ash disposal. Critical Revolution Environmental Science Technology, 20(1), 21-42.

Trefry, M. G. and Muffels, C. (2007). FEFLOW: A finite-element groundwater flow and transport modeling tool, Ground Water, 45(5), pp. 525–528. doi: 10.1111/j.1745-6584.2007.00358.x.

USEPA - US Environmental Protection Agency. (1994). Acid Mine Drainage Prediction. A technical document submitted U.S. Environmental Protection Agency, Washington, DC, doi: EPA 530-R-94-036.

USGS - U.S. Geological Survey Office of Groundwater. 2018. USGS MODFLOW and Related Programs. [ONLINE] Available at https://water.usgs.gov/ogw/modflow/. [Accessed 02 February 2018]

Vadapalli, V. R. K., Petrik, L. F., Fester, V., Slatter, P. and Sery, G. (2007). Effect of fly ash particle size on its capacity to neutralize acid mine drainage and influence on the rheological behaviour of the residual solids, World of Coal Ash (WOCA).

Valencic, A. (2013). Dust Suppression In Coal Ash Applications.A report submitted by the Dust Control Technology, Inc, Peoria, IL.

van Bart, A. (2008). Rison Groundwater Consulting Geohydrological Investigation : Komati Ash Dam Extension Final Report, (December 2007).

van den Berg, J. J., Cruywagen, L., de Necker, E., and Hodgson, F. (2001). Suitability and impact of power station fly ash for water quality control in coal opencast mine rehabilitation. Water Research Commission Report No. 745/1/01.

Van der Sloot, H.A., De Groot, G.J., Hoede, D, and Wjikstra J, (1993). Mobility of trace elements derived from combustion residues and products containing these residues in soil an groundwater. Comm Eur Communities, EUR, 14403, pp. 196

Vermuelen, P. D., and Usher, B. H. (2006). Recharge in South African underground collieries. Journal of Institute of Mining and Metallurgy, 106, 771-788.

Viljoen, M. (2015). Landscapes and Landforms of South Africa, pp. 23–29. doi: 10.1007/978-3-319-03560-4.

Visser, J.N.J., (1986). Lateral lithofacies relationships in the glacigenic Dwyka Formation in the western and central parts of the Karoo Basin. Transboundary Geologic Society South Africa. Vol. 89, pp. 373–383.

Ward, C. R., French, D., Stephenson, L., Riley, K. and Li, Z. (2009). Evaluating the interaction of coal ash leachates with rock materials for mine backfill studies, 3rd World of Coal Ash, WOCA Conference - Proceedings, pp. 1–13.

Waterloo Hydrogeologic. (2018). Groundwater modeling numerical methods: Which one should you use? Waterloo Hydrogeologic. [online] available at: https://www.waterloohydrogeologic.com/2013/08/26/groundwater-modeling-numerical-methods-which-one-should-you-use/. [Accessed 02 February 2018].

Weather South Africa (2017). South African Weather Services [online] available at www.weathersa.co.za. [Acessed 5 April 2018].

Whateley, M.G.K. (1980). Structural controls of sedimentation in the Ecca Group in northern Zululand. M.Sc. Thesis, University of Witwatersrand, Johannesburg, 149

Wolfe, W. E., Poston, R. W. and Butalia, T. S. (2001). The behaviour of coal combustion products in structural fills - A Case History', pp. 4–11.

Woods, J. and Cook, C. P. (2015). Modeling salt dynamics on the River Murray floodplain in South Australia : Modeling approaches – Appendices editor Goyder Institute for Water Research Technical Report Series No . 15 / 11', (15).

World Energy Outlook. (2011). International Energy Outlook 2018 Executive Summary. A report submitted by the World Energy Outlook 2011, http://www.iea.org, p. 577. doi: 10.1787/weo-2011-en.

Xenidis, A., Mylona, E. and Paspaliaris, I. (2002). Potential use of lignite fly ash for the control of acid generation from sulphidic wastes, Waste Management, 22(6), pp. 631–641. doi: 10.1016/S0956-053X(01)00053-8.

Yang, J. E., Kim, S. C., Kim, D. K., Oh, S. J., Kwon, H. H., Shim, Y. S., Ko, J. I. and Lee, J. S. (2011). Remediation technology for abandoned mine waste with coal combustion product (CCP). Conference proceedings from the 2011 World of Coal Ash Conference.

Yeheyis, M. B., Shang, J. Q. and Yanful, E. K. (2009). Chemical and mineralogical transformations of coal fly ash after landfilling, 2009 World of Coal Ash (WOCA) Conference, pp. 1–13. Available at: http://www.flyash.info/2009/047-yeheyis2009.pdf.

Yuan, C. G. (2009). Leaching characteristics of metals in fly ash from coal-fired power plant by sequential extraction procedure. Microchim. Acta., 165:91-96.

Zelenková, K., Hanise, B. and Kylychbaev, E. (2009). Earth observation for monitoring and observing environmental and societal impacts of mineral resources exploration and exploitation of civil society policies in a mineral extraction context.

Zhang, X. (2014). Management of coal combustion wastes. A report submitted by IEA Clean Coal Centre, Available at http://bookshop.ieacoal.org.uk/report/80575//83258/Management-of-coal-combustion-wastes,-CCC-231.

Zheng, C. P., & Wang, P. (1999). MT3DMS: A modular three-dimensional multispecies transport model for simulation of advection, dispersion, and chemical reactions of contaminants in groundwater systems; documentation and user's guide. Alabama, USA: Strategic Environmental Research and Development Program, Contract Report SERDP-99-1

Zhou, Y. and Li, W. (2011). A review of regional groundwater flow modeling, Geoscience Frontiers. Elsevier B.V., 2(2), pp. 205–214. doi: 10.1016/j.gsf.2011.03.003.

Ziemkiewicz, P., and Skousen, J. (1996). Overview of acid mine drainage at the source: control strategies. Morgantown, WV: West Virginia: University and the National Mine Land Reclamation Center.